A Study of Intracoronary Gene Transfer Using Stents Coated with Plasmid Vectors

A thesis submitted to the University of Manchester for the degree of Doctor of Medicine in the Faculty of Medical and Human Sciences

2011

Dr Paul David Williams

School of Medicine

Table of contents

Total word count: 46791

List of figures

List of tables

List of abbreviations

AAV	adeno-associated virus
Ad	adenovirus
BMS	bare metal stent
BSA	bovine serum albumin
CABG	coronary artery bypass grafting
CAD	coronary artery disease
CAG promoter	combination of CMV early enhancer element and chicken beta-actin promoter
cAMP	adenosine-3',5'-cyclic monophosphate
cDNA	complementary DNA
CMV	cytomegalovirus
CRE	cAMP-response element
CREB	cAMP-response element binding protein
CTGF	connective tissue growth factor
Cx	circumflex coronary artery
D	DNA nuclear transport sequence
ddH_2O	double-distilled water
DEPC	diethylpyrocarbonate
DES	drug eluting stent
DNA	deoxyribonucleic acid
dsDNA	double-stranded DNA
DTS	DNA targeting sequence
EBNA-1	Ebstein-Barr nuclear antigen-1
EBV	Ebstein-Barr virus
ECM	extracellular matrix
EDTA	ethylenediaminetetraacetic acid

EEL	external elastic lamina
EPC	endothelial precursor cell
GFP	green fluorescent protein
HE	enhancer region of the human smooth muscle myosin heavy chain promoter
HIV	human immunodeficiency virus
IEL	internal elastic lamina
ISR	instent restenosis
IVUS	intravascular ultrasound
LAD	Left anterior descending coronary artery
LB	lysogeny broth
MCP-1	anti-monocyte chemoattractant protein-1
MCS	multiple cloning site
MI	myocardial infarction
MIECMV	major intermediate-early CMV enhancer/promoter
MIEhCMV	major intermediate-early human CMV enhancer/promoter
MIEmCMV	major intermediate-early murine CMV enhancer/promoter
NOS	nitric oxide synthase
OCT	optimal cutting temperature compound
PBS	phosphate buffered solution
PCI	percutaneous coronary intervention
PCR	polymerase chain reaction
pDNA	plasmid DNA
QCA	quantitative coronary angiography
qPCR	quantitative real time polymerase chain reaction
RCA	right coronary artery

RE	enhancer region of the rabbit smooth muscle myosin heavy chain promoter *or* restriction endonuclease
RNA	ribonucleic acid
SLRP	small leucine-rich proteoglycan
SMC	smooth muscle cell
SMGA	smooth muscle gamma-actin
SRF	serum response factor
SVG	saphenous vein graft
TAE	tris-acetate-EDTA
TIMP-3	tissue inhibitor of metalloproteinase-3
TGF- β	transforming growth factor-β
VEGF	vascular endothelial growth factor
WPRE	woodchuck hepatitis virus post-transcriptional regulatory element

Statistics

Statistical calculations were performed using GraphPad Prism 3, GraphPad Software Inc. CA, USA

Power calculations were performed using software at:

http://www.dssresearch.com/toolkit/spcalc/power.asp

Declaration

No portion of the work referred to in this thesis has been submitted in support of an application for another degree or qualification of this or any other university or other institute of learning.

Copyright

Acknowledgements

Thank you to my supervisor Paul Kingston for your support, unabated enthusiasm and perennial optimism even when things weren't working out quite as anticipated. I would also like to thank Parisa Ranjzad for teaching me the ropes of basic science research, answering my endless supply of questions, and granting permission to reproduce Figure 4 with modifications.

I am grateful to the British Heart Foundation for funding my work.

The thesis is dedicated to Claire, Elsa and Isabella. Claire: without your constant support, love and patience I would not have been able to complete this endeavour. I started this research project with no children, and finished with two beautiful young daughters. Thank you to all three of my girls for the daily reminder that there is more to life than work!

Abstract

University of Manchester

Dr Paul David Williams

Degree of Doctor of Medicine (MD)

Title: A Study of Intracoronary Gene Transfer Using Stents Coated with Plasmid Vectors

Date: 24th June 2011

Percutaneous coronary intervention with stent deployment is the dominant form of revascularisation for patients with coronary artery disease. Although drug-eluting stents have reduced the incidence of instent restenosis, they are associated with late problems related to delayed vascular healing including late stent thrombosis. The use of gene-eluting stents offers the potential to deliver localised gene therapy to the vascular wall with the aim of both reducing restenosis and promoting endothelialisation.

Two candidate genes were investigated. Connective tissue growth factor (CTGF) promotes smooth muscle cell apoptosis and stimulates endothelial growth *in vitro*, and has an integral role in wound healing. Fibromodulin (FMOD) is involved in collagen metabolism and is a key mediator of scarless wound healing. Both genes have previously been shown to suppress restenosis in an *ex vivo* vein graft model.

Plasmids containing these two genes were constructed with an expression cassette specially designed to maximise transgene expression in vascular smooth muscle cells. These plasmids were coated onto coronary stents with a polymer and the effects of these gene-eluting stents were investigated in an *in vivo* pig coronary artery model. Previous work by our group has suggested that systemic β-blockade can affect the degree of transgene expression from viral vectors, and experiments were also performed to investigate the effect of β-blockers on plasmid-mediated gene expression.

At 28 days there was no significant difference in angiographic late loss or neointimal hyperplasia between the groups treated with stents coated with FMOD or CTGF and the group treated with stents coated with the marker gene *lacZ*. This lack of efficacy appeared to be as a result of extremely poor transgene expression rather than due to a genuine failure of the transgenes to elicit a relevant biological effect. There was no difference in *in vivo* gene expression demonstrated as a result of β-blockade, but again this result was probably due to limited transgene expression.

The potential causes of poor transgene expression in this study are reviewed and future directions for research on plasmid-mediated gene therapy are considered.

1 Introduction

Atherosclerotic coronary artery disease (CAD) is pandemic in the developed world and remains the most common cause of mortality[1]. Angina, symptomatic myocardial ischemia secondary to obstructive coronary stenoses, is responsible for an enormous symptom burden which is often refractory to medical therapy. In these cases, mechanical revascularisation either by means of coronary artery bypass grafting (CABG) or percutaneous coronary intervention (PCI) is frequently required. Since PCI was first performed in 1977, it has become the predominant method of revascularisation for patients with symptomatic CAD and 885,000 procedures were performed in Europe in 2004[2] and ≈1 million in the US in 2005[3]. The original procedure of balloon angioplasty alone had important limitations. In the short-term, vessel wall dissection and thrombus formation were common and restenosis (progressive luminal narrowing due to constrictive remodelling and neointimal hyperplasia) occurred in 20-50% of patients within 12 months, often necessitating a repeat procedure. The widespread use of coronary stents (and improvements in periprocedural antiplatelet therapy) substantially reduced the incidence of short-term complications and, by eliminating constrictive remodelling, the long-term risk of restenosis. However repeated revascularisation is still needed to treat in-stent restenosis (ISR) in ≈14% of patients receiving a bare metal stent (BMS)[4]. This represents a huge clinical and economic burden with recent estimates suggesting that ISR costs >$2.5 billion annually in the US alone[5].

There have been many different approaches to solving the problem of ISR, the vast majority of which have not been shown to have clinical utility. Several systemic pharmacological approaches have been shown to be ineffective in clinical trials despite promising preclinical data[6, 7]. Localised intracoronary radiotherapy (brachytherapy) briefly reached clinical practice but was found to be limited by significant long-term complications. Drug-eluting stents (DES) coated with antimitotic agents were the next major development to address the problem of ISR, with seminal early trials reporting minimal restenosis[8, 9]. Commentators proclaimed that the death knell had tolled for ISR[10].

However, DES have not lived up to their initial promise. Restenosis still occurs in high-risk patients such as those with diabetes[11] and, more worryingly, serious complications such as late stent thrombosis related to delayed endothelialisation of the stented segment have been recognised[12-20]. It has become apparent that safer, more effective methods of reducing restenosis are still required. Research is ongoing into coating stents with novel agents, including other antimitotic drugs and antibodies targeted at endothelial progenitor cells, and bioabsorbable stents have been developed. Currently, none of these approaches has been shown to have significant advantages over current stent technology. Gene therapy using coronary stents as a delivery mechanism offers an alternative approach to the problem of restenosis with the potential to modify the vessel wall response to injury favourably by both reducing neointimal formation and promoting rapid endothelialisation.

1.1 The mechanisms of restenosis

The normal arterial wall consists of three distinct layers (Figure 1). The intima, the innermost layer in contact with blood within the vessel lumen, consists of a single cell thickness layer of endothelial cells. The intima is bordered by the internal elastic lamina and surrounded by the media, which contains several layers of smooth muscle cells with separating elastic fibres. The media is separated from the adventitia by the external elastic lamina. The adventitia, the outermost coat, is composed primarily of collagen which gives the vessel structure, as well as anchoring it to adjoining structures. Occasional fibroblasts can be found within the adventitia.

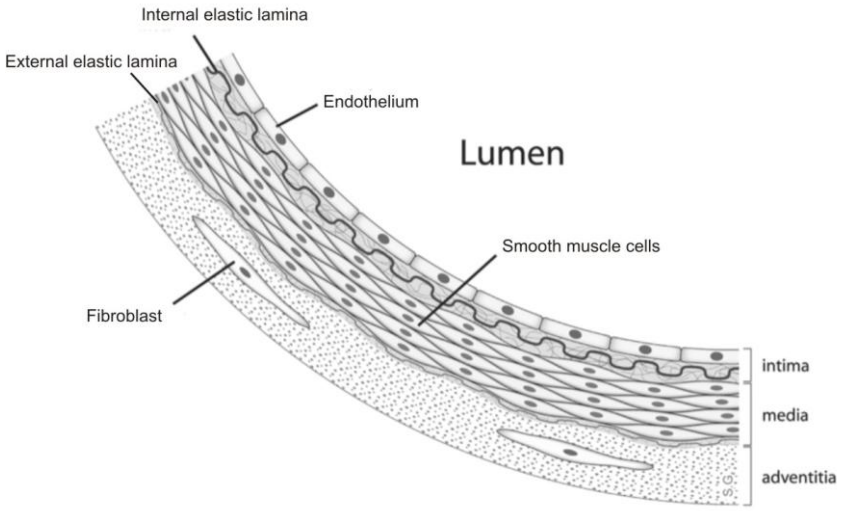

Figure 1 - Anatomy of the arterial wall

Adapted from diagram by Stijn Ghesquiere (under Creative Commons license)

Restenosis can be defined as a reduction in lumen size at a late timepoint following an initially successful intravascular interventional procedure. Restenosis following balloon angioplasty is primarily a result of both vessel wall remodelling and neointimal hyperplasia. Negative remodelling i.e. vessel shrinkage, was identified as a key contributor to the restenotic process by intravascular ultrasound (IVUS) studies in the mid-1990s[21, 22] and is thought to be related to neointimal extracellular matrix (ECM) remodelling, and increased collagen deposition by adventitial myofibroblasts[23]. The advent of routine coronary stent deployment in PCI has largely eliminated constrictive remodelling however[24], leaving neointimal hyperplasia as the sole major contributor to ISR. The pathophysiology of restenosis in the stent era has been reviewed in detail recently[25] and is illustrated in Figure 2.

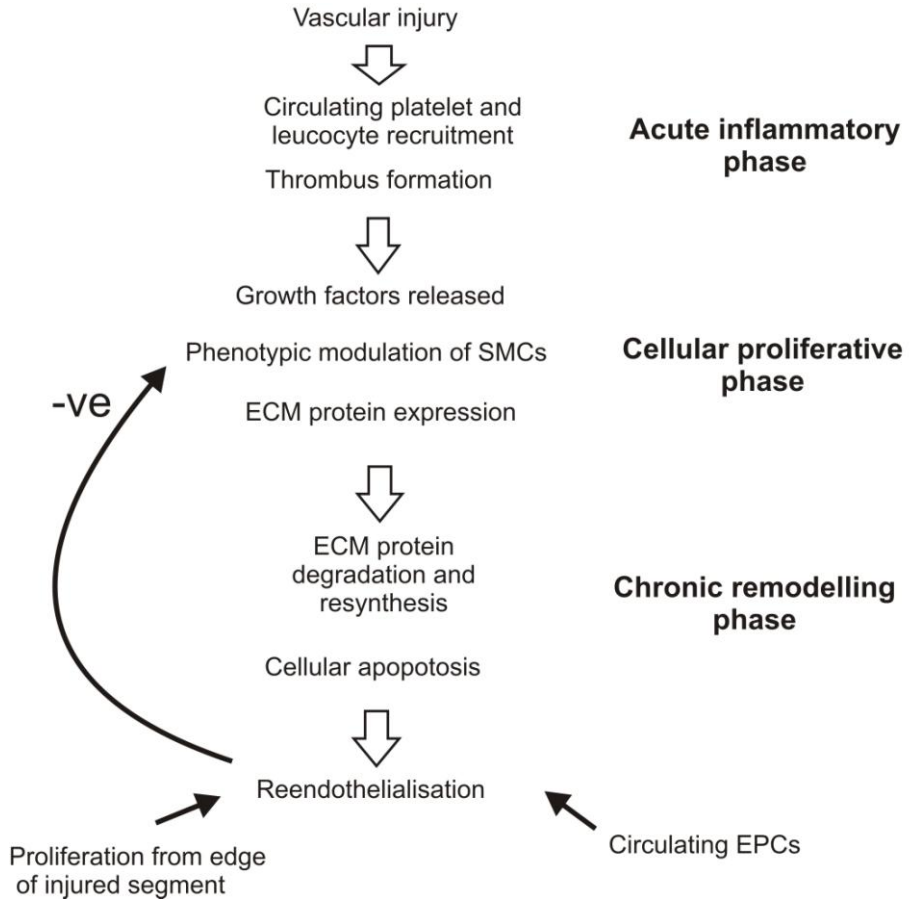

Figure 2 - Flow chart illustrating the restenotic process

ECM = extracellular matrix; EPCs = endothelial progenitor cells; SMCs = smooth muscle cells

The restenotic process can be thought of as a general wound healing response[26, 27]. Vascular injury by high pressure balloon injury or stent deployment causes immediate deendothelialisation, atherosclerotic plaque compression, and vessel stretch, often with dissection into the media and occasionally the adventitia. Circulating platelets are recruited and initiate thrombus formation. Platelet activation occurs via two distinct pathways, mediated by either collagen or tissue factor[28]. Firstly, exposure of collagen within the subendothelial ECM leads to platelet activation via glycoprotein VI, a collagen receptor on platelets, and via the interaction of platelet glycoprotein Ib-V-IX with collagen-bound von Willebrand factor. Secondly tissue factor, a membrane-bound cytokine receptor analogue found both within the vessel wall and in blood, forms a

complex with circulating factor VIIa thus initiating the proteolytic coagulation cascade leading to thrombin and fibrin generation, and subsequent platelet activation via cleavage of protease-activated receptor 4 on the platelet surface[28].

Activated platelets express P-selectin which causes leucocyte adhesion and rolling across the damaged endothelium, followed by stronger leucocyte adhesion and migration mediated by integrins (particularly leucocyte Mac-1[29]). Monocytes/macrophages accumulate within the vessel wall and, following stent deployment, cluster around the stent struts[30]. These cells can undergo phenotypic transformation into myofibroblasts[31]. The net result is a cycle of inflammation and thrombosis [32].

Growth factors released from SMCs, platelets and leucocytes induce a cellular proliferative phase. Normally vascular SMCs remain quiescent in the G0 phase of the cell cycle and possess a contractile function. Following vascular injury there is phenotypic modulation of SMCs[33] which enter the G1 phase of the cell cycle and migrate from the media to the intima where they proliferate[34] and increase the expression of ECM proteins[35]. Phenotypic modulation of adventitial fibroblasts to collagen-producing myofibroblasts also occurs and some of these cells migrate to the luminal surface of the vessel[36-39]. However it is unclear to what extent myofibroblasts contribute to neointimal formation. A study of SMC differentiation markers including smoothelin, a marker of late SMC differentiation, in a porcine coronary artery model found that SMCs rather than myofibroblasts represent the main cellular component of neointima; this suggests that the adventitial response may be unrelated to neointimal proliferation[40].

Although it was thought originally that the principal component of neointima was an excess of proliferative SMCs, it is now appreciated that the neointima in humans, at least after a few months, consists primarily of large amounts of proteoglycan-rich ECM, with few SMCs and numerous cell-depleted areas[41-43]. Interestingly, although animal models have shown that early exuberant intimal SMC proliferation may be an important contributor to the restenotic process, this phenomenon has never been demonstrated in humans. For instance, O'Brien and colleagues measured histone 3 mRNA expression, a sensitive marker of cell replication, in atherectomy specimens obtained from human

coronary restenotic lesions within three months of the original interventional procedure[44]. They found that the overall maximum percentage of replicating cells was less than 0.5%, although there were focal areas identified with higher levels of replication. These results raise the possibility that cellular replication may not contribute significantly to neointimal expansion in humans.

Neointimal ECM consists of varying quantities of proteoglycans (biglycan, versican and decorin) and glycoproteins (fibronectin, thrombospondin-1, osteopontin and tenascin-C), as well as the glycosaminoglycan hyaluronic acid and several members of the collagen family. Freshly deposited ECM is rich in the water-trapping macromolecules hyaluronic acid and versican[45], as well as the glycoprotein fibronectin[46]. The cytokine transforming growth factor-β(TGF-β) is overexpressed in the arterial wall early after vascular injury and is a key regulator of ECM gene expression.

Over a period of months, the neointima enters a chronic remodelling phase characterised by ECM protein degradation and resynthesis. Matrix metalloproteinases are important regulators of ECM remodelling and their expression is upregulated following vascular injury[47, 48]. Post-mortem human studies have shown that this process can extend for up to 18 months, with a gradual decline in cellularity, type III collagen, versican and hyaluronan content and a gradual increase in type I collagen and decorin[43, 49]. The finding of cell-depleted areas in chronic neointima suggests that SMC apoptosis occurs during this process[42]. After the initial development of neointimal hyperplasia during the first few months following stent deployment a degree of neointimal regression can occur. In a porcine model neointimal regression was demonstrated between two and six months which was associated with a reduction in proteoglycan content but with no change in SMC density or overall collagen content although, as demonstrated in the human post-mortem studies, there was a relative increase in type I and relative decrease in type III collagen at six months[50]. Late neointimal regression has also been demonstrated with BMS in humans and typically occurs after six months[51-53]. During very long-term follow-up there appears to be a triphasic response, with the initial ISR regressing between six months and three years before further progression after three years[54]. The mechanism for these late changes is unclear.

Functional vascular endothelium is essential for maintaining normal vessel wall function and permeability. Circulating platelets contribute to this physiological steady state by the constitutive release of proangiogenic cytokines and growth factors from platelet granules which bind to specific endothelial cell surface receptors[55]. The normal endothelium is a key producer of nitric oxide, a potent vasodilator and thromboregulator which inhibits platelet aggregation and SMC proliferation[56]. It has long been established that endothelial denudation alone, without disruption of the underlying media, results in significant neointimal formation[57]. As discussed earlier, endothelial disruption and exposure of subendothelial collagen and tissue factor leads to rapid platelet aggregation and thrombus formation; deployment of a coronary stent causes more endothelial disruption than balloon angioplasty alone[58]. The recent discovery that mice lacking the P2Y(12) platelet receptor have significantly less neointima formation following vascular injury[59] supports the theory that platelet aggregation and thrombus formation provide an important stimulus to neointimal formation, and as a consequence promoting re-endothelialisation may lead to a reduction in ISR.

Circulating CD34-positive bone marrow derived stem cells, which have the potential to differentiate into endothelial cells, have recently been identified: so-called endothelial progenitor cells (EPCs)[60]. Re-endothelialisation is now known to be a result of both local proliferation and migration of endothelial cells from the edge of the injured segment[57], and recruitment of circulating EPCs. A recent study has also highlighted the presence of bone-marrow derived smooth muscle progenitor cells which may contribute to the restenotic process[61]. In that study, coronary stenting induced recruitment of both types of progenitor cell from the bone marrow, an effect possibly mediated by Mac-1 integrin dependent activated neutrophils.

Facilitating endothelialisation might be expected therefore to reduce neointima formation, as well as reducing the risk of late stent thrombosis. This hypothesis is supported by evidence from recent animal studies. Vascular endothelial growth factor (VEGF), an endothelial mitogen, has been shown to reduce restenosis in several animal models[62-65]. Mobilisation of EPCs has been shown to promote endothelialisation and reduce neointimal hyperplasia in a rat model[66] and *ex vivo* transduction of EPCs with the nitric oxide synthase (NOS) isoform eNOS improved endothelialisation and reduced neointimal hyperplasia further whilst also reducing thrombosis[67]. There appear to be

important differences between NOS isoforms: adenoviral transfer of eNOS into the balloon injured rabbit carotid artery has been shown to both enhance endothelialisation and reduce neointimal hyperplasia, whereas transfer of iNOS impaired endothelialisation[68].

1.2 Clinical approaches to reduce restenosis

Our knowledge of the molecular and cellular mechanisms of restenosis has provided several potential therapeutic strategies. These can be broadly divided into five categories: reducing thrombosis, minimising inflammation, inhibiting cellular proliferation, modifying ECM deposition and enhancing endothelialisation. Pharmacological approaches include a vast array of anticoagulant, antiplatelet, antifibrotic, antioxidant and immunosuppressant agents, as well as antibiotics, statins, angiotensin-converting enzyme (ACE) inhibitors and β-blockers[69]. However, despite promising animal data none of these agents have been shown to be beneficial in human trials[6, 7], and it seems unlikely that a systemically administered therapy will reach sufficient local concentrations at the site of injury over an appropriate timeframe to be efficacious without causing side-effects.

Coronary stents have proved a major advance in the management of coronary artery disease. By remaining permanently in the coronary wall, stents act as a scaffold device and essentially eliminate acute vessel recoil and constrictive remodelling[24], thus significantly reducing the long-term risk of restenosis. Given that stents are now deployed in almost all PCI procedures, the current overriding clinical problem is that of ISR due to neointimal hyperplasia.

Intracoronary radiotherapy (brachytherapy) became the "gold-standard" for treating ISR in the late 1990s with impressive short-term results. However the difficulty of setting up a brachytherapy service, with complex licensing procedures for physicians, and the recognition of the problems of delayed restenosis[70, 71] and late stent thrombosis[72] limited uptake, and the devices have now been withdrawn from market[73].

Drug-eluting stents represented the next major development in combating restenosis. To date, DES have been coated with a biocompatible polymer and an anti-mitotic agent that targets cell division and inhibits neointimal proliferation primarily by reducing SMC

proliferation[25]. The first stents to reach clinical practice in 2003 were coated with either paclitaxel or sirolimus.

Early trials of DES demonstrated dramatic reductions in ISR by comparison with BMS, and a reduction in the need for repeat revascularization without evidence of systemic side-effects[8, 9, 74, 75]. These trials, however, offered relatively short-term follow-up, were not powered to examine safety end-points, and included only clinically stable patients with simple, newly-diagnosed lesions. Nonetheless, on the basis of this evidence, the uptake of DES was rapid and their use in clinical practice extended to higher risk patients with more complex lesions than were included in the original studies. In 2006, DES represented >90% of all stents implanted in some countries[5] and millions have been implanted worldwide.

However, DES do not represent a panacea for obstructive coronary disease. In high risk-groups such as diabetic patients, a significant minority of patients still develop restenosis [11] and there is increasing realisation that there can be a late "catch up" phenomenon, with the restenotic process only being postponed rather than eliminated [76-78]. Late incomplete stent malapposition and stent-related aneurysms, which are extremely rare with BMS, have been described[79, 80].

Of more concern are reports showing that vessels containing a DES are at increased risk of late stent thrombosis (defined as >30 days after implantation)[12-20]. This often catastrophic event manifests as acute myocardial infarction (MI) or sudden death and has a mortality rate that may be as high as 50%[81-83]. Studies of the potential mechanisms of late thrombosis in DES have implicated delayed healing and increased inflammation at the site of stenting[84, 85], characterised by persistent fibrin deposition, and incomplete endothelialisation of stent struts[86]. Delayed healing appears to be particularly marked in areas of stent overlap, where local drug concentrations are highest[86]; overlapping stents are very commonly deployed clinically in long lesions. Subsequent post-mortem and angioscopic studies have confirmed these findings in humans, and provided a pathophysiological explanation for late stent thrombosis[87-90]. Deendothelialisation remains significantly greater within DES at 6 months[89, 90], associated with a >5-fold increase in adherent thrombus in stented segments at this time point[90]. Delayed healing and the subsequent risk of late stent thrombosis appears to be a particular concern when

DES are implanted as the primary treatment for an MI (primary PCI) when there is often a large area of necrotic core at the site of plaque rupture[83]. Late incomplete stent apposition, which is more common with DES than with BMS, has also been linked to an increased risk of late stent thrombosis[91, 92].

As well as directly inhibiting local endothelial cell proliferation, other mechanisms have been proposed for the delayed endothelialisation seen with DES. Deployment of sirolimus-eluting coronary stents significantly suppresses the mobilisation and subsequent differentiation of endothelial progenitor cells from the bone marrow, possibly by reducing inflammation locally[61]. Deployment of sirolimus-eluting stents also reduces circulating levels of VEGF, as compared with BMS, in patients undergoing PCI for stable angina[93]. Localised hypersensitivity reactions to the polymer or drug coating on DES also represent another mechanism for late stent thrombosis[88, 94]. A recent study by Cook and colleagues showed increased eosinophilic infiltrates within coronary thrombus aspirated from patients presenting with late stent thrombosis, and this correlated with positive remodelling of the vessel wall and incomplete stent apposition. These findings suggest that DES can induce a chronic necrotising vasculitis secondary to localised hypersensitivity [92], although it is unclear whether this reaction occurs in response to the drug or the polymer (or both).

It is of some concern that registry data shows that the risk of stent thrombosis remains up to at least 3 years post-implantation, with a cumulative risk of 0.6% per year[95, 96], suggesting that DES can cause chronic deendothelialisation. Although the risk of stent thrombosis can be mitigated by the use of longer durations of oral antiplatelet medications, it is currently not clear when, if at all, it is safe to discontinue antiplatelet agents, and these drugs can significantly increase the long-term risk of bleeding complications.

In December 2006 the US Food and Drugs Administration's Circulatory Devices Systems Advisory Panel reviewed the current evidence surrounding this issue. They concluded that for licensed indications in relatively simple coronary lesions DES appear safe[19], but when used "off-label", in more complex disease and higher risk patients, the risks of late thrombosis, death and MI are possibly increased and prognosis may be worsened[13, 14, 16, 20]. Although several new DES have come to market[97, 98], they all use

similar anti-mitotic agents to the original DES and are likely to have similar problems with delayed healing, chronic deendothelialisation and late stent thrombosis. As a result, DES utilisation has fallen significantly as interventional cardiologists return to using BMS when possible.

Other stent-based technologies are in development. Clinical results with bioabsorbable stents have been disappointing so far; a recent trial with bioabsorbable magnesium stents, designed to degrade within a few months, demonstrated a revascularisation rate of 45% at 1 year, a rate substantially higher than with BMS [99]. Negative remodelling was a major contributor to restenosis in this study suggesting that stents need to maintain their structural integrity for substantially longer periods of time to provide sufficient vessel wall scaffolding. Drug-eluting bioabsorbable stents have also been implanted in humans but there is no long-term data on their safety or efficacy[100, 101].

Stents coated with anti-CD 34 antibodies, so-called "pro-healing" stents, have been designed which serve to capture circulating endothelial progenitor cells derived from the bone marrow[60]. However, as CD 34 is a marker for several types of bone marrow derived stem cells including smooth muscle progenitor cells, it is possible that these stents may actually exacerbate restenosis thereby counteracting any potential benefits gained from promoting endothelialisation[61]. Early published registry data support this theory with an 8 month restenosis rate of 19% in relatively short lesions in large vessels, results similar to that found with BMS[102]. A recently published randomised controlled trial showed a strong trend to increased adverse outcomes with anti-CD 34 antibody coated stents as compared to BMS in patients suffering myocardial infarction, including an increased risk of stent thrombosis[103].

Against this background, gene therapy with localised gene transfer to the coronary vasculature offers the potential to alter favourably the response of the arterial wall to stent implantation whilst avoiding the pitfalls of chronic deendothelialisation. The emergence of DES has demonstrated that coronary stents provide a viable platform to allow delivery of a therapeutic agent to the site of pathology, thus minimising systemic toxicity, and this same principle can be applied to the delivery of gene transfer vectors[62].

1.3 Gene therapy approaches to prevent restenosis

Gene transfer into the vascular wall was first demonstrated in 1989 using *ex vivo* transduction of endothelial cells with a retroviral vector and subsequent catheter-mediated introduction into porcine iliofemoral arteries[104]. Since then, a vast range of potentially beneficial genes have been investigated for their therapeutic potential in cardiovascular disease. Restenosis following vessel wall injury by PCI is an intuitively attractive avenue for vascular gene therapy as vectors can be delivered both locally and at the precise time of injury and, accordingly, there has been considerable research into this field. Unfortunately, despite extensive preclinical work, no transgene has been shown as yet to reduce restenosis in clinical studies. This subject has been extensively reviewed recently by others[105-108].

Vascular gene therapy requires the combination of a gene encoding a therapeutic protein, a vector to allow transduction or transfection of target cells, and a delivery system to allow sufficient exposure of the target cells to the vector[107]. All three of these factors crucially affect the efficacy and safety of gene transfer.

1.4 Choice of vector

Multiple vectors having been investigated for their use in cardiovascular gene therapy, and these can be broadly divided into those of viral and non-viral origin. The ideal vector for a given clinical application would be target cell specific with no expression elsewhere, result in therapeutic levels of transgene expression which are not attenuated by the host immune response, produce a duration of transgene expression appropriate to the clinical problem, pose no risk of toxicity either acutely, as a result of immunogenicity, or in the longterm, such as oncogenesis, and be cost-effective and easy to produce. Although recombinant viral vectors demonstrate high transfer efficiency and have been utilised in the majority of preclinical and clinical studies so far there are several issues which potentially limit their clinical utility. Many viruses are inherently immunogenic which can pose a safety concern as well as reducing efficacy. Repeated dosing is likely to result in an attenuated response due to the production of neutralising antibodies to vector antigens. There are also concerns over long-term risks, particularly with integrative viruses such as retroviruses and lentiviruses which are potentially oncogenic as a result of insertional mutagenesis. As will be discussed, non-viral gene

therapy using plasmid vectors represents a potentially much more attractive option for the prevention of coronary stent restenosis.

Three categories of virus represent the vast majority of work on cardiovascular gene therapy so far: adenovirus, adeno-associated virus (AAV) and lentivirus. Other retroviruses, sendaivirus, Semliki forest virus, herpes simplex virus and baculovirus[109] have all undergone preliminary investigation for cardiovascular gene therapy *in vitro* but have never been subject to clinical trials. The development of viral vectors for use in cardiovascular gene therapy has been the subject of a recent review by the author of this thesis[110].

Adenovirus is the most popular vector investigated in vascular gene therapy at present and most studies have used replication-deficient recombinant adenovirus 5 (Ad5) [111-118]. Adenovirus has several features which makes it attractive for gene therapy: a high nuclear transfer efficiency ensures a rapid onset of transgene expression, it has no mechanisms for integration into the host genome and therefore the risk of oncogenesis is remote, it can infect both dividing and quiescent cells, and it can be produced relatively easily in large quantities. However adenovirus has several limitations: the ability to transduce non-target organs as a result of a broad natural tropism, the presence of pre-existing neutralising antibodies in a substantial proportion of human adults and, most importantly, the induction of an immune response which limits the duration of transgene expression and can cause clinical side-effects[119, 120]. Despite extensive research and further development of the vector[121], immunogenicity remains a major hurdle to widespread clinical use and the death in 1999 of a patient in a clinical trial using high-dose adenovirus was attributed to an innate immune response[122]. Several good reviews on adenoviral vectors have been published[123, 124].

Recombinant adeno-associated AAV (rAAV) represents a potentially safer alternative to adenovirus for gene therapy as it is significantly less immunogenic and, unlike adenovirus, wild-type AAV has never been shown to cause human disease. Certain AAV serotypes have been shown to have cardiac tropism[125, 126]. However rAAV possess several disadvantages. The onset of transgene expression is substantially delayed as compared with other viral vectors as a result of slow nuclear transport and the need for the single-stranded genome to be converted to dsDNA prior to

expression[127]. The small packaging capacity (4.6 kb) severely limits the size of transgene and expression cassette that can be inserted. As with adenovirus, immune clearance of transduced cells can be a major problem, particularly given the high prevalence of neutralising antibodies in the general population[128, 129]. This immune response can be clinically relevant and a recent trial of AAV in patients with haemophilia B resulted in transient elevation of liver enzymes in two patients, likely as a result of immune rejection of transduced hepatocytes[130-132]. AAV is also very difficult to manufacture using currently available techniques. Despite these limitations, clinical trials have begun with this virus for the treatment of heart failure[133]. The phase 2 CUPID trial presented at the Heart Failure Congress in May 2010, showed that the treatment was safe and was associated with improvements in several measures of cardiac function and clinical status.

AAV may not represent an ideal choice of vector for the treatment of ISR given the relatively slow onset and limited duration of gene expression. In a comparative study of gene-eluting stents, stents coated with AAV serotype 2 demonstrated a significant decline in gene expression at 28 days following deployment, as compared with adenovirus-coated stents which showed stable levels of gene expression at this time-point[134]. However the exact duration of gene expression required to elicit a beneficial effect on neointimal formation remains unclear.

Although lentiviruses derived from HIV-1 have been used in several cardiovascular clinical trials, concerns remain about their long-term safety. Even though recombinant lentivirus has been rendered replication-deficient, there is the potential for homologous recombination to result in generation of wild-type HIV and, due to their integrative nature, there is a longterm risk of oncogenesis. Non-integrative lentiviruses have been developed[135] but have only been shown to result in transient gene expression in the cardiovascular system as a result of immune clearance[136]. Recombinant lentiviruses will require significantly more development before they can be considered for use in further clinical trials of cardiovascular gene therapy.

Given that currently available recombinant viruses do not represent ideal vectors with regards to vascular gene transfer for the reasons discussed above, recent attention has turned to non-viral vectors, including naked plasmid DNA, lipid-DNA, peptide-DNA

and polymer-DNA conjugates. Naked plasmid DNA represents the simplest form of gene delivery vector. Plasmids are found in virtually all bacterial species and consist of an extra-chromosomal DNA molecule which is usually circular and double-stranded. They can vary in size from 1 to over 200 kilobase pairs and usually encode proteins which engender antibiotic resistance to the host cell. A typical plasmid for use in gene therapy contains the gene encoding for the therapeutic protein, genes encoding for antibiotic resistance and a multiple cloning site (a short region containing several commonly used restriction sites which allows insertion of the transgene). Plasmids have the advantage of being easy to construct and readily produced in large quantities and of having an excellent safety profile, with virtually no risk of oncogenesis (as integration into the host genome is extremely inefficient) and very little immunogenicity as they contain no antigenic proteins. Plasmids have an extremely large DNA packaging capacity, being able to accommodate large segments of genomic DNA if required. They are very easy to handle as they remain stable at room temperature, unlike viruses which generally require storage at -80°C. However plasmid DNA has a gene transfer efficacy several orders of magnitude lower than with viral vectors[116] given poor uptake across the cellular membrane and the difficulty in targeting plasmids to the nucleus where transcription can occur. Many ways of improving gene transfer efficacy have been developed and will be discussed in detail in the following sections. Although plasmid DNA is also readily lost from dividing cells and can be subject to transcriptional silencing, resulting in a limited duration of transgene expression, this is not necessarily a significant concern in developing treatments for ISR as the pathological process is usually complete within several weeks to months.

Given the favourable safety profile and ease of handling, as compared with viral vectors, plasmid DNA represents the most attractive method of gene transfer in the coronary arteries. As will be discussed later, coronary stents are increasingly being used as a gene delivery system, and the advantages of plasmids in this setting are considerable. Although stent coating with viruses has to be performed at the time of the procedure due to their instability at room temperature, plasmids can be produced in large clinically relevant quantities and applied to stents in advance and there are no major storage concerns thus replicating the convenience of DES[137]. Proof of concept has

been established and plasmid-mediated gene transfer has already been demonstrated to have an effect on reducing neointima formation in animal models[62, 64, 138].

1.5 Improving plasmid-mediated gene transfer efficacy

Many different methods have been investigated in an attempt to improve plasmid gene transfer efficacy. It is worthwhile to consider the journey the vector has to make from the introduction into the host to the successful production of the desired transgene product, as at all stages there are formidable barriers to overcome. If introduced systemically the plasmid needs to avoid breakdown by serum nucleases and find its way to the target tissue whilst avoiding transfection of non-target organs. Naked pDNA given intravenously is rapidly eliminated by the liver making this route of administration impractical for this form of vector[139]. Once the plasmid has reached the target organ, the endothelium (if delivered intravascularly) is relatively impermeable given the large molecular weight of pDNA. The next considerable barrier consists of the target cell membrane. Cellular uptake is very inefficient with plasmids which, unlike viruses, do not have dedicated mechanisms to facilitate cell entry. Once inside the cell, the plasmid must avoid lysosomal and cytoplasmic nucleases before localising to the nucleus where transcription can occur. Plasmids can persist in extrachromosomal episomal form in quiescent cells but are rapidly lost from dividing cells. However, even when there is episomal persistence, plasmids are susceptible to transcriptional silencing and, as a result, duration of gene expression can be an issue with plasmid-mediated gene therapy.

At each stage of this journey there is the potential to improve plasmid gene transfer efficacy: physical techniques and carrier vehicles have been developed to aid target cell localisation and intracellular entry, nuclear localisation signals can aid nuclear trafficking and transcriptional targeting in terms of promoter and enhancer optimisation can increase target cell gene expression whilst reducing non-target organ expression. These methods will be discussed in the following sections.

1.6 Physical targeting of plasmids

The simplest method of physically delivering naked plasmid to a target organ is direct injection, e.g. intramuscular injection for skeletal or cardiac muscle gene therapy. This

is clearly impractical for vascular gene therapy and therefore initial attempts at delivering vectors to the vascular system *in vivo* involved balloon catheter systems. Although effective at gene delivery, with promising results from preclinical studies[64, 113, 115, 117], these systems had several important shortcomings. They usually involve prolonged vascular occlusion, which is not a viable option in the coronary tree given the deleterious consequences of even short periods of myocardial ischaemia, and they tend to cause significant vascular injury which may exacerbate neointimal proliferation. Human trials using balloon catheter systems for gene delivery have failed to show efficacy[112, 114].

The development and subsequent widespread use of coronary stents in clinical practice has provided a much improved system for gene delivery and balloon catheters have been rendered effectively redundant for the prevention of ISR. Coronary stents represent an ideal platform for gene transfer as they remain in the arterial wall permanently and thus allow sustained local exposure of the vessel wall to the gene vector whilst minimising the risk of non-target organ transfection. Stent deployment with a high pressure balloon causes localised vessel wall injury which results in two additional beneficial effects with regards to gene transfer. Firstly, endothelial denudation removes a potent barrier to plasmid transfer. Secondly, quiescent medial SMCs transform to a proliferative phenotype as a response to injury, as discussed above. This enhances gene transfer as nuclear transport can occur more readily in mitotic cells due to breakdown of the nuclear envelope[140]. As will be discussed later, effective plasmid-mediated gene delivery via coronary stents has already been demonstrated *in vivo.*

Other physical methods for increasing pDNA gene transfer efficacy exist. Cellular uptake of naked DNA can be increased by electroporation, whereby discharge of an electrical field increases the cell membrane's permeability to DNA, and this has been shown to increase transfection *in vitro* and *in vivo*[141, 142]. Although the difficulties in applying an electric shock to the target tissue limit the usefulness of this technique in the vascular system, one group has demonstrated increased transfection of plasmid DNA within the porcine femoral artery using a specially modified electroporation balloon catheter [143]. The gene gun, sonoporation and laser irradiation have all been shown to increase cell transfection in certain circumstances but none of these techniques is readily applicable to vascular gene therapy (see [144]).

Finally, carrier vehicles for pDNA have been developed to reduce susceptibility to circulating nucleases and/or target the plasmid to the target tissue and/or increase cellular membrane uptake of pDNA by endocytosis. The most commonly used are cationic liposomes and polymers which have been the subject of a recent review[145]. Carrier microbubbles which can be destroyed by local application of ultrasound have been used to improve plasmid delivery of VEGF in a model of peripheral artery ischaemia[144]. However, although these techniques may ultimately prove useful for other gene therapy applications, they do not appear to offer any appreciable advantages over stent-based plasmid delivery in treating ISR.

1.7 Transcriptional targeting and nuclear localisation

One way of addressing the issue of poor gene transfer efficiency with plasmids is to modify the transgene expression cassette. Modifications can involve the use of cell-specific promoters, the inclusion of enhancers and nuclear localisation signals and the removal of CpG dinucleotides. As the dominant cell in the arterial wall is the vascular SMC, this represents the logical target for vascular gene therapy.

Transgene expression is usually driven by strong constitutively active viral promoters such as the major intermediate-early human CMV enhancer/promoter (MIEhCMV), which is commonly used in vectors designed for vascular gene therapy[146]. Although SMC specific promoters exist, such as SM22α, these have consistently been shown to result in inferior SMC gene expression than the MIEhCMV promoter[147]. The major intermediate-early murine CMV enhancer/promoter (MIEmCMV) results in significantly greater transgene expression than MIEhCMV using an Ad5 vector in a wide variety of cell-types[148]. The 0.6kb truncated form of MIEmCMV has been shown to have increased activity as compared with the full length 1.5kb promoter[149] and has also been demonstrated to result in greater transgene expression than MIEhCMV in a wide variety of mammalian cell types using plasmid vectors[150].

The inclusion of *cis*-acting elements can further enhance transcription mediated by viral promoters. The woodchuck hepatitis virus post-transcriptional regulatory element (WPRE) increases transgene expression in a wide variety of cell types *in vitro* and is promoter and transgene independent[151, 152]. Enhancer regions of the mouse and rabbit smooth muscle myosin heavy chain promoters (ME and RE) have been investigated and

the inclusion of RE has been shown to increase vascular SMC transgene expression *in vitro*[153]. An enhancer element in the promoter region for the human VSMC α-actin gene (HE) has also been identified which demonstrates copy dependence and position and orientation independence when linked to the VSMC α-actin promoter[154]. However pairing of this enhancer with the SV40 promoter did not increase transgene expression[154]. The combination of MIEmCMV, RE and WPRE has been shown to dramatically increase SMC transduction using an Ad5 vector both *in vitro* and in porcine coronary arteries as compared with MIEhCMV alone[155].

The inclusion of an intron between the promoter and transgene has the potential to increase gene expression[156]. The inclusion of the EF-1α intron has been shown to significantly increase plasmid-mediated gene expression under the influence of the truncated MIEmCMV promoter[150] . The inclusion of a chimeric intron composed of the donor site from the first intron of the human beta-globin gene and the branch and acceptor site from the intron of an immunoglobulin gene increases gene expression driven by MIEhCMV[157].

The inclusion of a polyadenylation signal induces transcription termination by RNA polymerase II by adding approximately 200 adenylate residues to the 3'-end of the RNA transcript which increases RNA stability and subsequent translation. The late SV40 polyadenylation signal has been shown to increase levels of mRNA significantly more than the early SV40 polyadenylation signal[158].

Nuclear targeting represents an additional strategy to improve plasmid gene transfer efficacy and has been reviewed recently[140]. On entering the cell, plasmids have to travel to and enter the nucleus via the nuclear pore complex in order for transcription to occur[159]; the speed of nuclear transport is critical as naked DNA is susceptible to nuclease digestion whilst in the cytoplasm. Nuclear entry represents the most significant barrier to plasmid-mediated gene transfer in quiescent cells[160]. The nuclear envelope breaks down during mitosis and, as a result, nuclear transport is significantly increased in dividing cells although the process remains relatively inefficient. Dean and colleagues have demonstrated that the 72bp Simian Virus 40 (SV40) enhancer is required for nuclear localisation to non-dividing cells *in vitro*[161, 162]. The inclusion of the SV40 enhancer downstream of the transgene also increased gene expression from rat

mesenteric vasculature cells *in vivo* by 10-40X, with the primary mechanism appearing to be increased nuclear transport[142]. This sequence has been termed a DNA targeting sequence (DTS).

Gene therapy can be further refined by including nuclear localising DNA elements which contain binding sites for cell-specific transcription factors. This approach has the potential to increase gene transfer in target cells whilst improving safety by minimising non-target cell transfection. Dean and colleagues have identified a sequence consisting of 176bp of the chicken smooth muscle gamma-actin (SMGA) promoter, which when included downstream of the transgene acts as a DTS and results in SMC-specific gene expression. This region contains binding sites for SMC specific transcription factors: serum response factor (SRF; binding sites = SRE1 and SRE2) and the NK3 family of transcription factors (Nkx3-1 and Nkx3-2; binding site = NKE1), which can act as nuclear localisation signals (see Appendix 6.3). Mutation of these binding sites substantially reduces DNA nuclear import[163]. Successful SMC specific gene transfer with plasmids containing this sequence has been demonstrated in cultured SMCs[164] and in the rat mesenteric vasculature *in vivo*[165].

The association of the Epstein-Barr nuclear antigen-1 (EBNA-1) and its binding site *oriP*, both of which are derived from Epstein-Barr virus (EBV), can also aid nuclear transport[166]. The EBNA-1 protein binds to *oriP* and can facilitate nuclear entry - the inclusion of the *oriP* sequence in plasmids has been shown to increase transgene expression significantly in EBNA-1 expressing cells[167, 168]. The inclusion of the EBNA-1 gene and *oriP* binding site within the same plasmid has been shown to significantly improved plasmid-mediated transgene expression in cultured SMCs by a *cis*-acting mechanism[169].

As discussed above, the experimental data suggests that nuclear import presents a formidable barrier to successful gene therapy in stable, quiescent cells. Although arterial wall cells (specifically vascular SMCs) are non-dividing at rest, modification to a proliferative phenotype occurs in response to the vascular injury incurred during stent deployment. As a result, nuclear transport may not be a major limitation to gene therapy for the prevention of ISR.

Finally, although plasmids are inherently far less immunogenic than viral vectors they can still induce an inflammatory response. This has been related to the presence of unmethylated CpG dinucleotides which can lead to innate immune system activation via Toll-like receptors[170]. Completely CpG-free plasmids have been developed and have been shown to reduce inflammation and increase gene expression in a mouse model of cystic fibrosis[171]. However, as Toll-like receptors reside within endosomes, the presence of CpG dinucleotides is predominantly an issue with carrier-mediated plasmid delivery, for instance with liposomes. The complete elimination of CpG dinucleotides within a plasmid also dramatically limits the choice of promoter and enhancer elements which can be included which may outweigh any potential benefits in terms of reduced host immune response.

In summary, modification of the gene expression cassette can increase transgene expression by a variety of mechanisms and also increase target cell selectivity. In combination with intracoronary stents which can deliver a vector directly to the target tissue for a prolonged time period and overcome the endothelial barrier, this offers the potential for safe, effective gene therapy to the vascular wall.

1.8 Gene-eluting stents

The use of gene-eluting stents coated with a plasmid vector for the prevention of ISR is conceptually very similar to that of drug-eluting stents. Both plasmid-eluting stents and DES can be prepared in advance, stored at room temperature and deployed in an identical manner. Following stent deployment, a therapeutic agent is delivered at the site of pathology for a circumscribed period of time. The only difference between the two technologies is that the therapeutic agent with a gene-eluting stent is a protein manufactured by the host's own cells rather than an exogenously administered drug.

Ye and colleagues were the first group to demonstrate the feasibility of stent-mediated gene transfer in 1998, using custom bioabsorbable polymer stents impregnated with an adenovirus encoding for β-galactosidase[172]. Since then several further studies confirming the efficacy of gene-eluting stents with both viral and plasmid vectors have been published, which are summarised in Table 1.

Table 1 - Studies involving gene-eluting stents

Transgene	Vector	Model	Stent coating method	Method of vector application	Dose/stent	Primary outcome	Change in outcome	Reference
lacZ	Ad	Rabbit carotid	Custom bioabsorbable polymer stent	Incubated in virus stock ($1x10^8$ – $1x10^{10}$ pfu/ml)	Not reported	Transduction	Success	[172]
GFP	Plasmid	Porcine coronary	PLGA polymer	Dipcoated in polymer-plasmid mix	900-1100 µg	Transfection	Success (1% transfection)	[173]
GFP	Ad	Porcine coronary	Anti-Ad antibody-collagen coated stent	Incubated in virus-PBS solution for 1hr	$5x10^{10}$ viral particles/stent	Transduction	Success (5.9% total; 17% neointima)	[174]
GFP	Plasmid	Porcine coronary	Denatured collagen & PLGA polymer	Pipetted collagen-plasmid mix onto stents then dipcoated in polymer	500 µg	Transfection	Success (10.4% transfection)	[175]
lacZ, Luc, GFP	Plasmid	Rabbit iliac	Synthetic polyurethane polymer	Dipcoated in polymer-plasmid mix	120 µg	Transfection	Success	[137]
VEGF-2	Plasmid	Rabbit iliac	BiodivYsio stent (phosphorylcholine polymer)	Not reported (performed by Biocompatibles)	100 µg or 200 µg	Neointima formation Endothelialisation (NO production)	Decrease Increase	[62]
TIMP-3 & *lacZ*	Ad	Rat carotid	BiodivYsio stent	Pipetted onto stent	20 µl of 10^9 pfu/ml	Neointima formation	Reduction	[176]
lacZ	Ad & AAV	Rabbit iliac	BiodivYsio stent	Virus pipetted on stent	$5x10^9$ pfu/stent (Ad) $5.3x10^9$ drp/stent (AAV)	Transduction	Success 2.73% d3; 7.31% d28 (Ad) 5.78% d3; 2.12% d28 (AAV)	[134]
GFP, iNOS	Ad	Rat carotid	Bisphosphonate & anti-Ad Ab or D1 (recombinant Ad-receptor fragment)	3hr incubation in $5x10^{10}$ Ad particles/ml in 5% BSA/PBS	$10\text{-}15x10^9$ particles/ cm^2	Transduction Neointima formation	Success Reduction	[177]

lacZ, 7ND	Plasmid	Rabbit & monkey iliac	PVOH polymer	Dipcoated in polymer-plasmid mix	Not reported	Neointima formation	Reduction	[178]
iNOS, Luc & GFP	Ad	Rat carotid	Synthetic complex	Synthetic complex	$1x10^9$ particles	Neointima formation	Reduction	[179]
GFP	Plasmid	Rabbit carotid	Anti-DNA antibody-collagen coated stent	Incubated in solution of 20mcg plasmid in 200mcl Dulbecco's MEM	1.7 µg	Transfection	Success (3% total, 7% neointima)	[180]
lacZ, eNOS	Ad	Rabbit iliac	BiodivYsio stent	Virus pipetted on stent	50 µl; $5x10^9$ pfus/stent	Neointima formation Endothelialisation	Decrease Increase	[181]
GFP, iNOS	Plasmid	Pig coronary	Anti-DNA antibody-collagen coated stent	Incubated in solution of 20mcg plasmid in 200mcl Dulbecco's MEM	1.7 µg	Transfection Neointima formation	Success (2.6% total, 6% neointima) Possible decrease (morphometry data not reported)	[182]

Ad=adenovirus; AAV=adeno-associated virus; NOS=nitric oxide synthase; Luc=luciferase; GFP=green fluorescent protein; VEGF=vascular endothelial growth factor; PLGA=polylactic-polyglycolic acid; TIMP-3=tissue inhibitor of metalloproteinase-3; PVOH=polyvinyl alcohol; eNOS = endothelial nitric oxide synthase; iNOS = inducible nitric oxide synthase; 7ND = mutant monocyte chemoattractant protein-1; pfu = plaque-forming units; drp =DNase-resistant particles

The method of attaching the gene vector to the stent requires consideration. All currently available DES for clinical practice use a polymer coating to bind the drug, which can be applied by dipping or spraying. Concerns have been raised over a potential proinflammatory effect of these polymers. Van der Giessen and colleagues reported marked inflammatory reactions with subsequent neointimal thickening in five different biodegradable polymers and three different biostable polymers[183]. However in this study polymers were applied nonuniformly and as a thick layer (75-125μm strips as compared with 5-20μm applied by spraying on current clinically used DES) which may have increased the inflammatory response. In clinical practice using stents coated with thin layers of uniformly applied polymer, hypersensitivity reactions have been reported but appear to be rare[94]. Bioabsorbable polymers such as polylactic acid may offer potential advantages in terms of longterm safety and are available on some of the newer DES to reach the market[184].

Although the majority of research has centred on the use of polymers for drug elution, synthetic and naturally occurring polymers, such as collagen, have been used successfully for gene elution (see Table 1). Alternatives to polymers for vector binding to stents have also been studied. Klugherz and colleagues have successfully demonstrated cell transduction using adenovirus bound via anti-viral antibodies[174], and plasmids have been bound to stents using anti-DNA antibodies by another group[180, 182], but both of these studies also used collagen to coat the stents. Fishbein and colleagues recently demonstrated successful viral tethering to bare metal stents using an entirely synthetic 3-component complex[179]. Brito and colleagues immbolised poly(beta-amino ester) precondensed plasmid DNA-containing cationic liposomes or lipopolypexes onto stainless steel stents using a gelatin coating[185]. Marker gene transfection was then demonstrated *in vivo* following deployment of these stents in rabbit iliac arteries.

1.9 Choice of target gene

A huge range of candidate therapeutic transgenes have been studied to prevent restenosis and this field has been extensively reviewed[108]. These genes can be somewhat arbitrarily divided into strategies that reduce SMC proliferation and migration, inhibit thrombosis, reduce ECM deposition or enhance endothelialisation. However, transgenes exist which have multiple potentially beneficial, or pleiotropic, effects. Given the

complexity of the restenotic process, it is probable that either a single pleiotropic gene or multiple transgenes with different actions will be required for a clinically therapeutic effect.

VEGF has been perhaps the most studied transgene in the field of restenosis and highlights the difficulties in extending basic science research to the clinical setting. VEGF is proangiogenic but also has been shown to be vital for vascular homeostasis and endothelial integrity[186]. In the rabbit iliac model, plasmid-mediated gene transfer of VEGF causes rapid reendothelialisation and reduced intimal thickening following vascular injury[64] and stent deployment[65]. Recently Walter and colleagues demonstrated successful transfection and a reduction in neointima formation in a rabbit iliac model using a plasmid encoding for VEGF-2 bound with a phosphorylcholine polymer to a bare metal stent[62].

However clinical studies of VEGF gene therapy for restenosis have been disappointing. A pilot study with ten patients showed that catheter-mediated delivery of VEGF plasmid DNA in a plasmid-liposome complex at the same time as coronary stenting was safe and well tolerated[114]. However a larger follow up clinical trial using a perfusion-infusion catheter and VEGF plasmid-liposome or VEGF adenovirus showed no difference in restenosis at 6 months[112]. These negative results may be at least partly explained by low gene transfer at the site of injury, an issue which has the potential to be overcome with the techniques discussed in the previous sections. However they clearly demonstrate that promising results in preclinical studies do not necessarily lead to clinically meaningful results.

Table 1 shows the other transgenes which have demonstrated reductions in neointima formation when bound to gene-eluting stents in animal models. These include tissue inhibitor of metalloproteinase-3 (TIMP-3)[176], nitric oxide synthase[179, 182] and the anti-monocyte chemoattractant protein-1 (MCP-1) gene, which encodes a mutant MCP-1 protein called 7ND which acts as a dominant negative inhibitor of MCP-1[178]. Gene-eluting stents have not been trialled in humans at the time of writing.

As discussed in Section 1.2, DES coated with potent anti-mitotic drugs successfully reduce neointima formation via inhibition of SMC proliferation and migration, but also

inhibit endothelial cell proliferation and subsequent re-endothelialisation with potentially serious clinical consequences. Repair of vascular injury has many parallels to cutaneous wound healing (see Section 1.1), with neointimal formation analogous to scar formation. Therefore therapies which enhance vascular healing and repair offer an intuitively attractive approach to the problem of restenosis.

This study will investigate two candidate transgenes which have been shown to have important roles in wound healing: connective tissue growth factor and fibromodulin.

1.9.1 Connective Tissue Growth Factor (CCN2)

Connective tissue growth factor (CTGF) or CCN2 is one of six secreted proteins making up the CCN (cyr61, ctgf, nov) family, each numbered by their order of discovery. The consensus amongst researchers in the field is that CCN members should not be called by their original names, which were often misleading; the preferred name for CTGF is therefore CCN2[187]. However CTGF currently remains the most commonly used term in the scientific literature and thus will be used throughout the rest of this thesis. CCN proteins are characterised by an extremely high cysteine content, consist of four (or three for CCN5) discrete domains, and regulate many important biological processes in multiple tissues including cell migration, proliferation, adhesion, differentiation, survival and stimulation of ECM production. Although they are not generally considered to be growth factors (which typically stimulate cellular growth and proliferation via specific receptors), CCN members have key roles as extracellular signal modulators between the cell surface and ECM and modify the signalling of other molecules such as TGF-β and integrins[188]. Several recent reviews have been published on the biology of CTGF[189-191].

1.9.1.1 Structure and function *in vitro*

CTGF was first discovered in the conditioned medium of human umbilical vein endothelial cells in 1991[192] and is the best characterised of the CCN family. It is a 38kDa mosaic protein with four discrete modules aligned in tandem, each encoded by a separate mRNA exon: a non-functional insulin-like growth factor binding domain-like region (IGFBP), a Von-Willebrand factor type C like domain (VWC), a thrombospondin-1-like domain (TSP-1) and a C-terminal module which contains a

heparin-binding cysteine knot (CT) domain (Figure 3). A further exon encodes for a signal peptide required for secretion from the cell. The hinge regions between the domains are susceptible to proteolytic cleavage, particularly the region between VWC and TSP-1 and the region between TSP-1 and CT. These cleavage products have been identified in biological fluids[193]. Although a specific CTGF receptor has not been identified, it is thought that these four functional domains can act both independently and interact with each other[190]. The CT domain allows CTGF to associate with cell membranes and the ECM via heparan sulphate containing proteoglycans (HSPGs)[194] and cell surface integrins[195] and the LDL receptor related protein has been shown to bind to the TSP-1 domain[196, 197]. Although CTGF appears to play a vital role in normal biological processes such as tissue repair, chondrogenesis, osteogenesis and angiogenesis[191], excess production has been linked to fibrotic disorders in a variety of organ systems.

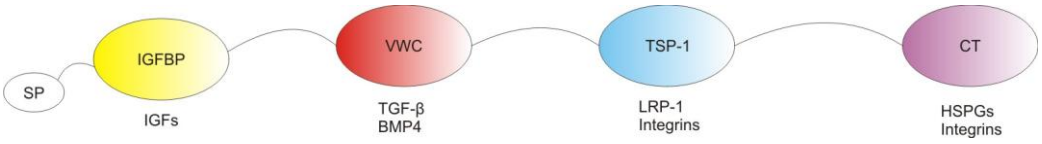

Figure 3 – Structure of CTGF

CTGF consists of a signal peptide required for secretion (SP) and four discrete modules: an insulin-like growth factor binding domain (IGFBP), a Von-Willebrand factor type C domain (VWC), a thrombospondin-1 domain (TSP-1) and a heparin-binding cysteine knot (CT) domain. The hinge region between VWC and TSP-1 and that between TSP-1 and CT are both susceptible to proteolytic cleavage. The molecules to which each domain has been shown to bind are shown.

In vitro studies have shown that CTGF has little activity in isolation, but in association with other cytokines and growth factors, such as TGF-β, it can lead to fibroblast proliferation and myofibroblast differentiation[198, 199], and stimulation of collagen and ECM production by both fibroblasts[200] and SMCs [201]. CTGF has been shown to

stimulate adhesion, migration and proliferation of endothelial cells[202, 203], and promote endothelial cell survival in growth factor-deprived conditions which would normally result in apoptosis[203]. The effect of CTGF on endothelial migration and adhesion appears to be mediated by integrins, cell surface receptors which interact with the ECM and trigger intracellular signalling cascades. The integrin $\alpha_v\beta_3$ appears to be critical for this effect and binds to the CT module[203]. Inhibition of CTGF with antisense RNA and oligonucleotides results in reduced endothelial proliferation in culture[202]. CTGF has been shown to be expressed from cultured vascular endothelial cells *in vitro*[192, 204] suggesting that CTGF has an important role in maintaining endothelial cell homeostasis, possibly via autocrine regulation[202]. As well as its pro-angiogenic activities, CTGF also appears to be able to modulate the effect of other pro-angiogenic molecules: CTGF has been shown to bind to VEGF via the TSP-1 domain and reduce VEGF-induced angiogenesis *in vitro* and *in vivo*[205].The role of CTGF in the regulation of endothelial function and angiogenesis has been reviewed recently[206].

Studies of the effect of CTGF on SMC proliferation have given conflicting results, suggesting that the effect of CTGF is dependent on the cellular context. A study using cultured rat aortic SMCs showed that CTGF promotes SMC migration and proliferation[201]. However, CTGF has also been shown to inhibit SMC proliferation and initiate apoptosis in cultured human SMCs by activating caspase 3[207-209]. Oemar and colleagues demonstrated that CTGF is expressed in high levels in intimal SMCs cultured from human atheromatous carotid arteries. These cells were not proliferating, as indicated by negative staining for PCNA, suggesting that CTGF does not stimulate SMC proliferation *in vivo*[210]. As with TGF-β, CTGF appears to have a dose-dependent effect on some tissues. Liu and colleagues demonstrated that at lower concentrations CTGF resulted in increased proliferation of human embryonic fibroblasts, whereas at higher concentrations CTGF had a growth inhibitory effect[211]. As a specific CTGF receptor has not yet been identified, differences in non-specific receptor distribution and subtypes may explain some of these differences.

TGF-β is known to be a major inducer of CTGF expression[212] and CTGF has been considered to primarily act as a profibrotic downstream mediator for TGF-β[213]. Conversely, CTGF can directly bind TGF-β1 via the Von-Willebrand factor domain and enhance its ability to bind to TGF-β receptors[214]. However, CTGF can be constitutively

expressed independently of TGF-β[215] and other factors such as endothelin-1 can induce its expression via TGF-independent pathways[216, 217]. CTGF expression has also been shown to be suppressed by TNF-α and prostacyclins[218, 219] and induced by glucose, thrombin, angiotensin II and hypoxia (via hypoxia-inducible-factor-1)[220-224]. CTGF therefore has both TGF-β dependent and independent actions and is likely to have different effects in different tissues depending on the local cell types and concentrations of growth factors. CTGF can bind fibronectin via the cysteine knot domain[225] and it has been suggested that CTGF acts as an adaptor molecule, promoting and modulating the binding of ECM proteins to their cell surface receptors[189].

1.9.1.2 Function *in vivo* and role in wound repair and vascular healing

The exact biological actions of CTGF *in vivo* remain to some extent unclear. CTGF expression has been shown to be present in normal uninjured adult tissue in a mouse model, with high levels present in the cardiovascular system (particularly the aorta and coronary arteries) and the gonads[226].

The development of CTGF knockout mice has allowed important observations of the function of CTGF *in vivo.* CTGF is vital for chondrogenesis as homozygous knockout mice die shortly after birth due to widespread skeletal dysmorphisms as a result of impaired chondrocyte proliferation and ECM remodelling[227]. CTGF is also necessary for normal bone development[228, 229]. Although CTGF has been shown to increase collagen production *in vitro,* it is not required for collagen synthesis *in vivo* as levels of collagen II and X are not decreased in knockout mice. However levels of the ECM components aggregan & link protein are severely reduced.

Evidence from *in vivo* studies supports the *in vitro* data suggesting that CTGF plays a key role in angiogenesis[191, 203, 230]. VEGF expression is reduced in knockout animals suggesting that CTGF induces VEGF expression, which may represent one pathway for its proangiogenic effects. Despite this CTGF is not a *necessary* requirement for angiogenesis *in vivo,* as demonstrated by a retinal injury study in CTGF-knockout mice[231],

CTGF has been shown to be involved in wound healing in several *in vivo* models[211, 212, 232], and this action appears to be dependent on the presence of TGF-β. Mori and

colleagues showed that subcutaneous injection of either TGF-β or CTGF alone into the skin of newborn mice caused only a brief reaction, but that injection of both TGF-β and CTGF together resulted in a persistent fibrotic reaction[232]. A recent report demonstrated a beneficial effect of parenterally administered recombinant CTGF on the healing of burn wounds in the rhesus-monkey[211]. A study of virally mediated transfer of Cyr61, another member of the CCN family closely related to CTGF, recently showed beneficial effects with regards to angiogenesis. After femoral artery excision in rabbits, administration of an adenovirus carrying the Cyr61 gene resulted in significantly improved revascularisation of the ischaemic hindlimb as compared with control or VEGF[233].

Excessive expression or activity of CTGF has been shown to play a role in several human diseases. It is associated with fibrotic disorders in a variety of organ systems, including the liver, skin, kidney and heart, and the excess CTGF in these conditions appears to be largely derived from fibroblasts and myofibroblasts[234-237]. CTGF may also play a role in the development of atherosclerosis and has been shown to be expressed in high levels from SMCs in human atherosclerotic lesions, but not from those in normal arteries[210]. CTGF accumulates within the shoulders of human complicated atheromatous plaques and appears to stimulate monocyte migration *in vitro* which may offer a mechanism for promoting atherogenesis[238]. CTGF has been shown to be upregulated in the left atrial myocardium of patients with atrial fibrillation and may be a regulator of atrial scarring in this condition[239].

Two other members of the CCN family, CCN1 and CCN3, have similar amino acid sequences to CTGF (CCN2) and their role in vascular function and repair has also been investigated. CCN3 is constitutively expressed in the vascular media and is localised to VSMCs[240]. A recent paper investigated the vascular role of CCN3[241]. Administration of CCN3 protein inhibited VSMC proliferation and migration *in vitro* independently of TGF-β signalling. Unlike CTGF knockout mice, CCN3 knockout mice survive to adulthood and have a normal vascular phenotype. However vascular endothelial injury of the femoral artery using a photochemically induced thrombosis method resulted in markedly increased neointimal formation and reduced endothelialisation in CCN3-null mice suggesting that CCN3 has important roles in normal vascular healing.

The role of CCN1 appears to be in contrast to CCN3. CCN1 stimulates adhesion and migration of rat VSMCs *in vitro*[242]. CCN1 knockdown mice generated using lentiviral delivery of siRNA demonstrate significantly impaired VSMC proliferation which can be reversed by replenishment of CCN1. Balloon injury of knockdown mice resulted in significant suppression of neointimal hyperplasia in a rat carotid artery balloon injury model which could be reversed by lentiviral gene transfer of CCN1 to the vascular wall.

1.9.1.3 CTGF - a potential therapy for instent restenosis?

In summary, CTGF is involved in wound healing, angiogenesis and chondrogenesis and is overexpressed in fibrotic and atherosclerotic lesions. TGF-β represents one of the most potent inducers of CTGF action. CTGF induces collagen and elastin synthesis, promotes the migration and survival of endothelial cells, and may have varying effects on SMC migration, proliferation and apoptosis depending on the cellular context.

Given the potentially beneficial effects on endothelial cell function and inhibition of SMC proliferation via apoptosis, and its integral role in animal models on wound healing, it is proposed that local overexpression of CTGF will both reduce restenosis and promote re-endothelialisation following coronary stent deployment. Our group has recently demonstrated a reduction in neointima formation following adenovirus-mediated gene transfer of CTGF in a human saphenous vein graft *ex vivo* model **(unpublished data)**. The mechanisms for this effect have not yet been investigated. It is hypothesised that any reduction in intima formation will be more marked *in vivo* when the potential effects of CTGF on improved endothelialisation will be apparent.

1.9.2 Fibromodulin

Fibromodulin is a member of the small leucine-rich proteoglycan (SLRP) family, which consists of eleven structurally and functionally related members; the others include decorin, biglycan, and lumican[243]. The SLRP family has been less studied than the CCN family and hence their functions both *in vitro* and *in vivo* are less well understood.

A 59-kDa protein extracted from bovine articular cartilage was first described in 1986 [244] and was later named fibromodulin in 1989[245, 246]. Fibromodulin is present in most connective tissues and is expressed at high levels in tendon and cartilage. It has been shown to be present in the intima of atherosclerosis-prone human internal carotid and

atheroma-free internal mammary arteries using a proteomics-based approach[247] and in normal arteries and atherosclerotic lesions from apoE/LDLr knockout mice[248].

The human fibromodulin gene (FMOD) is located on chromosome 1q32[249] and has two translated exons which generate a 376 amino acid 40-kDa protein[250]. The human form of fibromodulin is homologous to the bovine form with an overall sequence homology of 90%. Fibromodulin consists of a central domain containing ten leucine-rich repeat domains bordered by disulphide-bonded terminal sequences[251]. The core protein possesses N-linked oligosaccharide chains between the leucine-rich repeats which can be substituted with between one and four keratan sulphate chains via N-glycosidic linkage[252]. There is a tyrosine-rich domain at the N-terminus. A schematic representation of fibromodulin is shown in Figure 4.

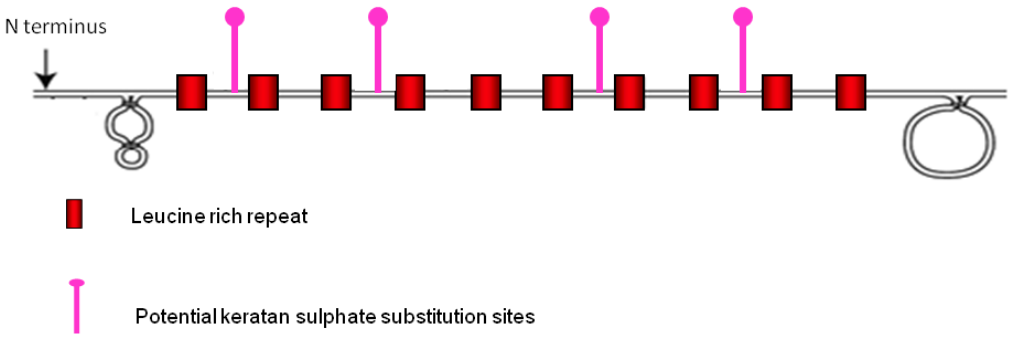

Figure 4 – Structure of fibromodulin

Fibromodulin consists of a core protein with 10 leucine rich repeat domains flanked by two disulphide bonded domains. There are up to 4 keratan sulphate chains between the leucine rich repeat domains.

Fibromodulin binds to fibrillar collagen and helps regulate fibril diameter during its formation and protects the fibrils from proteolytic damage by collagenases[253].

The roles of fibromodulin *in vivo* are still being elucidated. Fibromodulin knockout mice (Fmod-/-) are viable, fertile and do not exhibit any major functional deficits[254].

However electron microscopy reveals abnormal tendon collagen architecture with an increase in the population of small diameter fibrils and these animals are prone to arthritis, confirming that fibromodulin contributes to collagen fibrillogenesis *in vivo*.

Recent reports suggest that fibromodulin may be important in the pathogenesis of osteoarthritis, and most current research focuses on its role in this condition. The fibromodulin gene is upregulated in the cartilage of osteoarthritic joints[255]. Fibromodulin has been shown to activate the complement pathway and its cleavage stimulates proteolytic enzymes, including matrix metalloproteinases, which may lead to persistent joint inflammation[256].

As well its putative role in the development of osteoarthritis, it has also been proposed that fibromodulin acts as a mediator of wound healing. A remarkable feature of foetal wound healing is the absence of scar tissue formation. Soo and colleagues examined fibromodulin expression in a foetal rat model of scarless healing[257]. In this model, ontogenetic transition from scarless healing to adult-type healing with scar occurs between days of 16 and 18 of gestation. They showed that significant fibromodulin expression occurred 36 hours following injury at day 16 gestation. However adult-type healing following injury at day 19 gestation was associated with a down-regulation in fibromodulin expression. Stoff and colleagues investigated the potential therapeutic role of fibromodulin on wound healing in a rabbit *in vivo* model[258]. Following creation of a full-thickness incisional wound and suturing, adenovirus encoding for human fibromodulin was injected intradermally. Scar formation was significantly reduced in the Ad-Fibromodulin animals as compared to two control groups.

The mechanism for the effect of fibromodulin on healing has been proposed to be due to an inhibition of activity of TGF-β1, which is considered to be a key profibrotic cytokine. Fibromodulin has been shown to sequester TGF-β into the extracellular matrix[259]. A recent study showed that overexpression of fibromodulin by human fibroblasts resulted in a decrease in TGF-β1 and TGF-β2 expression, with increases in expression of TGF-β3 (which acts as a functional antagonist to TGF-β1) and TGF-β type II receptors[258]. There were also effects on matrix metalloproteinase activity with an up-regulation in secretion of MMP-2, TIMP-1 and TIMP-2 and a down-regulation in secretion of MMP-1 and MMP-3.

Gene transfer of the related SLRP decorin has been shown to reduce neointima formation in animal models of arterial injury, primarily as a result of a decrease in ECM volume rather than a reduction in cell number within the intima[49, 260]. Fibromodulin is a more potent antagonist of TGF-β1 activity than decorin, but has a lesser effect on TGF-β3[259]. As TGF-β3 acts as a functional antagonist of TGF-β1 activity and exogenous TGF-β3 reduces cutaneous scarring[261], fibromodulin might be expected to be more effective at suppressing neointima formation than decorin.

The effects of fibromodulin on arterial injury have not been studied but our group recently investigated the effect of gene transfer of fibromodulin and decorin on neointima formation in an *ex vivo* organ culture model of human saphenous vein graft disease[262]. Delivery of the transgene was with an adenoviral vector and analysis was performed 14 days after infection. Both SLRPs reduced neointima formation as compared to placebo. However fibromodulin was a significantly more potent inhibitor of neointima formation than decorin. This reduction in neointima is likely to be at least partly explained by antagonism of TGF-β1. Another possible mechanism relates to the effect of fibromodulin on collagen formation and inhibition of collagenases. Fibrillar collagen has been shown to inhibit SMC migration which in turn contributes to the development of neointima[263].

In summary, fibromodulin is expressed in connective tissue including the vascular wall of healthy and diseased arteries. The function of fibromodulin function *in vivo* is incompletely understood but it is involved in collagen development and maintenance and is thought to play a key role in cutaneous wound healing, mediated by its antagonist effect on TGF-β1 activity. As with CTGF, fibromodulin gene expression has been shown to reduce neointima formation in an *ex vivo* saphenous vein graft model.

Given the beneficial effects of fibromodulin on scarless wound healing and the positive results demonstrated *ex vivo* in the vein graft model, it is hypothesised that overexpression of fibromodulin will also result in a reduction in neointima formation following coronary artery stent deployment *in vivo*.

1.10 The influence of beta-adrenergic antagonists on transgene expression

The treatment of most human diseases involves the use of pharmacological therapy. Given that gene therapy is essentially just an alternative means of delivering a biologically active "drug", in this case a peptide expressed from a therapeutic transgene by transfected cells, the potential exists for interactions between gene therapy agents and standard pharmacological therapies. This may have important clinical implications, particularly as patients entered into early trials of new gene therapies tend to have advanced disease refractory to standard treatment and are usually on multiple medications. One such interaction which has been reported recently is between beta-adrenergic receptor antagonists (β-blockers) and the human CMV promoter (MIEhCMV), which has been used in almost all clinical trials of cardiovascular gene therapy to date[264].

β-blockers are amongst the widely prescribed pharmaceutical agents for the treatment of cardiovascular disease. Multiple large randomised clinical trials have unequivocally demonstrated both symptomatic and prognostic benefit in patients with heart failure and following myocardial infarction, and as a result their routine use in these patient populations receives the highest level of recommendation in international guidelines[265, 266]. They are also widely used as antiarrhythmic, antianginal and antihypertensive agents. Unsurprisingly there is a very high rate of concomitant β-blocker therapy in patients enrolled in trials of cardiovascular gene therapy, with some studies reporting rates of use as high as 90%[112, 267].

The clinical effects of β-blockers occur as a result of numerous mechanisms but include alterations in gene expression mediated via the cyclic AMP system. The β-adrenergic receptor pathway represents a classic example of a second messenger system. Stimulation of β-adrenergic receptors with catecholamines results in activation of adenylyl cyclase by G proteins and an increase in intracellular adenosine-3',5'-cyclic monophosphate (cAMP). cAMP activates protein kinase A which translocates to the nucleus where it can in turn activate the transcriptional factor cAMP-response element binding protein (CREB). CREB can then bind to regions of DNA called cAMP-response elements (CRE), eight–base pair palindromic DNA sequences (TGACGTCA)

which are found upstream of many eukaryotic genes. Binding of a CBP (CREB binding protein) co-activates CREB and results in alterations in downstream gene expression[268].

Several copies of the CRE are present within both the human and murine CMV promoters (MIEhCMV and MIEmCMV)[264] and binding of CREB promotes transcription of the downstream gene. β-receptor stimulation therefore has the potential to increase transgene expression under the transcriptional regulation of these promoters via the CREB pathway and β-receptor blockade may attenuate this response.

This hypothesis was examined in a recent study by our group[264]. β-receptor stimulation with isoprenaline resulted in increased transgene expression from both MIEhCMV and MIEmCMV promoters in cultured coronary SMCs, which was inhibited by β-blockade. The effect of isoprenaline was shown to be mediated by the CREB pathway as CRE-decoy oligonucleotides inhibited the isoprenaline-induced enhancement of gene expression. This effect was then confirmed *in vivo.* Marker gene expression (*lacZ*) following adenovirus-mediated gene transfer within a porcine coronary artery model was significantly reduced in animals receiving β-blockers as compared to those receiving no β-blocker.

Although β-blockers have been demonstrated to reduce transgene expression from CMV promoters following viral gene transfer into the vascular wall, this effect has not been studied using plasmid vectors. Given that, for the reasons discussed in Section 1.4, plasmids represent a more attractive choice of vector than viruses for vascular gene therapy, it is essential to know whether this interaction also applies to plasmid-mediated transgene expression.

1.11 Research objectives

Previous work from our group has identified a potentially beneficial effect on neointima formation following adenoviral delivery of CTGF in a SVG model of restenosis. Analysis of previously prepared slides will be carried out and further CTGF infections of human saphenous veins will be performed to assess for possible mechanisms for this effect.

The next goal of this study is to improve plasmid-mediated transgene expression in vascular SMCs via expression cassette modification. Plasmids will be constructed

containing various combinations of the RE enhancer, the HE enhancer and the fragment of the smooth muscle gamma-actin (SMGA) promoter, which acts as a DNA targeting sequence. The most effective expression cassette at eliciting transgene expression will be ascertained by measurement of *in vitro* transfection of coronary arterial SMCs.

Transgene expression of both FMOD and CTGF has been shown to reduce neointimal proliferation in a vein graft *ex vivo* model. The next goal is to investigate the effects of plasmid-mediated gene expression of these two transgenes delivered via gene-eluting stents in a porcine coronary artery model.

Once the most effective expression cassette has been identified from the earlier experiments, three plasmids will be constructed using this expression cassette containing the cDNA for the therapeutic genes CTGF and FMOD, and the marker gene *lacZ* respectively. The ability of these plasmids to elicit transgene expression *in vitro* will be confirmed.

Dose finding studies will be performed *in vivo* using gene-eluting stents coated with several different doses of the plasmid encoding the *lacZ* marker gene in a pig coronary model. Stents coated with the optimal dose of plasmid identified will then be prepared for each of the three transgenes and deployed in pig coronary arteries. Following sacrifice at 28 days, morphometric assessment will identify whether there has been an effect on neointimal hyperplasia.

Further stent deployments will allow quantitation of the degree of transgene expression in the stented vessel segments using qPCR. If there is evidence of a biological effect, a variety of histological and immunohistochemical techniques will be performed to assess to what extent differences in neointimal hyperplasia are accompanied by differences in ECM deposition, reendothelialization and apoptosis.

The final goal is to investigate the effect of systemic β-blocker administration on plasmid-mediated gene expression *in vivo*. β-blockers have been shown to reduce transgene expression from CMV promoters following vascular gene transfer with viral vectors *in vivo*. It is unclear however whether this applies to plasmid-mediated gene transfer and this will be investigated in the pig coronary model using gene-eluting stents.

1.11.1 Summary of research objectives

- Further investigate mechanistic effects of adenovirus-mediated gene transfer of CTGF on neointima formation in the SVG model
- Investigate combinations of promoters to develop an improved expression cassette for plasmid-mediated transgene expression in coronary SMCs
- Construct plasmids containing the CTGF, FMOD and *lacZ* transgenes with the most efficient promoters
- Confirm the identity and function of these newly created plasmids (transfection *in vitro* and PCR)
- Prepare gene-eluting stents coated with several doses of p*lacZ*
- Confirm intact DNA elution from prepared stents
- Identify the optimal plasmid dose in eliciting marker transgene expression *in vivo* in a pig coronary artery model
- Prepare gene-eluting stents coated with the optimal dose of *lacZ*, CTGF and FMOD
- Assess the effects of CTGF and FMOD gene transfer *in vivo* in a pig coronary artery model of instent restenosis
- Assess the effects of systemic β-adrenoreceptor blockade on plasmid-mediated transgene expression *in vivo* in a pig coronary artery model

2 Methods and materials

2.1 Cell culture techniques

For *in vitro* assessment of gene transfer cell culture was performed with human coronary artery smooth muscle cells (HCSMC) and two cell lines: A-10 cells and HEK 293 cells. All work was performed under sterile conditions in a laminar flow hood in a dedicated tissue culture facility. Cell incubation was performed at 37°C with 5% CO_2. The general principles of cell culture are described below for HCSMCs and the differences are then discussed for A10 and HEK 293 cell culture.

2.1.1 Growing up and maintenance

Cryopreserved stocks of human coronary artery smooth muscle cells (TCS Cellworks, Bucks, UK) were thawed in a waterbath at 37°C. When a small amount of ice pellet was still present, the contents of the cryovial were transferred into a 15ml centrifuge tube containing 9ml of pre-warmed SMC medium (TCS Cellworks; see Appendix 6.1). The cells were pelleted by centrifugation at 1500rpm for 10 minutes, the supernatant was removed and the cells were resuspended in 6ml of SMC medium. The cell suspension was transferred into a 25cm^2 cell culture flask and incubated at 37°C with 5% CO_2.

The culture medium was changed every 48-72 hours. The old medium was aspirated and the cells were washed with pre-warmed phosphate buffered solution (PBS). The PBS was aspirated and fresh pre-warmed SMC medium was added.

Cell passage was performed when the cells reached 80-90% confluency. The old medium was removed and the cells were washed with pre-warmed PBS. 1-5ml of pre-warmed trypsin 0.25%/EDTA 0.02% (Sigma) was added and the flask was incubated at 37°C for 3-5 minutes until cell detachment had occurred. Pre-warmed SMC medium was added to neutralise the trypsin and the cell suspension was titurated to break up cell clumps. The cell suspension was divided at a ratio of 1:3 or 1:4 between 25cm^2, 75cm^2 or 175cm^2 flasks (depending on the initial flask size) before being returned to the incubator at 37°C with 5% CO_2.

2.1.2 Production of stocks

A 175cm^2 flask of SMC cells at 80-90% confluency was trypsinised and neutralised with SMC medium. The cell suspension was transferred into a sterile 15ml tube (Falcon) and the cells were pelleted by centrifugation at 1,500rpm for 10min. The supernatant was aspirated and the cell pellet resuspended in 10ml of Freezing Medium (see Appendix 6.1 for composition). The cell suspension was transferred into cryovials in 500µl aliquots. The vial was wrapped in cotton wool, placed in a polystyrene container and left in a –80°C freezer overnight. The following day the cryovial was transferred to a liquid nitrogen storage tank.

2.1.3 A-10 cells

A-10 cells (ATCC, Virginia, USA; catalogue no: CRL-1476) are a clonal cell line derived from the thoracic aorta of rat embryos and possess many of the characteristics of smooth muscle cells. In particular, they have been shown to resemble neointimal SMCs[269] and have been used in previous studies investigating vascular gene therapy for restenosis[173, 174].

Cell culture techniques were similar to the protocol above except A-10 medium was used instead of SMC medium (see Appendix 6.1 for composition).

2.1.4 HEK 293 cells

293 cells (Microbix, PD-02-01) are derived from human embryonic kidney fibroblasts. The original cell line was transformed with the E1A region from adenovirus type 5 DNA sheared by passage through a fine needle. The resultant cell line is very easy to transfect using dedicated liposome-based techniques (e.g. 293fectin, Invitrogen).

Cell culture techniques were similar to the protocol above except 293 medium was used instead of SMC medium (see Appendix 6.1 for composition).

2.2 Adenovirus-mediated gene transfer to saphenous vein graft segments

2.2.1 Adenovirus titration

The titre of stock adenovirus (Ad5-CTGF) was determined using an end-point dilution assay. $5x10^3$ 293 cells in 100µl warmed 293 medium were seeded into each well of a 96-well plate 24 hours before the titration. Serial dilutions of the viral stock were then prepared in 293 medium, starting with the 1:1000 dilution (10^{-3}) to 10^{-13}. The 293 cells were infected with the different virus dilutions as stated above with ten wells for each group. The remaining wells of the 96-well plate were used as negative controls for the presence of cytopathic effect (CPE). The plates were incubated at 37°C for 10 days with the addition of 100µl media every 3 days to prevent the pH of the medium changing or the medium evaporating. After 10 days wells were examined for the appearance of CPE. CPE-positive wells were analysed using an inverted phase-contrast microscope and the fractions of CPE-positive wells in each row were calculated. The titre was determined according to the formula: titre (pfu/ml) = $10^{(x+0.8)}$. X refers to the sum of the fractions of CPE-positive wells.

2.2.2 Surgical preparation

Harvested segments of human saphenous vein which were excess to surgical requirements were obtained from patients undergoing coronary artery bypass grafting. Side-branch ligation had already been performed. The segments were stored in organ transfer medium (see Appendix 6.1) at 4°C prior to transfer to our laboratory and processing on the day of surgical harvest.

2.2.3 Adenoviral transduction and culture of saphenous vein segments

All tissue culture steps were performed in a category 2 laminar flow cabinet using autoclaved equipment and taking all possible care to maintain sterility. The saphenous vein specimen was transferred into a 35mm tissue culture dish containing organ culture medium warmed to 37°C. The vessel was washed out with phosphate buffered saline (PBS) and cut into segments of approximately 2cm length. One end of each segment was closed with a Ligaclip (Ethicon) and nylon suture and any excess fluid was

removed from the lumen. Luminal instillation of either thawed Ad5-CTGF or Ad5-*lacZ* was performed with a dose of 1 x 10^8 plaque forming units (pfus) in 100µl of PBS and the proximal end of the segment was closed with a further Ligaclip and suture. Incubation of the segment was performed in organ culture medium at 37°C for one hour. Following this incubation period, the end clips were removed and the vessel was opened longitudinally with sterile scissors and washed with PBS. The segment was stretched and pinned onto a strip of sterile polyester gauze placed into a glass petri plate into which a 4mm layer of Sylgard 184 encapsulating resin (Dow Corning) had been cast. The opened vein was covered with fresh organ culture medium and incubated at 37°C with 5% CO_2. The culture medium was replaced every 48 hours.

2.2.4 Snap freezing of vein segments and slide preparation

Processing was performed following either three, seven or fourteen days of incubation. The segment was washed in PBS and cut into two using sterile scissors. One half was placed in a storage tube and directly snap-frozen in liquid nitrogen. The other half was placed into a 5ml syringe from which the tip had been excised and which had been filled with optimal cutting temperature compound (OCT). The syringe was snap frozen in liquid nitrogen and the OCT block was transferred to a 15ml centrifuge tube. The OCT-embedded frozen segments were cut into 12µm sections using a cryostat and placed onto Superfrost microscope slides. All specimens were stored at -80°C whilst awaiting further processing.

2.2.5 Indirect immunohistochemistry and immunofluorescence

The initial slide preparation was similar for both immunohistochemistry and immunofluorescence. Slides with mounted sections were removed from the -80°C freezer, allowed to warm to room temperature and squares were drawn around the sections with a water-repellent delimiting pen (Dako, Cambridgeshire, UK). Fixation with 10% buffered formalin (Sigma) for 15 minutes was followed by three 5 minute washes in phosphate buffered solution (PBS). Immersion in Triton-X100 0.1% was performed for 10 minutes to reduce surface tension and allow reagents to cover the whole tissue section. Following three further washes in PBS, non-specific antigen blocking was performed with 1% bovine serum albumin (BSA) in PBS for 60 minutes. The primary antibody was diluted to an appropriate concentration (see Table 2) with 1%

BSA in PBS and applied to each section. For negative control slides, 1% BSA was applied without primary antibody. The slides were incubated at 4°C overnight.

Table 2 - Antibodies used for immunohistochemistry and immunofluorescence

Type	Antibody	Dilution	Supplier (Cat no)
Primary	Rabbit anti-CTGF	1:200	Abcam (ab6992)
Primary	Rabbit anti-fibromodulin	1:200	A gift kindly provided by Dr PJ Roughley, Shriners Hospitals for Children, Canada
Secondary	Goat biotinylated anti-rabbit IgG	1:200	Vector labs (BA-1000)
Secondary	Goat anti-rabbit IgG, Cy5 conjugate, species adsorbed: human, mouse, rat	1:400	Millipore UK (AP187S)

The following day the sections were washed with PBS. For immunohistochemistry, endogenous peroxidase activity was blocked by incubation with 0.3% hydrogen peroxide in absolute methanol for 30 minutes followed by a further PBS wash. An appropriate concentration of diluted secondary antibody (biotinylated for immunohistochemistry; fluorophore-conjugated for immunofluorescence; see Table 2) was applied and the sections were incubated for 1 hour at room temperature followed by a PBS wash.

For immunohistochemistry, processing was performed with the Vectastain ABC kit (Vector laboratories, Peterborough, UK). The slides were incubated in the ABC reagent, consisting of Avidin DH and biotinylated horseradish peroxidise H, for 30 minutes followed by a PBS wash. The slides were then incubated in diaminobenzidine tetrahydrochloride (DAB, Vector labs) for 5 minutes. If nickel chloride was added the precipitate was grey/black rather than brown. The slides were washed in dH_2O and serial dehydration of the slides with increasingly concentrated alcohol solutions (50%, 70%, 90%, 100%, 100%) and two xylene washes was performed with 2 minutes

incubation in each solution. Mounting medium and a coverslip was applied to each slide.

For immunofluorescence, following secondary antibody binding, the slides were counterstained with DAPI for nuclear staining. Vectashield mounting medium (Vector labs) and a coverslip was applied and the perimeter was sealed with nail varnish.

DAB-stained sections were imaged with light microscopy. Immunofluorescent sections were imaged with a Zeiss LSM 5 Pascal confocal laser scanning microscope using two channels. Collagen autofluorescence was detected via excitation at 488nm and detection between 505-600nm. Cy5 antibody binding was detected via excitation at 633nm and detection >650nm.

2.2.6 Assessment of proteoglycan content with Alcian blue staining

Alcian blue staining was performed as previously described[270]. Frozen samples were warmed to room temperature, weighed and fixed via immersion in 100% ethanol at 4°C for 20 minutes in the original tube. Specimens were then air-dried on paper for approximately 30 minutes. The samples were immersed in 1ml Alcian Blue (0.5% w/v in 0.1M HCl) at 4°C overnight in microcentrifuge tubes. The following day, the samples were washed briefly with 70% ethanol and then immersed in 5ml guanidine hydrochloride 8M at 4° overnight. Calibration of a spectrophotometer was made using guanidine hydrochloride as a blank and absorbance of the specimens was measured at 595nm. Proteoglycan content was considered to be proportional to the A_{595}/weight.

2.2.7 Assessment of collagen content with picosirius red staining

Microscope slides had been prepared by our group containing sections of vein graft segments previously infected with either Ad5-CTGF or Ad5-*lacZ* and stained with picosirius red. The area of red birefringent staining under circularly polarised light, which is proportional to collagen content, was measured using QWindows software (Leica) and a Leica Quantimet 600S digital analysis system [111].

2.3 Manipulation and cloning of plasmid DNA

2.3.1 Restriction endonuclease digestion

All restriction endonucleases and buffers were supplied by Promega (Southampton, UK) unless otherwise specified. DNA digestion reactions were performed using the manufacturer's recommended buffer for single enzyme digests and the buffer with the best compromise of efficiency in the case of double enzyme digests. Digests were carried out in a total volume of 20µl, except for when gel extraction was planned in which case a volume of 50µl was used. Unless specified otherwise, digestion reactions were performed in a waterbath at 37°C for one hour. A typical digestion reaction would consist of:

	For diagnosis (µl)	**For extraction (µl)**
DNA	1-5 (typically 100-200ng)	1-10 (typically 2-5µg)
Buffer (10X)	2	5
Enzyme (10U/µl)	1	3
dH_2O	12-16	32-41
Total volume	20	50

2.3.2 Agarose gel electrophoresis

Following restriction enzyme digestion DNA fragments were identified and quantified using agarose gel electrophoresis. A typical 1% agarose gel was made by dissolving 500mg agarose into 50ml of 1x TAE buffer and adding ethidium bromide to intercalate DNA and allow identification of DNA fragments under ultraviolet light. 15µl of 1kb DNA ladder (Invitrogen, Paisley, UK; 15615-024) was used for DNA fragment identification and quantification; with this volume there was calculated to be 75ng DNA at the 1636bp band. Digital images were taken using the UVIpro Platinum system (UVItec, Cambridge, UK).

2.3.3 Gel extraction and purification

Following restriction enzyme digestion and gel electrophoresis, the DNA fragment of interest was excised using a scalpel blade and purified using the Qiaquick gel extraction kit (Qiagen, West Sussex, UK). This system uses a silica membrane to bind DNA in high salt buffer prior to washing and elution with ddH_2O. The procedure removes primers, nucleotides, enzymes, mineral oil, salts, agarose, ethidium bromide, and other impurities from DNA samples.

2.3.4 DNA ligation

T4 DNA ligase and the ligase buffer were supplied by Promega. The size and concentration of both the insert and vector DNA were used in the following equation to calculate the amount of each required for ligation reactions involving molar ratios of insert to vector of 1:1, 3:1 and 5:1. A typical ligation reaction would contain 100-200ng vector and be carried out in a total volume of 20µl at 4°C overnight. Restriction enzyme digested vector without insert was used as a control.

$$\text{wt. vector (ng)} \times \frac{\text{size insert (kb)}}{\text{size vector (kb)}} \times \text{molar ratio (i:v)} = \text{wt. insert (ng)}$$

Assuming the vector and insert were both identical sizes and had a concentration of 100ng/µl, a typical reaction would consist of:

Molar ratio (i:v)	**1:1 (µl)**	**3:1 (µl)**	**5:1 (µl)**	**Control (µl)**
Vector	1	1	1	1
Insert	1	3	5	0
T4 DNA ligase	1	1	1	1
Ligase buffer	2	2	2	2
ddH_2O	15	13	11	16
Total volume	20	20	20	20

Once the ligation process was complete, bacterial transformation of the plasmid DNA solutions was performed.

2.3.5 Bacterial transformation using heat shock

Transformation-competent *E. Coli* cells stored at -70°C were thawed on wet ice. 50µl of competent cells were mixed with 10µl DNA ligation reaction solution and incubated on ice for one hour. The cells were then heat shocked by immersion in a water bath at 42°C for 45 seconds. Following rapid cooling on ice for 10 minutes, 700µl of LB broth was added and the cells were incubated at 37°C with continuous shaking for one hour. 150µl of the cell suspension was then pipetted and spread over an LB-ampicillin agar plate which was incubated at 37°C overnight.

The following day, individual bacterial colonies were selected and inoculated in 5ml of LB broth containing ampicillin at a concentration of 100µg/ml. The bacteria were grown overnight at 37°C with continuous shaking prior to DNA purification the following day. Appropriate restriction enzyme digestion was then performed of the purified plasmid to identify colonies producing the correct ligation product.

2.3.6 DNA purification

Qiagen Mini-, Midi-, and Maxi-prep kits were used according to the quantity of DNA required (Qiagen). For DNA which was used in subsequent *in vitro* transfection or *in vivo* experiments EndoFree kits were used to minimise the quantity of bacterial endotoxin. All kits work on the same principle of alkaline lysis. Bacterial cells cultured under appropriate antibiotic selection were pelleted, resuspended and lysed with an alkaline buffer containing RNase A. Following neutralisation, the bacterial lysate containing chromosomal DNA, detergent, salt and proteins was cleared either via centrifugation or using a filtration unit. Plasmid DNA was bound to an anion-exchange resin under low-salt and pH conditions and RNA, proteins and low molecular weight impurities were removed with a medium-salt wash. Plasmid DNA was eluted in a high-salt buffer and then concentrated and desalted by isopropanol precipitation. For endotoxin-free purification, incubation with an endotoxin removal buffer was performed following bacterial lysate clearing.

Typical culture volumes and DNA yields were 5ml and 10-20μg DNA for a Miniprep, 100ml and 75-100μg DNA for a Midiprep, and 250ml and 250-500μg DNA for a Maxiprep.

Large scale plasmid purification for use in the *in vivo* stent experiments was performed by PlasmidFactory GmbH & Co. KG (Beilefeld, Germany).

2.4 Construction of novel plasmid expression cassettes

The previously constructed pGEG.Psi-*lacZ* plasmid was used for cloning experiments (Figure 5). This plasmid is approximately 14kb in size and has been demonstrated by our group to elicit high level transgene expression in smooth muscle cells (**unpublished data**). pGEG.Psi-*lacZ* contains an expression cassette consisting of the truncated murine MIECMV promoter, a chimeric intron consisting of the donor site from the first intron of the human beta-globin gene and the branch and acceptor site from the intron of an immunoglobulin gene (obtained from the pCI vector, Promega[157]), the transgene (*lacZ* cDNA), the Woodchuck hepatitis virus post-transcriptional regulatory element (WPRE), and the late SV40 polyadenylation signal. The plasmid also includes the *cis*-acting EBNA1 gene driven by a CAG promoter, the complementary oriP binding site for the EBNA1 protein, and the ampicillin resistance gene. The bacterial origin of replication is ColE1.

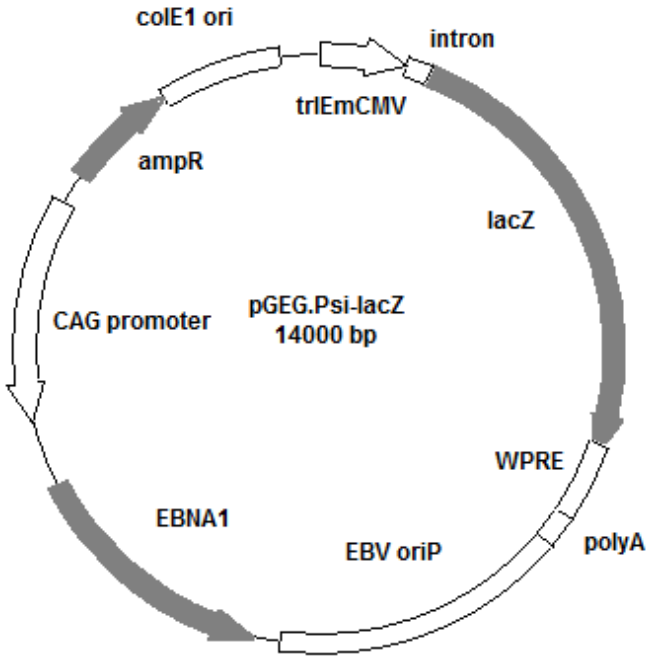

Figure 5 - Diagram of pGEG.Psi-*lacZ*

See text for description. amp^r=ampicillin resistance gene; SV40 PolyA=late SV40 polyadenylation signal; trIEmCMV=truncated murine CMV promoter

To facilitate construction of the plasmids with novel expression cassettes, a 708bp custom DNA sequence was synthesised (Genscript, New Jersey, USA). This consisted of a 176bp fragment of the chicken smooth muscle gamma-actin promoter, which has been shown to act as a DNA targeting sequence within SMCs (D), two copies of the 107bp enhancer fragment of the rabbit smooth muscle myosin heavy chain promoter (RE), and two copies of the 109bp enhancer fragment of the human VSMC α-actin promoter (HE). These elements were separated by various restriction sites to facilitate cloning experiments (see Appendix 6.3 for details).

The custom DNA sequence was ligated into the pGEG.Psi-*lacZ* plasmid immediately upstream of the MIEmCMV promoter to create pGEG-**D2RE2HE**-Psi-*lacZ*. Restriction

enzyme digestion and religation of pGEG- **D2RE2HE**-Psi-*lacZ* was performed to create six further plasmids with the following combinations of HE, RE and D (see Appendix 6.3.2 for specific cloning protocol).

pGEG- **2RE2HE** –Psi-*lacZ*

pGEG- **D2HE** –Psi-*lacZ*

pGEG- **D2RE** –Psi-*lacZ*

pGEG- **DREHE** –Psi-*lacZ*

pGEG- **DRE** –Psi-*lacZ*

pGEG- **D** –Psi-*lacZ*

Following cloning and purification, plasmid identities were confirmed by restriction digests.

2.5 Assessment of transgene expression in vitro

Two methods of cell transfection were used to assess transgene expression *in vitro*: liposome-mediated transfection (or lipofection) and electroporation.

2.5.1 Smooth muscle cell transfection

2.5.1.1 Liposome-mediated transfection

Liposome-mediated transfection (lipofection) uses proprietary cationic liposomes which can electostatically bond with negatively charged pDNA. These complexes are also positively charged which enhances cellular uptake via electrostatic interaction with the negatively charged cell membrane.

The success of liposome-mediated transfection is highly dependent on the cell-type studied. Original studies showed extremely poor gene transfer efficiency using this

technique in vascular wall cells, including VSMCs[271]. For instance, in a study using rat VSMCs only 5% of cells transfected successfully as compared with 50% of COS-7 cells[272]. Serum-free medium may increase the effectiveness of liposomal gene delivery[273] and optimising conditions, particularly the liposome formulation and liposome:DNA ratio, has been reported to improve the transfection rate in VSMCs to approximately 50%[274].

On the day prior to transfection, cells were trypsinised and counted. $3x10^5$ cells were seeded into each well of a 6-well plate and returned to the incubator overnight to give approximately 90% confluency on the following day. As transfection with plasmids encoding for the *lacZ* transgene was to be assessed by visual inspection of X-gal, a cell monolayer on the base of the well was sufficient. However assessment of transgene expression of the therapeutic genes CTGF and FMOD required indirect immunocytochemistry and therefore a collagen-coated coverslip (BD BioCoat Cellware coated with rat tail collagen type I (BD Biosciences, Bedford MA; cat no: 354089) was placed into each well of the 6-well plate prior to cell seeding and lipofection.

On the day of transfection the cells in the 6-well plate were washed with PBS, 800µl of pre-warmed OptiMEM I reduced serum media (Invitrogen; #51985-026) was added to each well and the plate was returned to the incubator.

The following solutions were then prepared for each transfection experiment: 2µg plasmid was made up to 100µl with OptiMEM, and an appropriate amount of lipofectamine solution (depending on the cell-type to be transfected) was added to 100µl OptiMEM. For HEK-293 cells 10µl of 293fectin was used; for A10 cells 6µl of Lipofectamine LTX and 2µl of PLUS reagent was used (both Invitrogen).

These two solutions were allowed to stand for 5 minutes at room temperature and then mixed together. The resultant solution was left to incubate at room temperature for 30 minutes to allow DNA-lipofectamine complexes to form. Each lipofectamine-DNA mixture was added to one well of the 6-well plate and the plate was returned to the incubator for 5-6 hours.

Following transfection the cells were washed again with PBS, 2ml of the appropriate culture medium was added to each well and the plate was returned to the incubator. Transfection efficacy was assessed at 24-48 hours.

2.5.1.2 Nucleofection

In order to quantify the gene transfer efficiency of the novel expression cassettes, HCSMC transfection experiments were conducted *in vitro*.

Electroporation was performed with Amaxa's Nucleofector technology (Lonza Cologne AG, Germany) which uses a combination of optimised electrical parameters generated by a Nucleofector device and cell-type specific reagents to allow efficient DNA transfer into the cytoplasm and nucleus. Nucleofection allows efficient transfection of both dividing and quiescent cells.

Briefly, the nucleofection protocol was as follows. Human coronary artery smooth muscle cells were cultivated as described in the previous section to approximately 70-80% confluency and harvested by trypsinisation. A cell count was performed with a haemocytometer and an appropriate volume was centrifuged at 100g for 1 minute and resuspended in Nucleofector solution to make a final concentration of 0.5-1 x 10^6 cells/100µl. 100µl of this cell suspension was mixed with 1-5µg plasmid DNA and transferred to a cuvette. The cuvette was placed in the Nucleofector device and the A-33 programme was run. Following nucleofection, 500µl of pre-warmed SMC medium was added to the cuvette and the suspension was aspirated and seeded into 3 wells of one 6-well plate. The cells were incubated at 37°C with 5% CO_2 and the medium was changed at 18 hours post-nucleofection.

At 72 hours, the cells were washed with PBS and 500µl of cell lysis buffer was added to each well (see Appendix 6.1). The lysed cells were transferred to a microcentrifuge tube and stored at -20°C in preparation for β-galactosidase and total protein assays.

2.5.2 β-galactosidase assay

β-galactosidase activity can be assayed by addition of a synthetic sugar, o-nitrophenol-β-D-galactopyranoside (ONPG). β-galactosidase cleaves ONPG into galactose and o-

nitrophenol (ONP), which is a yellow colour and can be quantified using a spectrophotometer. Enzyme activity is directly proportional to the absorbance at 420nm.

The following solutions were placed into a microcentrifuge tube on ice:

ONPG 4mg/ml in PBS (substrate)	100µl
10mM $MgCl_2$/0.45M β-mercaptoethanol (buffer)	45µl
Lysed cell sample, diluted with PBS	345µl

The tubes were incubated at 37°C for one hour. The reaction was terminated with the addition of 510µl of 1M Na_2CO_3, which denatures ONPG and renders it inactive. A blank sample was prepared to control for spontaneous lysis of ONPG, which used the above solutions but cell lysis buffer diluted with PBS instead of the lysed cell sample. Samples were transferred to cuvettes and absorbance was measured at 420nm using a spectrophotometer.

2.5.3 Protein assay

The BCA protein assay reagent kit was used (Pierce, Illinois, USA) which is based on bicinchoninic acid (BCA) for the colorimetric detection and quantitation of total protein. Cu^{2+} is reduced to Cu^{1+} by protein in an alkaline medium. Cu^{1+} is then detected using a reagent containing BCA, with two molecules of BCA chelating with one cuprous ion to form a purple-coloured reaction product.

A set of cuvettes were prepared containing known protein concentrations to create a standard protein curve. Blank samples consisted of the cell lysis buffer alone. The BCA working reagent was prepared by mixing 50 parts of reagent A with 1 part of reagent B. 25µl of each standard or unknown sample was pipetted into a pair of wells on a 96-well microplate and 200µl of the working reagent was added to each well and mixed thoroughly. Two wells were prepared for each sample. The plate was incubated at 37°C for 30 minutes and then cooled to room temperature. Absorbance was measured at 570nm on a plate reader.

The average 570nm absorbance measurement of the blank samples was subtracted from each of the standard and unknown sample measurements. A standard curve was plotted using the known protein concentrations and the blank-corrected 570nm measurements.

2.5.4 Calculation of transgene expression

The β-galactosidase activity (which is proportional the 420nm absorbance) was divided by the protein concentration (which is proportional to the 570nm absorbance) for each sample to give an estimation of expression of the *lacZ* gene per cell. This calculation gives an estimation of the β-galactosidase activity controlled for protein content but does not have a meaningful unit of measurement as it is a ratio of absorbances. The mean of the values from the three wells prepared for each plasmid nucleofection was then calculated.

2.6 Construction of plasmids for use in vivo

Plasmids encoding for the *lacZ*, CTGF and FMOD genes with the expression cassette identified by the experiments detailed in section 2.5 to result in the greatest transgene expression in human coronary smooth muscle cells (pGEG-2RE2HE-Psi) were required for the *in vivo* experiments. Following cloning, large scale plasmid purification of the three plasmids was performed by PlasmidFactory.

2.6.1 Cloning strategy for *lacZ* encoding plasmid

pGEG-2RE2HE-Psi-*lacZ* was constructed as part of the experiments investigating expression cassette optimisation (see Section 2.4, Appendix 6.3.2 and Figure 6).

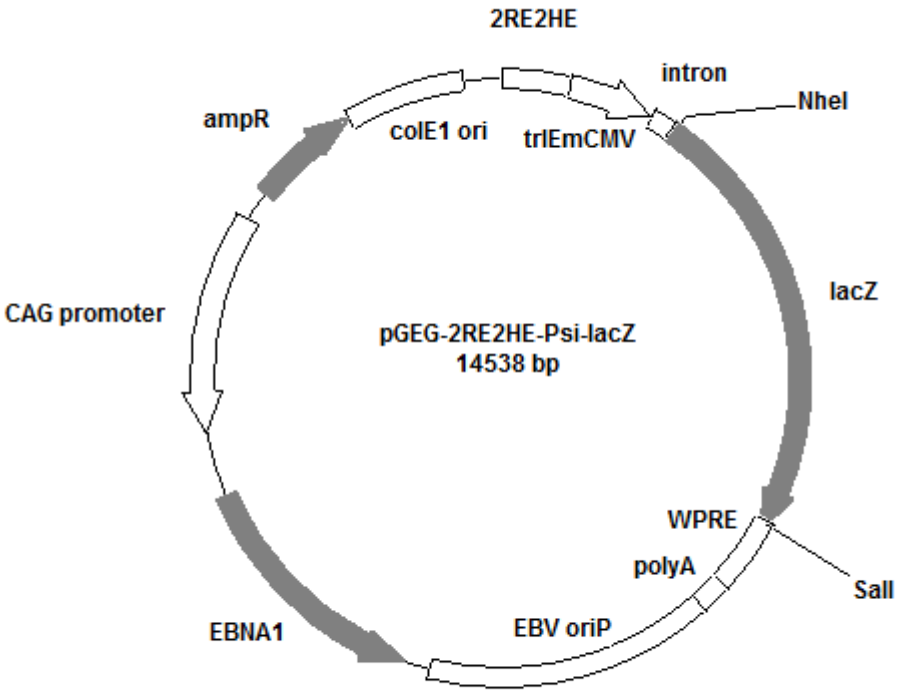

Figure 6 – Diagram of pGEG-2RE2HE-Psi-*lacZ*

2.6.2 Cloning strategy for CTGF encoding plasmid

A plasmid encoding for the human CTGF consensus coding DNA sequence (CCDNS; see Appendix 6.4.1 for DNA sequence), pΔE1CI-CTGF, was kindly provided by Dr Kingston (see Figure 7) and the CTGF transgene was removed via digestion with SalI and NheI. pGEG-2RE2HE-Psi-*lacZ* (Figure 6) was also digested with SalI and NheI to remove the *lacZ* transgene. The CTGF transgene was then ligated into this backbone to create pGEG-2RE2HE-Psi-CTGF (Figure 8), preserving the NheI and SalI sites.

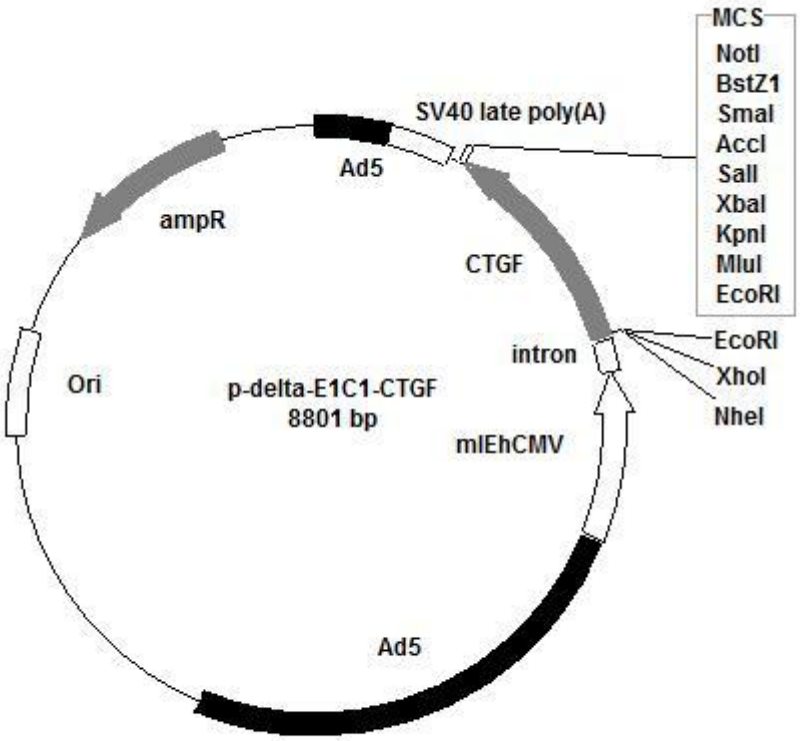

Figure 7 – Diagram of intermediary plasmid pΔE1CI-CTGF

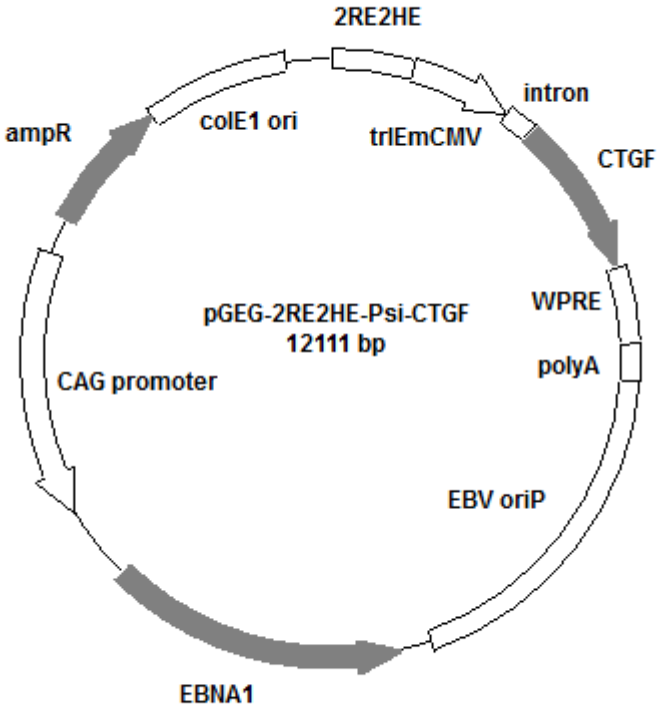

Figure 8 – Diagram of pGEG-2RE2HE-Psi-CTGF

2.6.3 Cloning strategy for fibromodulin encoding plasmid

Insertion of the FMOD transgene into the pGEG-2RE2HE-Psi backbone was considerably more complex than insertion of CTGF due to the paucity of convenient RE sites. Custom oligonucleotides and an intermediary plasmid were required to facilitate cloning.

A shuttle vector, pCI (Figure 9), was digested with HindIII, which cut a single restriction site 749bp into the CMV promoter, and NotI, which cut at a single RE site in the MCS, to remove a 350bp fragment.

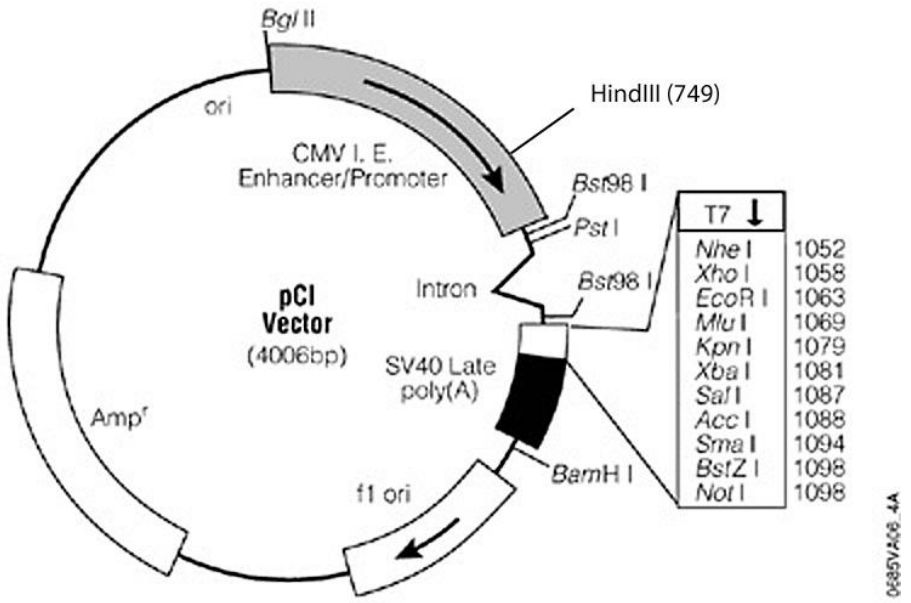

Figure 9 – Diagram of pCI shuttle vector

Two 30bp custom complementary oligonucleotides were ordered (Sigma-Aldrich Ltd, Poole, UK) and annealed using a PCR machine to create a polylinker. Table 3 shows the RE sites in the polylinker. The 5' end was designed to be compatible with a digested HindIII sticky end but not regenerate a new RE site, and the 3' end was designed to be compatible with a digested NotI sticky end but again not to regenerate a new RE site. This polylinker was ligated into the pCI backbone to create pCI-polylinker.

Table 3 – Oligonucleotides used to facilitate cloning of fibromodulin encoding plasmid

Strand 1	agc-tctaga-agctt-aaaaaa-gctag-ctcga
Strand 2	ggc-ctcgag-ctagc-tttttt-aagct-tctag
Annealed product	agc-tctaga-agctt-aaaaaa-gctag-ctcga gatct-tcgaa-tttttt-cgatc-gagctc-cgg
RE sites	**HindIII** – XbaI – HindIII – NheI –XhoI –**NotI**

Bold type indicates RE sites that the polylinker is compatible with but which do not reconstitute on binding.

pCI-polylinker was digested with HindIII and NheI. A plasmid containing bovine fibromodulin cDNA (see Appendix 6.4.2 for DNA sequence), pΔPREK1-FMOD, was kindly provided by Dr PA Kingston (Figure 10). Digestion was performed with HindIII and XbaI to remove the FMOD gene. The XbaI sticky end on the FMOD transgene is compatible with NheI allowing the FMOD gene to be ligated into the digested pCI-polylinker to create pCI-FMOD. Ligation of XbaI and NheI does not regenerate a new RE site.

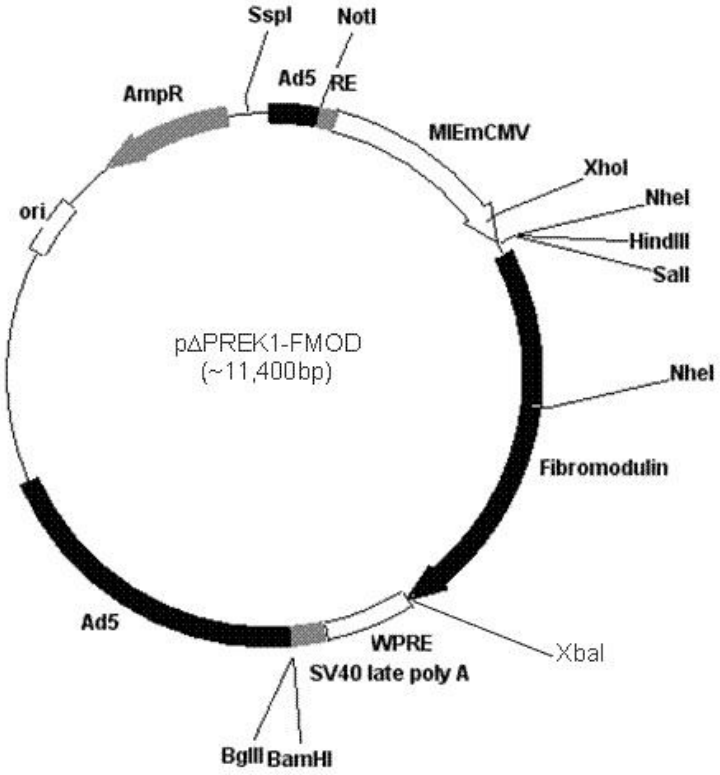

Figure 10 – Diagram of pΔPREK1-FMOD

The FMOD gene was then removed from pCI-FMOD with digestion by XbaI and XhoI (which were added with the polylinker). The *lacZ* gene was then removed from pGEG-2RE2HE-Psi-*lacZ* with NheI and SalI digestion (see Figure 6). NheI sticky ends are compatible with XbaI, and XhoI sticky ends are compatible with SalI, although neither binding regenerates an RE site. This allowed the FMOD gene to be ligated into the pGEG-2RE2HE-Psi backbone to create pGEG-2RE2HE-Psi-FMOD (Figure 11).

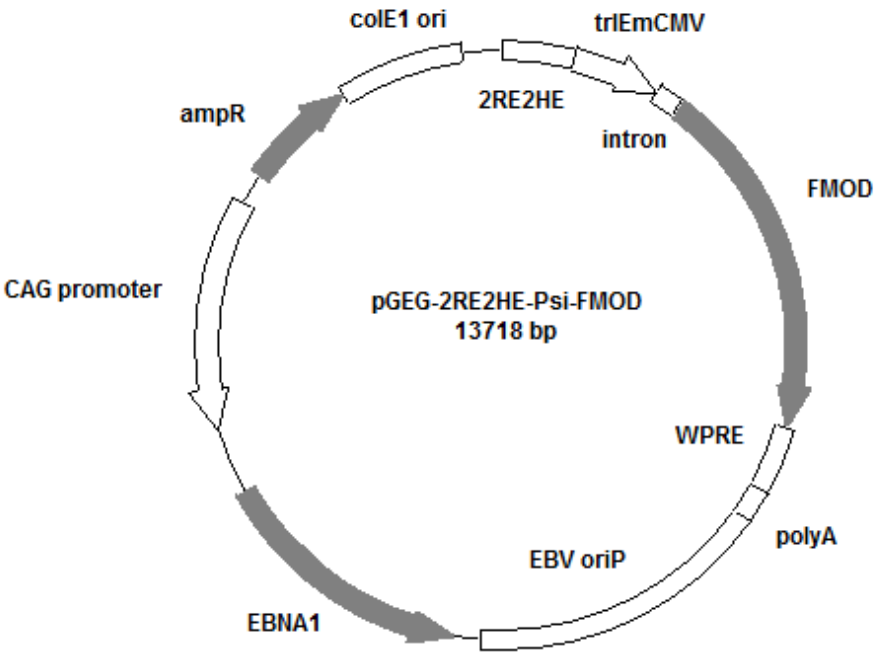

Figure 11 – Diagram of pGEG-2RE2HE-Psi-FMOD

2.6.4 Confirmation of identity and function of plasmids

Following cloning and purification, the identity of the three plasmids planned for use *in vivo* was confirmed by restriction digests, polymerase chain reaction and by transfection *in vitro*.

2.6.4.1 Polymerase chain reaction

The polymerase chain reaction (PCR) amplifies a small quantity of a specific piece of DNA by several orders of magnitude. Two primer oligonucleotides, which contain sequences complementary to two target regions at either end of the DNA segment of interest, and a DNA polymerase are required. Thermal cycling in a PCR machine with multiple cycles of DNA melting, annealing and elongation results in a chain reaction in which the DNA template is exponentially amplified.

PCR was performed to confirm the identity of the newly constructed FMOD and CTGF plasmids. Custom primers for the CTGF and FMOD transgenes were designed (Invitrogen; Table 4) to give expected bands of 1003bp (CTGF) and 1020bp (FMOD). The binding sites for these primers are illustrated in Appendix 6.4.The four primers were each designed to have an approximate melting temperature (Tm) of 55°C. The concentration of primers and annealing temperature were optimised with a series of PCR experiments to minimise non-specific binding.

Table 4 – CTGF and FMOD PCR primers

CTGF forward	5' - ccg ccg cca gta tgg gc - 3'
CTGF reverse	5' - aag atg tca ttg tct ccg gg - 3'
FMOD forward	5' - ctc cct ctc ctg ggc cc - 3'
FMOD reverse	5' - tcg ttg cca tcc agg cgc - 3'

A typical 50µl PCR reaction mix would consist of:

	Concentration	Volume (µl)	Final concentration
PCR nucleotide mix (#C1141; Promega)	10mM each	1	0.2mM each dNTP
GoTaq DNA polymerase (#M3171; Promega)	5u/µl	0.25	1.25u
Upstream primer	Variable	5	0.1-1µM
Downstream primer	Variable	5	0.1-1µM
Template DNA	Variable	5	<0.5µg/50µl
GoTaq green reaction buffer	5X	10	1X
dH_2O		23.75	

A typical PCR reaction was as follows:

1.	Denature	95°C	5min
2.	Denature	95°C	15s
3.	Anneal	Variable	15s
4.	Elongate	72°C	1min 30s (approx 1min/kb extension)

(Steps 2-4 repeated X30)

5.	Final elongation	72°C	10min
6.	Hold	4°C	∞

PCR was then performed with the original plasmids from which the transgenes were derived and with the newly constructed plasmids.

2.6.4.2 Confirmation of transfection *in vitro*

The ability of the three plasmids to transfect cells and produce the desired transgene was assessed in both 293 cells and A10 cells using liposome-mediated transfection in 6-well plates as described in section 2.5.1.1. Transfection efficiency was assessed at 24-48 hours.

For the *lacZ* encoding plasmid, successful transfection and production of the transgene was assessed with X-gal staining of the wells using the same technique detailed in section 2.8.3.1.

For the FMOD and CTGF encoding plasmids, successful transgene production was confirmed with indirect immunocytochemistry and immunofluorescence with similar methodology to section 2.2.5. Briefly, the culture medium was carefully aspirated from

the well and the cells were washed with PBS taking care not to disrupt the cell monolayer on the collagen coated coverslip. The cells were fixed with 4% paraformaldehyde for 15 minutes, washed with PBS, permeabilised with 0.1% Triton X-100 for 10 minutes and washed again with PBS. Non-specific antibody binding was blocked with a 30 minute incubation in 1% BSA. A strip of parafilm was placed on the lid of the 6-well plate and 60µl of the appropriate primary antibody (diluted in 1% BSA – see Table 2) was spotted for each coverslip. Each coverslip was removed from its well and placed monolayer down onto the spot of primary antibody. The coverslips were placed in a humid box and left at 4°C overnight.

The following day the coverslips were returned to their wells and washed with PBS. The appropriate secondary antibody (Cy5 for immunofluorescence – see Table 2) was spotted onto a strip of parafilm and the coverslips were again placed monolayer down onto the spot. The coverslips were placed in a humid box at room temperature for 1 hour followed by a further PBS wash. Nuclear counterstaining was performed with DAPI (4'-6-Diamidino-2-phenylindole, Sigma) which forms fluorescent complexes with natural double-stranded DNA. The coverslips were coated with DAPI for 15 minutes. The coverslips were then briefly dipped in dH_2O, blotted dry and placed with the cell monolayer down onto a microscope slide spotted with Vectashield mounting medium (Vector labs). The perimeter was sealed with clear nail varnish and the slides were stored in the dark at 4°C.

The slides were imaged with a Zeiss LSM 5 Pascal confocal laser scanning microscope using two channels. The first channel utilised a mercury lamp to assess nuclear staining (pseudoDAPI mode) and the second channel assessed Cy5 antibody binding with excitation at 633nm and detection at >650nm.

2.7 Development of gene-eluting stents

Dr Kingston (Vascular Gene Therapy Unit, University of Manchester) had formed a research agreement with Medtronic, Inc. (Minneapolis, MN, USA) who had committed to provide polymer-plasmid coated coronary stents for use within our *in vivo* experiments. Shortly after the research project commenced Medtronic's European interventional cardiology division unexpectedly closed, which led to considerable uncertainty as to whether the company would be able to provide the stents within an

appropriate timescale for the research to be completed in. There was initially therefore no choice but to investigate alternative methods of coating stents with a polymer-plasmid mixture.

2.7.1 Method 1: coating with polyvinyl alcohol/plasmid mix

This method has been previously described by Egashira and colleagues[178] and their protocol was kindly provided by Professor Egashira (Kyushu University, Fukuoka, Japan):

	conc.	amount（μl）	final conc.
PVA	5%	810	2.31%
plasmid		500	
heparin		125	
TC-310	40%wt	36.5	0.83%
EtOH	100%	280	
		1751.5	

Polyvinyl alcohol in the form of GOHSENOL EG-05 was obtained (Nippon Gohsei, Inc. Osaka, Japan) and a 5% solution was mixed slowly with plasmid to dissolve. The heparin and TC-310 (titanium sulphate to act as a cross-linking agent) were added followed by alcohol.

Dip-coating of stents with this solution was attempted in our laboratory. However this lead to an uneven coat of polymer with marked webbing between the stent struts. There was no easy way of controlling the amount of polymer mixture (and hence plasmid) on each stent.

It was decided that this was process was impractical for *in vivo* experiments and was therefore not investigated further; a commercial polymer company with experience in coating coronary stents was approached.

2.7.2 Method 2: dip-coating with urethane/plasmid mix

Preparation of stents by this technique was performed by Surface Solutions Laboratories, Inc. (Carlisle, MA, USA). Surface Solutions provided the stents used previously in the gene-eluting stent experiments performed by Takahashi and colleagues[137].

3x16mm stainless steel coronary stents (Boston Scientific; Natick, MA, USA) were dip-coated with a solution containing 17.6% w/w plasmid DNA and a hydrophilic urethane polymer and allowed to dry. Three weights of coating were obtained by dipping 3 times, 5 times and 7 times giving an estimated weight of plasmid DNA of approximately 260µg, 350µg, and 720µg respectively.

These experiments were performed prior to the development of the plasmids designed for use *in vivo*. Therefore a plasmid previously constructed by our group (pGEG-PRIK-*lacZ*; ~14kb) was used.

A sample stent manufactured by Surface Solutions is shown in Figure 12. It can be seen that, although the polymer application appears uniform throughout the length of the stent there is considerable webbing between the stent struts.

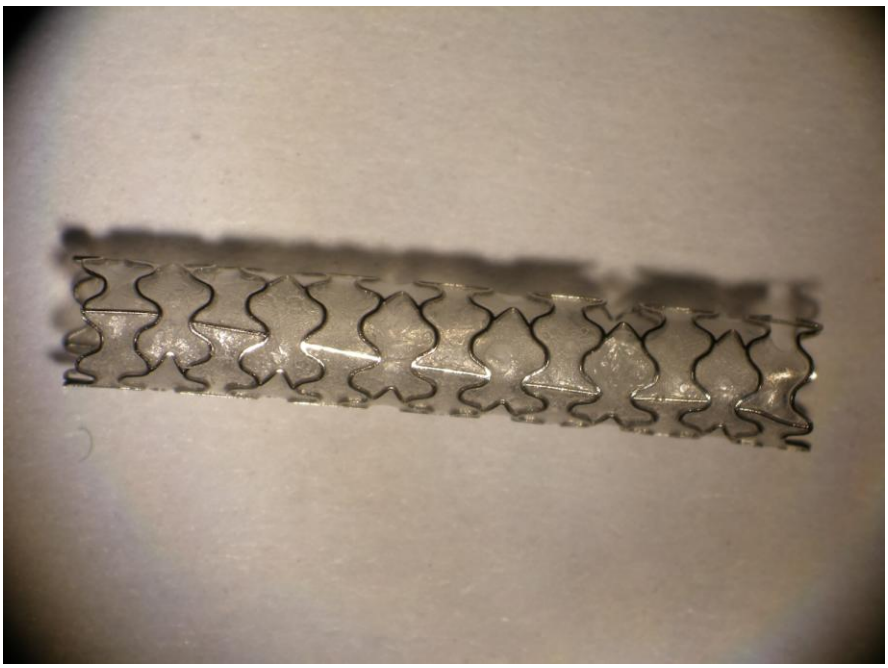

Figure 12 – Polymer-plasmid coated coronary stent prepared by Surface Solutions

Plasmid elution was assessed by incubation in TE buffer at 37 degrees with constant shaking. The buffer was changed at various time intervals and DNA concentration was quantified using a Nanodrop spectrophotometer (Thermo Scientific). Restriction digests were performed to confirm intact plasmid elution.

These stents were investigated *in vivo*. Stents were deployed into both the LAD and Cx coronary arteries of four pigs as described in Section 2.8. In total, four stents coated with a plasmid-polymer mixture (pGEG-PRIK-*lacZ*) and four stents coated with polymer mixture alone were deployed. Following sacrifice at 7 days, en face X-gal staining was performed as described in Section 2.8.3.1.

2.7.3 Method 3: spray-coating of polymer and poragen followed by dip-coating in plasmid solution

After several months of discussion, Medtronic finally agreed to perform the plasmid-eluting stent preparation at their World headquarters in Minneapolis, USA. These stents were therefore used for the *in vivo* work, as they were ready in time for the main experiments to be completed, and were of a substantially higher quality than those produced by the alternative methods described above. The technique Medtronic used is briefly described below. However this process was of a proprietary nature and we were not party to the full details of the polymer used or the coating method.

3.5 x 15mm stainless steel stents were spray-coated with a primer coat and a polymer coating containing a poragen. The stents were then soaked in water to allow the poragen to dissolve and create a porous coating. A solution containing the plasmid was leached into the pores, which were closed with gentle heating. For the dosing experiments the *lacZ*-eluting plasmid containing the expression cassette which was found to elicit the maximal transgene expression was applied to stents at one of three theoretical loading doses: 100μg, 200μg and 400μg DNA. The dose which provided the highest gene expression would then be used for the subsequent therapeutic experiments.

Figure 13 illustrates one of the polymer-plasmid coated stents provided by Medtronic. Although the stents prepared by Medtronic and Surface Solutions were all stainless steel, the Medtronic stent struts appear white whilst the Surface Solutions struts still appear metallic (Figure 12). This indicates there is considerably more polymer coating

on the Medtronic stents. As with the Surface Solutions stents, there is a fine polymer webbing which can be seen between some of the stent struts.

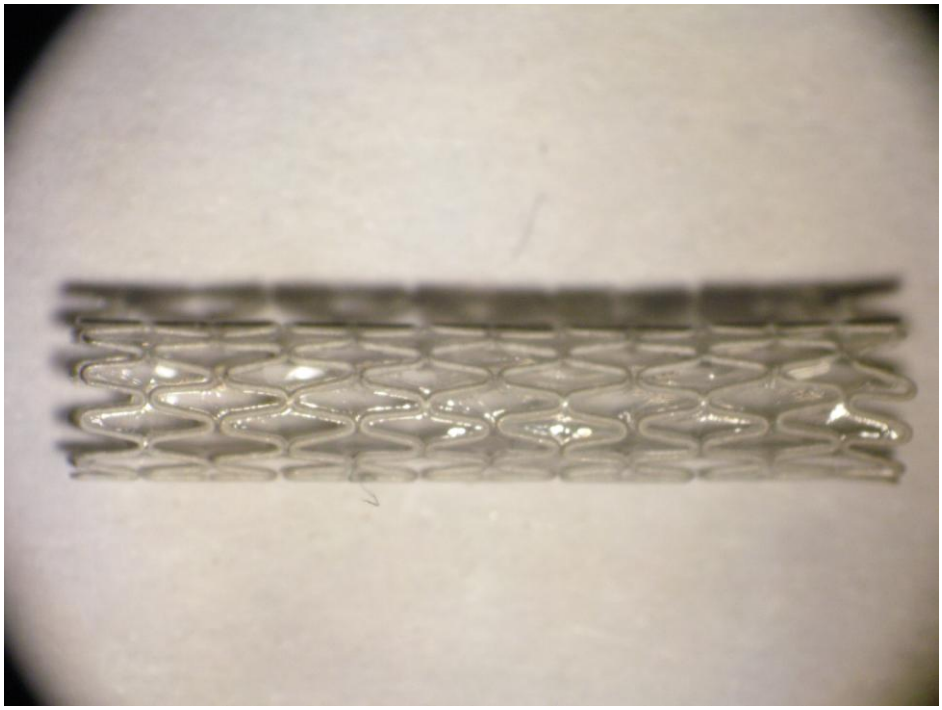

Figure 13 – Polymer-plasmid coated coronary stent prepared by Medtronic

DNA elution was assessed by Medtronic in the USA. The stents were incubated in PBS at 37 °C with constant shaking and then DNA concentration was quantified using the Quant-iT Picogreen dsDNA assay kit (Invitrogen).

Once the stents had been delivered, DNA elution was rechecked in our laboratory by incubation of stents in TE buffer and quantification with a Nanodrop spectrophotometer as described for Method 2. Restriction digests were then performed to confirm intact plasmid elution.

2.8 Assessment of in vivo action of gene-eluting stents

2.8.1 Stent deployment procedure

Juvenile male large white pigs of approximately 20-25kg weight were obtained commercially and housed in the University of Manchester Biological Services Facility. All surgical procedures conformed to the UK Animals (Scientific Procedures) Act 1986 and were authorised by the Home Office.

To reduce the risk of stent thrombosis, dual antiplatelet therapy (aspirin 150mg and clopidogrel 150mg) was administered on the day prior to the procedure and on the day of the procedure itself[275]. Aspirin 75mg and clopidogrel 75mg were then continued daily following the procedure until the time of sacrifice.

2.8.1.1 General anaesthesia

Induction of anaesthesia was obtained via inhalation of nitrous oxide (2L/min), oxygen (4L/min) and 4% isoflurane (Abbot Laboratories). Following application of lidocaine spray to the larynx to reduce the risk of laryngospasm, endotracheal intubation was performed and the tube was secured (Figure 14). General anaesthesia was maintained using 2.5% isoflurane and oxygen (4L/min) via the gas circuit of an anaesthetic machine. During the procedure electrocardiograph and arterial oxygen saturation readings were continually monitored.

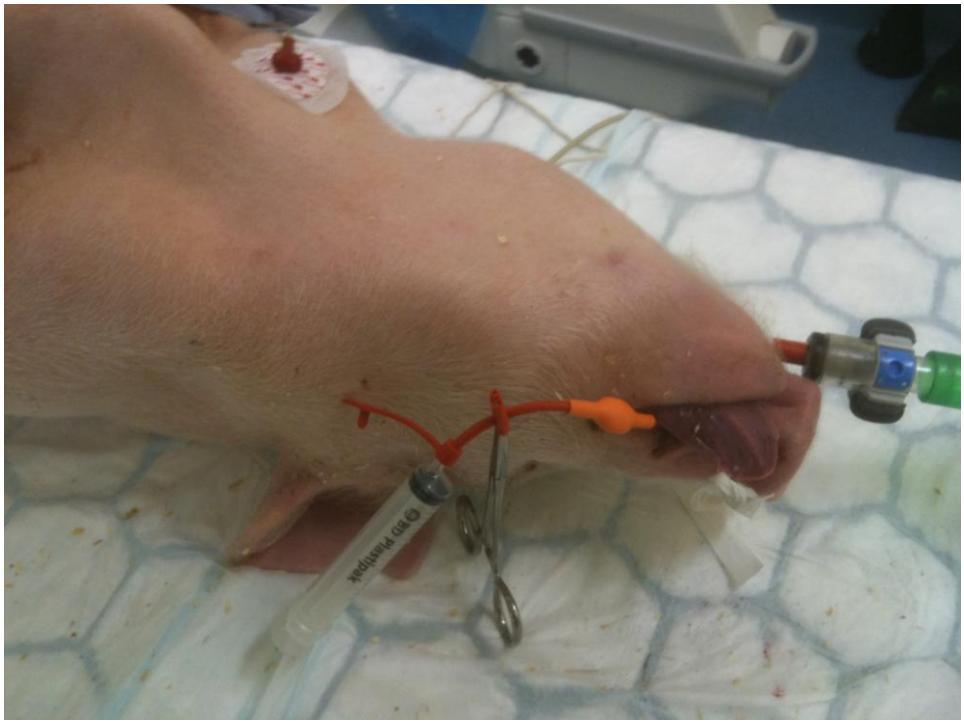

Figure 14 – Pig following induction of general anaesthesia and tracheal intubation

2.8.1.2 Coronary catheterisation and stent deployment

Full aseptic technique was adhered to throughout the procedure. The surgical site was cleansed with chlorhexidine solution and a 5cm left paratracheal incision was made midway between the xiphisternum and the left mandibular angle. The left carotid artery was identified and mobilised using blunt dissection. The artery was tied off cranially with an 0 gauge silk suture (Johnson & Johnson) and a further silk suture was applied loosely to the proximal artery to allow closure at the end of the procedure. Arterial access was obtained using a 7 French safe sheath inserted via the Seldinger technique and 5000 Units of heparin was administered intra-arterially for periprocedural anticoagulation. Anti-arrhythmic agents were not given routinely.

A 7 French guide catheter, either an Extra Backup (EBU) 3.5 or Judkins right 4 (JR4) catheter (Guidant) was passed into the left main stem of the left coronary artery. Diagnostic angiograms were obtained during selective injection of contrast medium (Omnipaque 350; GE Healthcare) via fluoroscopy with an OEC Cardiac 9600 image intensifier (GE Medical Systems). Typically right anterior oblique 30° (RAO) and left anterior oblique 30° (LAO) views would be sufficient to identify suitable coronary artery segments for stent deployment: in most cases the proximal segments of either the left anterior descending (LAD) or proximal circumflex (Cx) coronary arteries were used. Segments without side-branches were preferred to reduce the risk of side-branch occlusion and periprocedural myocardial infarction. A 0.014” BMW guide wire (Guidant) was passed into the distal coronary artery and the stent (which had been crimped onto a monorail balloon system) was passed over the wire to the target vessel segment. The stent was deployed by balloon inflation to between 8 and 18 Atm of pressure depending on the experimental protocol and vessel size. Following stent deployment, the balloon was deflated and removed and an angiogram was obtained to confirm that there were no vascular complications such as vessel dissection or intracoronary thrombus. Quantitative coronary angiography (QCA) was performed during the therapeutic studies prior and following stent deployment. The steps of the stent deployment procedure are illustrated in Figure 15.

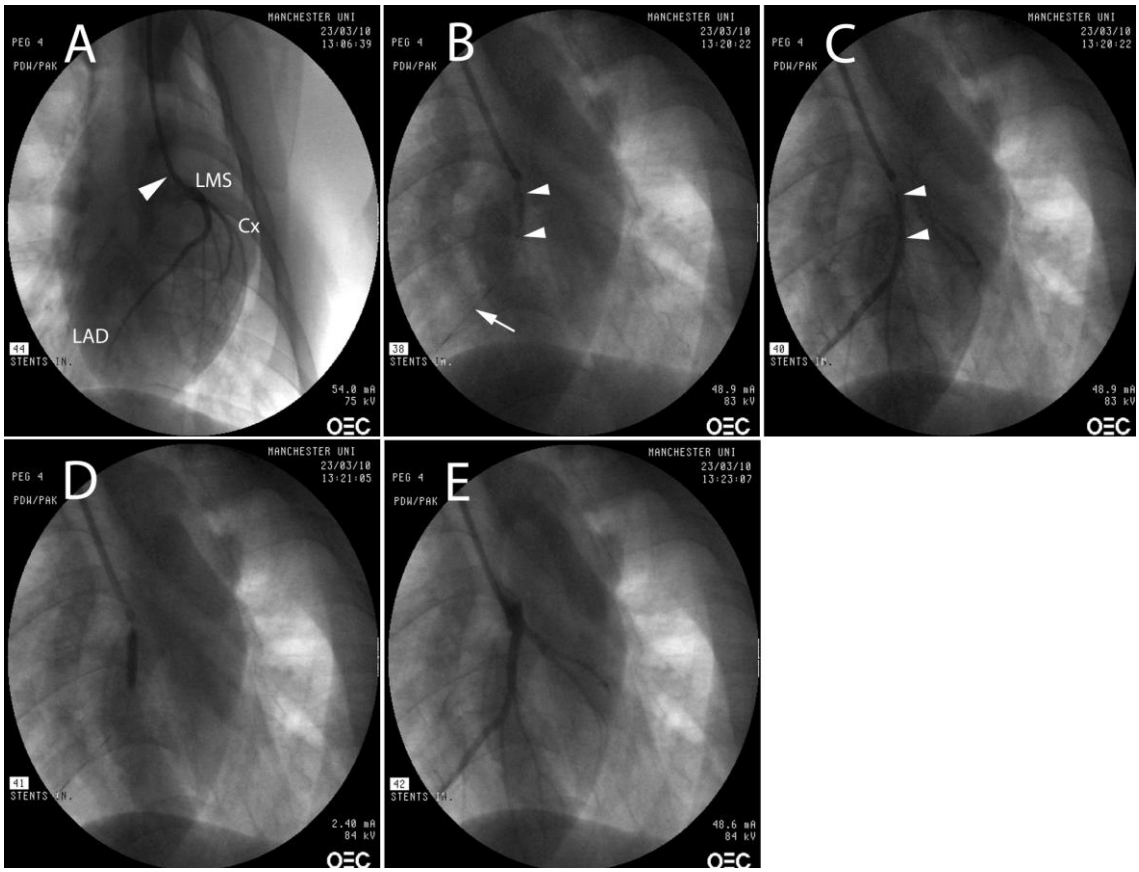

Figure 15 – Coronary angiograms demonstrating stent deployment procedure

Panel A illustrates a right anterior oblique (RAO) coronary angiogram with the guide catheter (arrowhead) sitting in the ostium of the left main stem (LMS) of the left coronary artery which subsequently bifurcates into the left anterior descending (LAD) and circumflex (Cx) arteries. Panels B and C show stent positioning before and after contrast injection: a guidewire is passed into the distal LAD (arrow) and the stent balloon, with radioopaque markers at each end (arrowheads), is placed in the target vessel segment. The stent is subsequently deployed by balloon inflation (panel D). Following balloon removal a final angiogram is taken to ensure there are no vascular complications (panel E).

Following all stent deployments, the arterial sheath was withdrawn and the 0 gauge silk suture applied to the proximal carotid artery was tied off to achieve haemostasis. The wound was closed in layers using an 0 gauge absorbable Vicryl suture (Johnson & Johnson). Intramuscular buprenorphine was given at the end of the procedure for post-operative analgesia.

The inhalational anaesthetic agents were stopped, the animal was transferred back to the housing area, and the endotracheal tube was removed. The animal was closely observed during recovery and then remained in the housing area until the time of sacrifice.

2.8.2 Sacrifice and extraction of stented coronary artery segments

Induction of anaesthesia was obtained via inhalational agents as previously described. For the therapeutic studies, repeat coronary angiography was performed via a right carotid artery cutdown as described in the previous section. Euthanasia was achieved with a bolus injection of 100mg/kg of pentobarbitone sodium 20% (Animalcare Ltd, York), either administered directly into the arterial catheter or into an ear vein cannula if repeat angiography was not performed.

A left thoracotomy was performed via an incision along the left parasternal border which was extended at each end via two intercostal incisions. The rib segment was then everted to allow easy access to the thoracic cavity. The visceral and parietal pericardium was stripped from the surface of the heart and the heart was mobilised. The intracoronary stents could then be identified by gentle palpation. Traction was applied to the heart, avoiding applying any pressure to the stents, and the great vessels were cut with scissors allowing removal of the whole heart from the thoracic cavity.

2.8.2.1 Removal and storage of stented segments

The following steps were performed for tissue analysis experiments. Following heart extraction, the stented segments were carefully dissected out and any excess adventitial fat was removed. The vessel segment was cut longitudinally through both the vessel wall and stent with scissors and then opened to expose the luminal surface. This allowed the stent to be carefully removed with forceps.

The segment could then be divided and either directly snap frozen in liquid N_2 or embedded in OCT solution and then snap frozen in liquid N_2. The segments were stored in a freezer at -80°C until further processing was performed.

2.8.2.2 Pressure perfusion of coronary artery segments

For the therapeutic studies, which required cross-sectional morphometric analysis of the stented segments, pressure perfusion with formaldehyde was performed to ensure that the coronary arteries were fixed at a similar diameter to that seen *in vivo.*

The heart was transferred to a fume cupboard immediately following extraction. The connection end of a venous giving set was placed into the aortic root and a seal created around the plastic tubing with several artery forceps. 110ml of 37-41% formaldehyde solution was injected into a 1 litre bag of 0.9% normal saline to make a 4% formaldehyde solution. This bag was placed into a pressure cuff inflated to 100mmHg pressure and connected to the giving set to deliver formaldehyde to the aortic root, and hence to the coronary arteries, at approximately physiological arterial pressure. Following delivery of 1 litre of 4% formaldehyde over approximately 15 minutes, the stented arterial segment was dissected out with a scalpel and stored in a 50ml tube containing 4% formaldehyde at room temperature until further processing was performed.

2.8.3 Processing of stented coronary artery segments

2.8.3.1 X-gal stain for visual assessment of β-galactosidase activity

X-gal staining can be used to assess expression of the β-galactosidase protein by *lacZ* transfected cells. It can be performed on whole tissue segments en face, or on coronary artery sections which had been cut with a cryostat.

X-gal ((5-bromo-4-chloro-3-indolyl-β-D-galactopyranoside) is cleaved by β-galactosidase to yield colourless galactose and 5-bromo-4-chloro-3-hydroxyindole. The latter is subsequently oxidised to 5,5'-dibromo-4,4'-dichloro-indigo, an insoluble intense blue precipitate. X-gal staining solution was made by adding 500µl of freshly made X-gal solution to 19.5ml of buffer solution (see Appendix 6.1 for compositions).

Stored coronary artery segments or slide-mounted cryostat sections were removed from the -80°C freezer and allowed to warm to room temperature. Fixation was performed with 4% paraformaldehyde for 30 minutes and then the segments were washed twice with PBS. They were then permeabilised with 0.1% Triton-X 100 for 10 minutes

followed by two further PBS washes. The segments were incubated in X-gal staining solution at 37°C overnight followed by two PBS washes the following day. Blue staining was assessed by light microscopy.

2.8.3.2 β-galactosidase and protein assay to quantify transgene expression

β-galactosidase assay was performed to quantify the degree of *lacZ* transgene expression in transfected coronary artery segments.

A pestle and mortar was cleaned with 70% ethanol and allowed to air dry. The pestle and mortar were placed in a polystyrene container containing enough liquid N_2 to cover the mortar; the lid of the box was left closed to prevent further evaporation of liquid N_2. The mortar was half-filled with liquid N_2, removed from the box and placed on the open bench. The frozen tissue segment was removed from storage at -80˚C and placed in the mortar, ensuring that it remained submerged in liquid N_2 at all times. The tissue was ground until it became a fine powder and the liquid N_2 was allowed to evaporate. An empty tube was weighed and the powdered tissue was scraped into the tube using a spatula. The tube was then re-weighed and the tissue weight calculated. 10ml of Lysis Buffer per 1g of tissue weight was added and the tissue lysates stored at -80˚C until required.

On the day of processing, the samples were removed from the -80°C freezer and allowed to warm to room temperature. β-galactosidase and protein assay were then performed as described previously (Sections 2.5.2 and 2.5.3) and the degree of transgene expression could be calculated.

2.8.4 Dose finding stent study

In our group's most recent previous study of intracoronary β-galactosidase expression[264], activity in vessel lysates was 0.005±0.002iu/mg protein/min. A group size of 5 vessels will afford an 80% power of detecting a two-fold increase in β-galactosidase activity (i.e. an increase to 0.01±0.004) with P=0.05 (one-tailed test). There were planned for four groups (3 different plasmid doses and a control group) of 5 vessels each, meaning that twenty

vessels would need to be treated. Two vessels would be treated in each animal and therefore ten animals would be required.

3.5x12mm stents were prepared by Medtronic coated with one of three doses of plasmid encoding for *lacZ* or with polymer alone (with no plasmid). Stent deployment was performed within ten pigs, with each animal receiving two of the above stent types: one within the proximal LAD and one within the proximal circumflex. Stents were deployed at 8Atm.

Sacrifice and vessel harvesting was performed at 7 days. Following stent removal, the stented segment was divided into two. One half was embedded in OCT solution and snap frozen in liquid nitrogen and the other half was directly snap frozen in liquid nitrogen and processed for en-face X-gal staining. The OCT embedded vessel segment was cut into 20μm sections with a cryostat and stained with X-gal solution as described in Section 2.8.3.1.

2.8.5 Therapeutic stent study

In our group's previous study of stent-mediated gene transfer of the secreted TGF-β type II receptor (RIIs)[276], mean luminal area at 28 days in control vessels was 0.55±0.8mm^2 compared with 2.02±1.23mm^2 in vessels receiving RIIs. A group size of 10 animals will afford an 89% power of detecting a difference of the same magnitude with P=0.05 (two-tailed test).

30 pigs were randomised to receive a single 3x12mm stent loaded with plasmid encoding for either CTGF, FMOD or *lacZ* (control) with 10 pigs in each group. All stents were prepared by Medtronic. The stents were deployed in the proximal LAD at 14Atm pressure aiming for a stent:vessel oversizing ratio of 1.1-1.2. According to the manufacturer's product information, at 14Atm pressure the 3mm stents will expand to a theoretical diameter of 3.33mm (stent area 8.7mm^2) and therefore target vessel diameters of 2.5-2.8mm as assessed by QCA were used if possible.

Vessel harvesting was performed at 28 days. Repeat coronary angiography and QCA calculation was performed prior to sacrifice. Following heart extraction, pressure perfusion and fixation of the coronary arteries was performed as described in Section 2.8.2.2.

2.8.5.1 Processing of fixed stented segments for morphometric analysis

This was performed by the osteoarticular pathology department of the University of Manchester. The fixed stented artery segments were removed from storage in 4% formaldehyde and placed in 70% ethanol for 2 days to prevent buffer salts in the formaldehyde from precipitating. They were then placed in an automatic processor at 4°C and the following wash cycles were performed: 100% ethanol X 3, chloroform (to removed any lipid from the sample), 100% ethanol X 3 and LR White for Hard Tissue resin (London Resin Company). The samples were then warmed to room temperature, placed in trays half-filled with LR White resin and placed in a vacuum container overnight to remove any excess ethanol or chloroform. The resin was changed and the samples were placed in a pressure container at 60 PSI with dry nitrogen which was then placed in a 42°C oven overnight to polymerise the resin under anaerobic conditions.

The samples were broken out of their containers and mounted onto an aluminium chuck. 8μm sections were cut from the proximal, mid and distal segments of the stented artery with an LKB powered microtome with a tungsten carbide D-profile blade. The sections were floated on a water meniscus to flatten them and were then mounted onto a Mylar sheet and placed on a hot plate. Staining of the sections was performed with toluidine blue (in which proteoglycans appear pink) and Miller's elastic stain counterstained with picosirius red (in which collagen appears yellow, muscle appears red and elastic tissue appears blue). A drop of Loctite ultraviolet (UV) adhesive (Glass Bond) was placed onto the section and a microscope slide adhered to the sample in a UV box. The Mylar sheet was peeled off and another drop of Glass Bond was placed on the slide and a coverslip placed on top.

2.8.5.2 Morphometric analysis of stented segments

Visualisation of the slides was performed with a Leica DMLB microscope and analysis and computed morphometry was performed using Leica Qwin software.

For each section the cross-sectional area of the lumen, stent, internal elastic lamina (IEL) and external elastic lamina (EEL) were measured. The neointimal thickness (defined as the average of the minimum distance between each stent strut and the lumen) was calculated.

From the above measured parameters, the neointimal area (IEL area – lumen area) and media area (EEL area – IEL area) were calculated.

Vessel injury was assessed using a modification of the scoring system originally described by Schwartz[277], in which vessel stretch as well as deep injury can be quantified[278]. This scoring system is shown in Table 5 and a mean injury score for each section was calculated.

Table 5 – Injury score (assessed for each stent strut)

0	No IEL deformation
1	IEL deformed < 45º (stretch)
2	IEL deformed > 45º (stretch)
3	Ruptured IEL (deep injury)
4	Ruptured EEL (deep injury with complete medial rupture)

2.8.6 Mechanistic stent study

The processing methods described above to allow accurate morphometric measurements of the stented vessel segments rendered the tissue unsuitable for further analysis. Therefore a further series of stent deployments was performed to allow assessment of transgene expression using quantitative PCR and to enable further exploration of the mechanisms for any effect on the degree of neointimal hyperplasia demonstrated in the therapeutic experiments.

A total of three CTGF-coated, three FMOD-coated and one *lacZ* coated stent (all 3x12mm) were deployed at 14Atm in the proximal LAD of seven pigs. The vessels were harvested at 7 days. Following stent removal, the stented vessel segment was divided into two. One half was snap frozen in liquid N_2 and stored at -80°C for RNA extraction and quantitative PCR. The other half was embedded in OCT and snap frozen in liquid N_2 for sectioning at a later date.

2.8.6.1 Assessment of transgene expression by quantitative polymerase chain reaction

RNA extraction

The arterial segments were removed from storage at -80°C. All equipment to be used was sprayed with RNaseZap (Ambion) to remove RNase contamination. The arterial segment was cut into small pieces and placed in a dounce homogenizer with 0.5ml TRIzol (Invitrogen) to lyse tissues and cells. The tissue was homogenized until no solid tissue was visible, incubated at room temperature for 15 minutes and centrifuged for 5 minutes at 4000g. The supernatant was transferred into a new tube and 0.2ml of chloroform was added. The tube was vortexed and incubated at room temperature for 3 minutes, followed by centrifugation at 12000g for 15 minutes at 4°C. The upper aqueous phase (which contains the total RNA) was removed carefully with a pipette and placed in a new labelled tube. 0.25µl of ice-cold isopropanol, to precipitate the RNA, and 2µl of GlycoBlue (Ambion), to aid identification of the nucleic acid pellet, were added and the tube was incubated at room temperature for 10 minutes. Further centrifugation at 12000g for 10 minutes at 4°C was performed and the supernatant was removed. The RNA pellet was washed with 0.5ml of 75% ethanol followed by a final centrifugation run at 7500g for 5 minutes at 4°C. The supernatant was removed and the pellet was allowed to dry for a few minutes at room temperature and then resuspended in 50µl DEPC-treated water. The RNA concentration was quantified with a NanoDrop spectrophotometer and stored at -80°C until use.

Complementary DNA synthesis

The SuperScript VILO cDNA synthesis kit (Invitrogen) was used to generate complementary DNA (cDNA) from the extracted RNA. This contains an enzyme mix including a reverse transcriptase and an RNase inhibitor, and a reaction mix including random primers, $MgCl_2$, and dNTPs in a buffer. The following components were placed in a tube on ice and mixed:

VILO reaction mix 5X	4µl
SuperScript enzyme mix 10X	2µl
RNA 2µg	variable
DEPC-treated water	to make 20µl

The tube was placed in a PCR machine and incubated at 25°C for 10 minutes, 42°C for 60 minutes and 85°C for 5 minutes. The cDNA was diluted 20-fold in DEPC-treated water, quantified with a NanoDrop spectrophotometer and then stored at -20°C until use.

Quantitative polymerase chain reaction

The quantitative real time polymerase chain reaction (qPCR) aims to amplify and simultaneously quantify a region of a targeted DNA molecule. The Taqman system from Applied Biosystems (ABI; California, USA) utilises a specific probe for the gene of interest, which contains a reporter dye at the 5' end and a quencher dye which suppresses fluorescence at the 3' end. During PCR the annealed probe is cleaved by AmpliTaq Gold DNA polymerase at the 5' end freeing the reporter dye resulting in increased fluorescence which can be monitored in real time.

Gene quantification requires analysis of an endogenous control gene which accounts for variability in the initial concentration and quality of total RNA (and therefore cDNA). Duplex PCR was performed using the target gene primers and endogenous control gene primers, with different reporter dyes, in the same reaction. Previous work from an allied group has identified the human 18S ribosomal RNA gene to work as a reliable housekeeping gene (with a relatively constant level of gene expression) in pigs. Therefore a Taqman gene expression assay for 18S rRNA with the VIC reporter dye (ABI; #Hs99999901_s1) and Taqman gene expression assays for human CTGF (#Hs00170014_m1) and bovine fibromodulin (#Bt03212663_m1) with the FAM reporter dye were used.

Each duplex qPCR reaction consisted of:

Taqman Master Mix 2X	10µl
Taqman gene assay (FMOD or CTGF)-FAM 20X	1µl
Taqman 18S rRNA gene assay-VIC 20X	1µl
cDNA (diluted 1:20)	5µl
DEPC-treated water	3µl

The PCR reaction solutions were transferred to a MicroAmp 96-well plate. Reactions with both the FMOD and CTGF primers were performed for each sample in duplicate. Non-template controls substituted the cDNA for DEPC-treated water.

Analysis was with an Applied Biosystems 7500 Fast Real-Time PCR System. The threshold cycle (C_T) is the cycle at which a statistically significant increase in fluorescence is detected. C_T is measured for the S18 housekeeping gene (with the VIC dye) and for the target gene (with the FAM dye) for each sample.

$$\Delta C_T \text{ sample} = C_T \text{ target gene} - C_T \text{ endogenous control (S18)}$$

The mean ΔC_T of the reference samples (those transfected with *lacZ* or the non-targeted transgene) was calculated. The fold-change (RQ) for each target sample can then be calculated as follows:

$$\Delta\Delta C_T = \Delta C_T \text{ sample} - \text{mean } \Delta C_T \text{ reference samples}$$

$$RQ = 2^{-\Delta\Delta CT}$$

2.8.7 Assessment of effect of β-blockers on plasmid-mediated transgene expression

Stent implantation was performed within six pigs. Three of the pigs were loaded with 10mg of bisoprolol, a selective β1-receptor blocker, for 3 days prior to the procedure,

whereas the other three pigs did not receive a β-blocker. Heart rate was measured after induction of general anaesthesia to ensure adequate β-blockade.

Two stents were implanted into each pig: a 3.5x12mm stent prepared by Medtronic coated with polymer and an estimated 400μg of *lacZ* plasmid deployed at 10Atm, and a 3x12mm Liberté bare metal stent (Boston Scientific, MA, USA) deployed at 14Atm. The deployment pressures were selected to ensure a similar diameter of balloon expansion. The choice of artery to which a plasmid-coated stent was delivered was random, with one stent deployed within the proximal LAD and the other within the proximal Cx.

Sacrifice and vessel harvesting was performed at 7 days. Following stent removal, the stented vessel segment was divided into two. One half was snap frozen in liquid N_2 for en face staining with X-gal. The other half was snap frozen in liquid N_2 for β-galactosidase staining and protein assay to assess transgene expression.

3 Results

3.1 Adenovirus infection of saphenous vein graft segments

Previous work from our group has identified a potentially beneficial effect on neointima formation following adenoviral delivery of CTGF in a SVG model of restenosis. Analysis of sections from these previous experiments, which had already been stained with picosirius red, was performed. Further specimens of human saphenous vein were infected with Ad-CTGF to enable further mechanistic assessments.

3.1.1 Picosirius red staining

Collagen content, as assessed by area of red birefringent staining, was significantly greater in the *lacZ*-infected group compared with the CTGF-infected group (Figure 16; mean $3.18x10^6$ pixels vs. $1.86x10^6$; P=0.019). However when collagen content was controlled for the total area of the section this difference was no longer significant (Figure 17; mean 0.78 vs. 0.70; P=0.14).

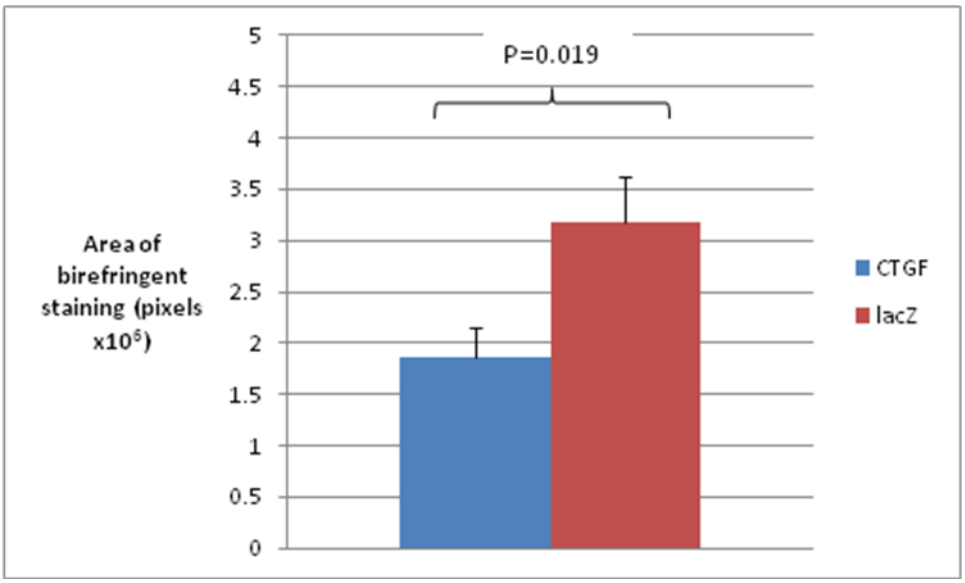

Figure 16 – Collagen content as assessed by area of red birefringent staining with picosirius red

Total collagen content is significantly greater in the *lacZ* infected sections as compared to the CTGF infected sections. Results are shown as mean (+- standard error). CTGF group = 11 sections; *lacZ* group = 8 sections

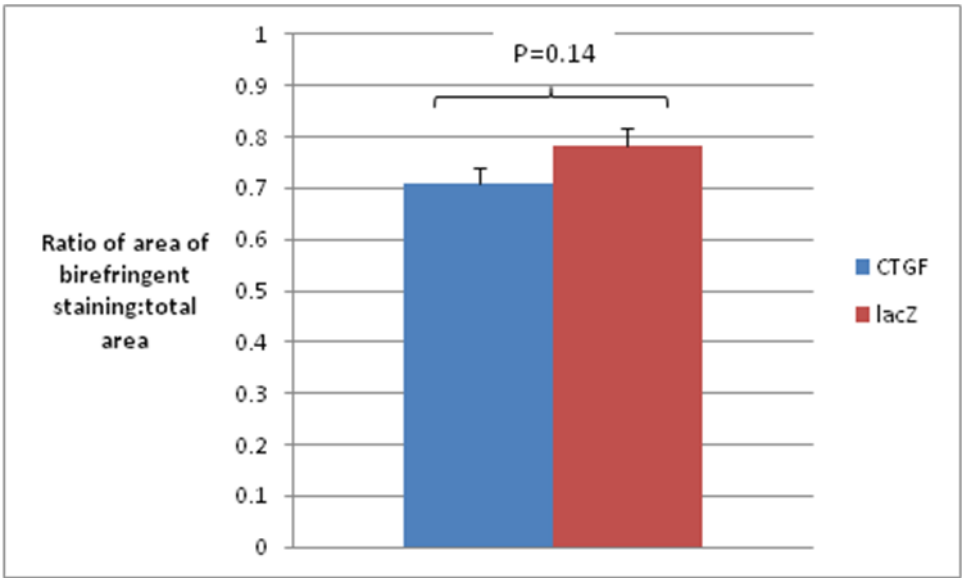

Figure 17 - Collagen content as assessed by ratio of area of red birefringent staining to total section area

There is no significant difference between the *lacZ* and CTGF infected sections in the proportion of collagen in the vessel wall. Results are shown as mean (+- standard error). CTGF group = 11 sections; *lacZ* group = 8 sections

3.1.2 Saphenous vein graft infections

A total of 17 vein segments were virally infected, with 9 segments infected with Ad5-*lacZ* and 8 segments infected with Ad5-CTGF. These segments were processed at various time points as shown in Table 6 with the OCT embedded sections subsequently being used for immunofluorescence and the direct frozen segments being used for Alcian blue staining.

Table 6 - Method of processing of virally infected vein segments (numbers indicate number of vein segments)

	lacZ		**CTGF**	
Day	**OCT**	**Direct**	**OCT**	**Direct**
3	4	0	3	0
7	7	7	7	7
14	4	3	6	5

3.1.3 Alcian blue staining

There was no difference in proteoglycan content between the *lacZ*- and CTGF-infected groups at 7 days (mean A_{595}/weight 0.42 vs. 0.33; P=0.12) or at 14 days (mean A_{595}/weight 0.31 vs. 0.35; P=0.65) as assessed by this technique.

3.1.4 Immunohistochemistry & immunofluorescence

CTGF was present primarily in the endothelium and intima of both the Ad5-*lacZ* and Ad5-CTGF infected segments; representative sections are illustrated in Figure 18 and Figure 19 (immunohistochemistry) and Figure 20 (immunofluoresence). There was no difference in overall CTGF content between the *lacZ* and CTGF groups, as assessed by immunofluorescence, at any timepoint and also no change in CTGF content between days 3, 7 and 14 in either group (see Table 7).

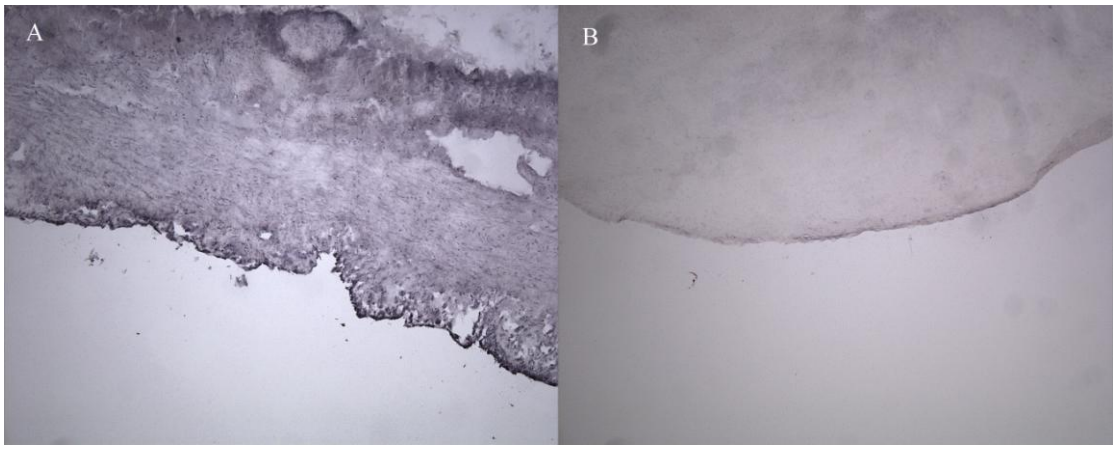

Figure 18 – CTGF binding in *lacZ*-infected SVG section at day 3

Representative sections from 4 vein graft infections with 3 sections stained from each experiment. A=anti-CTGF primary antibody; B=control (no primary antibody); x10 magnification

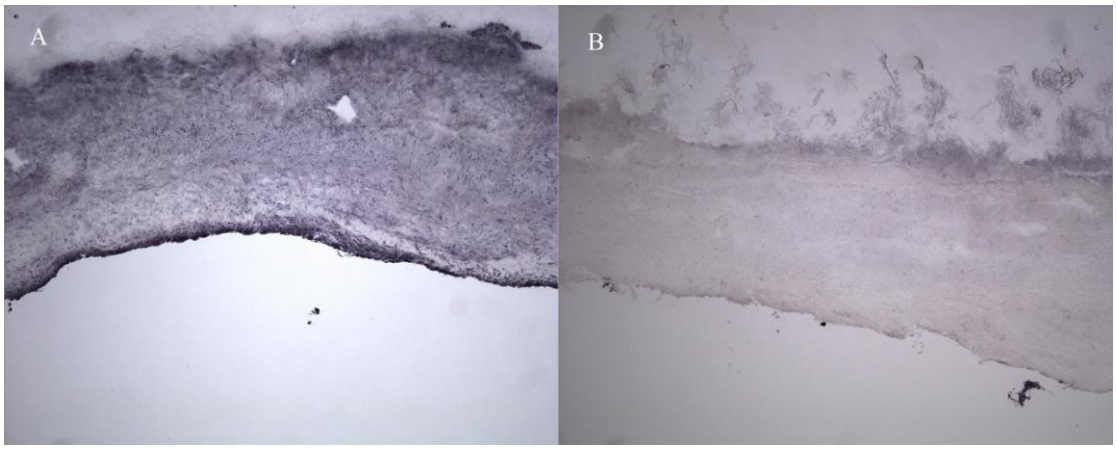

Figure 19 - CTGF binding in CTGF-infected SVG section at day 3

Representative sections from 3 vein graft infections with 3 sections stained from each experiment. A=anti-CTGF primary antibody; B=control (no primary antibody); x10 magnification

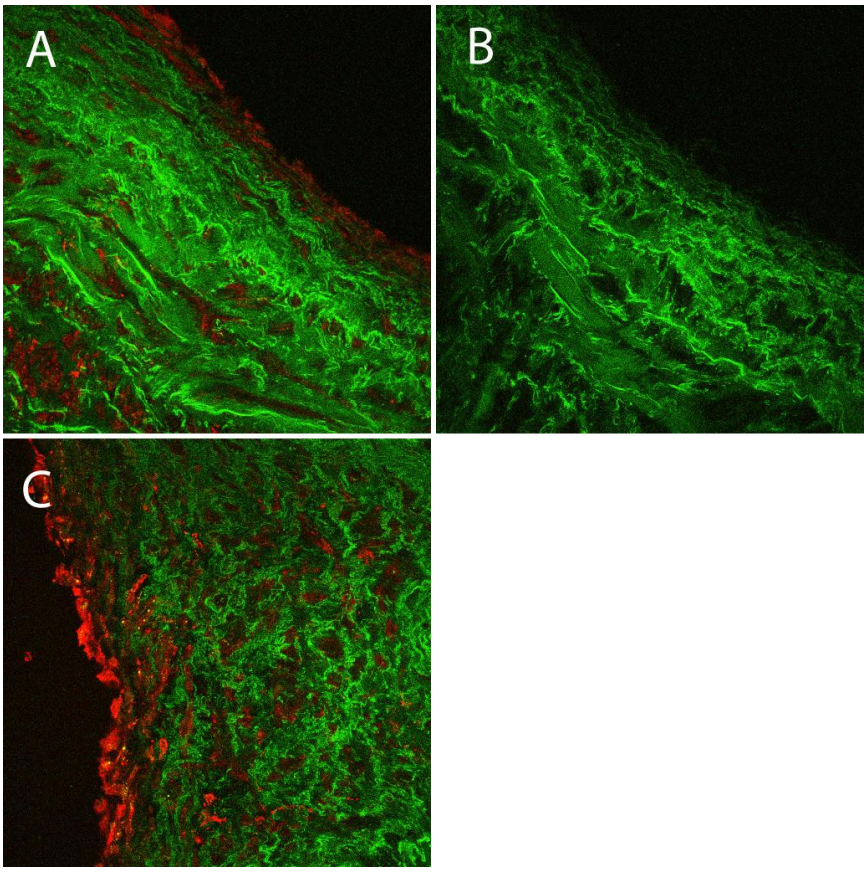

Figure 20 - Immunofluorescence of SVG sections with anti-CTGF antibody

Representative sections at day 7 following infection. 6 infections were performed for each transgene and 3 sections were processed from each specimen at this timepoint. A=Ad5-CTGF-infected; B=control (no primary antibody); C=Ad5-*lacZ*-infected; Green=collagen autofluorescence; red=anti-CTGF antibody binding; x40 magnification

Table 7 - Mean intensity of staining of anti-CTGF antibody

	Day 3	**Day 7**	**Day 14**
lacZ	35.4 (4)	30.9 (6)	32.0 (5)
CTGF	28.0 (3)	29.7 (6)	33 (7)

Values in brackets indicate number of specimens analysed

3.2 Confirmation of identity of lacZ plasmids with different promoter elements

The expected band sizes following specific restriction digests and gel electrophoresis of the newly constructed plasmids are detailed in Table 8. Confirmatory gels are shown in Figure 21, Figure 22 and Figure 23. In Figure 22 some of the plasmids have been subject to partial digests as evidenced by additional visible bands which are of weaker intensity than the smaller bands below and also correspond to the sum of the smaller bands. These can be seen for the D2RE2HE, D2RE, DREHE and 2RE2HE plasmids.

Table 8 – Expected DNA fragment sizes following restriction enzyme digests

	XhoI	**SwaI**	**PmlI**	**BstBI**	**NotI & SpeI**
D2RE2HE	4 (9100, 4500, **900**, 400)	2 (14000, **400**)	2 (14000, **200**)		4 (5500, 5500, 3000, **700**)
D2HE	3 (9100, 5000, 400)	2 (14000, **200**)	2 (14000, **200**)		
D2RE	4 (9100, 4500, **600,** 400)	2 (14000, **200**)	2 (14000, **200**)	2 (14000, **100**)	
DREHE	4 (9100, 4500, **600**, 400)	2 (14000, **200**)	2 (14000, **200**)	1 (linearised, 14000)	
DRE	3 (9100, 4900, 400)	2 (14000, **100**)	2 (14000, **200**)		
D	3 (9100, 4800, 400)	1 (linearised, 14000)	1 (linearised, 14000)		4 (5500, 5500, 3000, **200**)
2RE2HE	4 (9100, 4400, **900,** 400)	1 (linearised, 14000)	1 (linearised, 14000)		
Backbone	3 (9100, 4600, 400)	0 (uncut)	0 (uncut)	0 (uncut)	3 (5500, 5500, 3000)

The boxes detail the expected number of bands with the approximate fragment sizes in brackets (bp). Figures in bold indicate easily identifiable additional bands as compared to the control pGEG.PSi-*lacZ* plasmid.

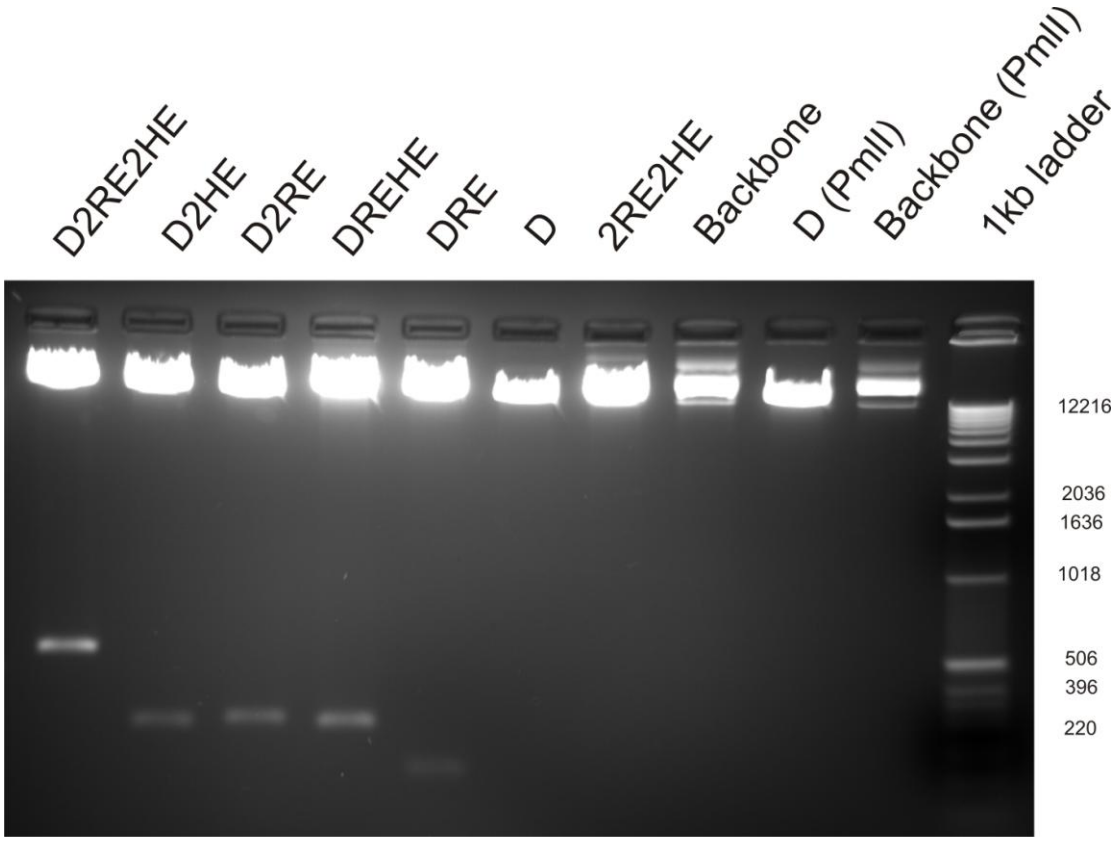

Figure 21 – SwaI and PmlI digest of novel plasmids

Lanes 1-8 = SwaI; lanes 9-10 = PmlI; backbone = pGEG.PSi-*lacZ*

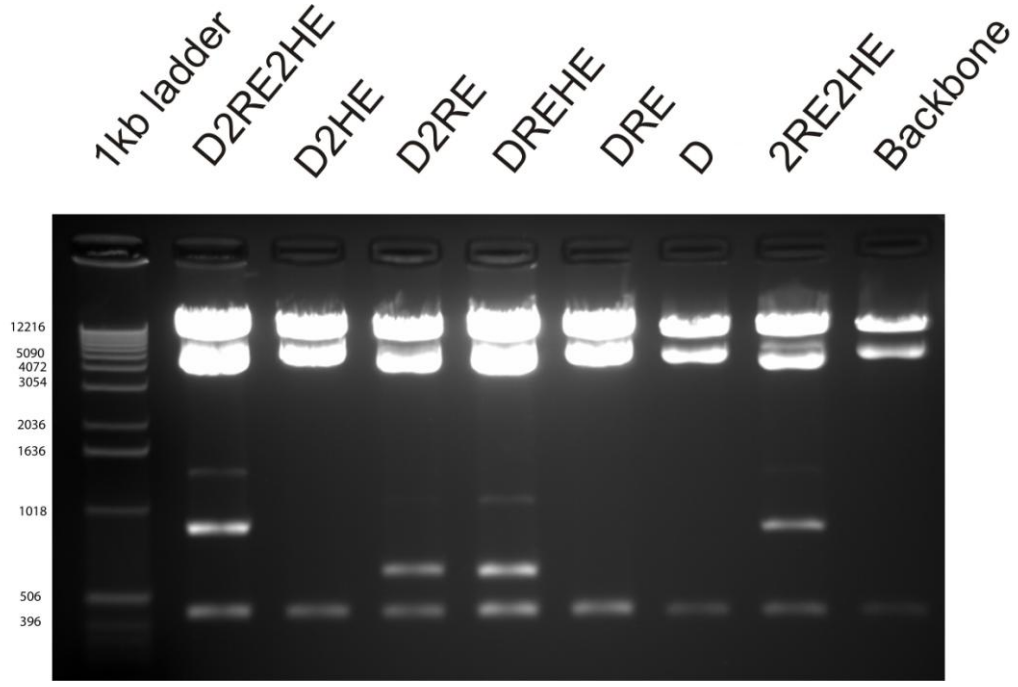

Figure 22 - XhoI digest of novel plasmids

Backbone = pGEG.PSi-*lacZ*

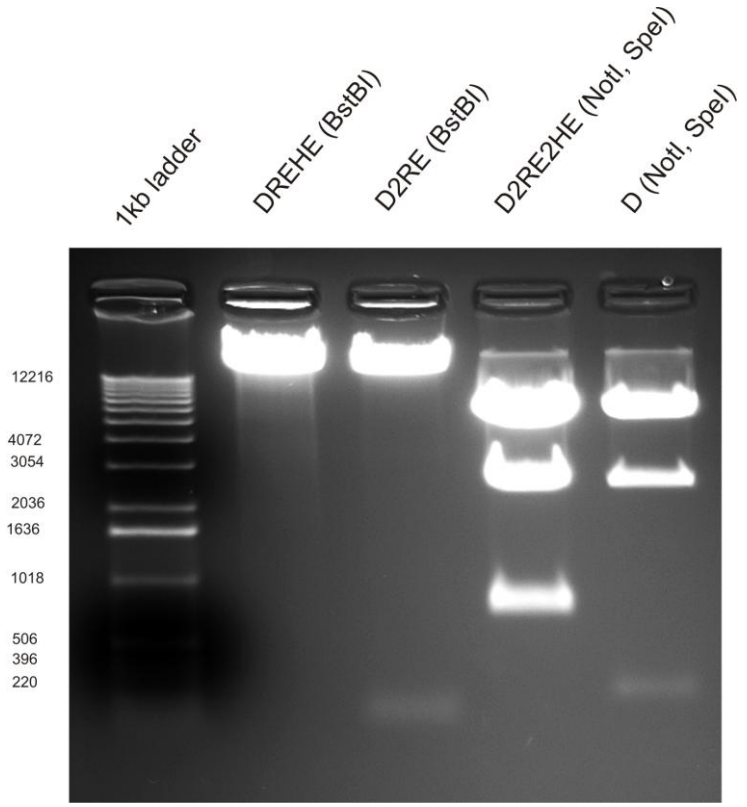

Figure 23 - Further confirmatory digests of novel plasmids

3.3 Quantification of transgene expression with novel expression cassettes

Figure 24 illustrates the relative transgene expression of plasmids containing the novel expression cassettes in human coronary SMCs following nucleofection. Transgene expression was approximately 12-fold greater with the 2RE2HE insert than with the original pGEG.Psi-*lacZ* plasmid (P=0.041) and approximately 11-fold greater than a construct with the inclusion of the D element as well as 2RE2HE (P=0.041). There was no statistically significant difference between any of the other expression cassettes and the original plasmid.

Given that the addition of the 2RE2HE enhancer elements resulted in significantly greater transgene expression than with the pGEG.Psi-*lacZ* plasmid, pGEG-2RE2HE-Psi-*lacZ* was selected as the control plasmid for use in the *in vivo* experiments and the therapeutic plasmids were constructed using the same expression cassette.

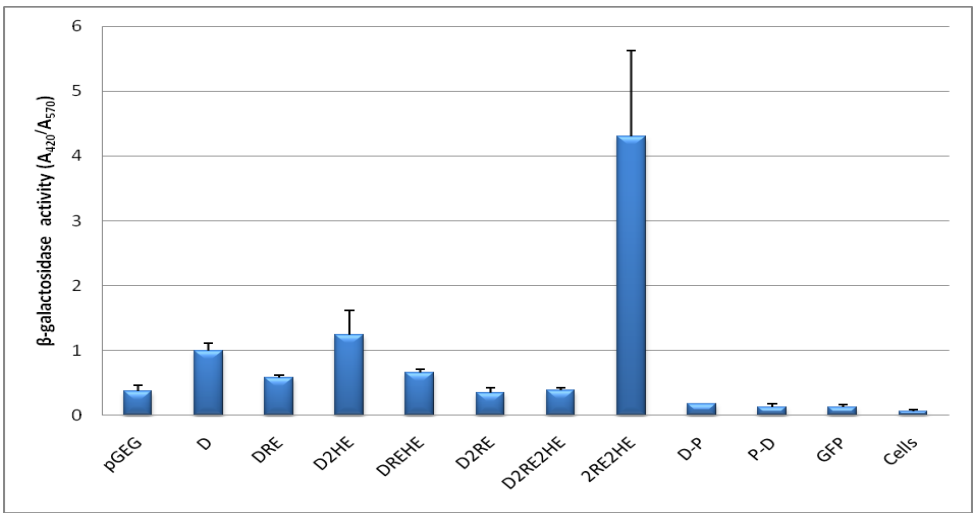

Figure 24 – β-galactosidase activity in cell lysates of cultured human coronary arterial SMCs following nucleofection with plasmids containing novel expression cassettes

Results are expressed as the ratio of β-galactosidase activity (A_{420}) to protein (A_{570}). pGEG = pGEG.PSi-*lacZ* plasmid. Controls were as follows: D-P = DNA without nucleofection programme; P-D = nucleofection without DNA; GFP = green fluorescent protein (control plasmid); Cells = cells alone without DNA or nucleofection. The bars indicate the mean of 3 experiments (+- standard error).

3.4 Confirmation of identity of putative therapeutic constructs to be used in vivo

The identity of pGEG-2RE2HE-PSi-*lacZ* had already been confirmed in the earlier experiments. The identity of pGEG-2RE2HE-CTGF and pGEG-2RE2HE-FMOD were confirmed with restriction digest patterns, PCR, and with transfection of cells *in vitro*.

Restriction digest

Table 9 shows the expected bands to be seen on agarose gel electrophoresis following selected restriction enzyme digestion of pGEG-2RE2HE-CTGF and pGEG-2RE2HE-FMOD. The expected bands that would be seen for the original pGEG-2RE2HE-Psi-*lacZ* are also shown. Figure 25 and Figure 26 show the gels following selected restriction digests confirming the identity of pGEG-2RE2HE-CTGF and pGEG-2RE2HE-FMOD respectively.

Table 9 – Expected digest patterns for selected restriction enzymes

Transgene	**Restriction Enzyme/s**	**Expected bands for new plasmid**	**Expected bands for pGEG.Psi-*lacZ***
CTGF	XhoI	4 (6729, 4043, 858, 438)	4 (9021, 4043, 858, 438)
CTGF	NheI, PmlI	3 (10262, 1407, 399)	2 (14360, 1407)
CTGF	NheI, SbfI	2 (11358, 710)	1 (linearised)
FMOD	BamHI	4 (12566, 850, 160, 106)	1 (linearised)
FMOD	SpeI	4 (5607, 3617, 2713, 1744)	3 (12180, 6573, 533)
FMOD	BglII	3 (12857, 564, 213)	0 (uncut)

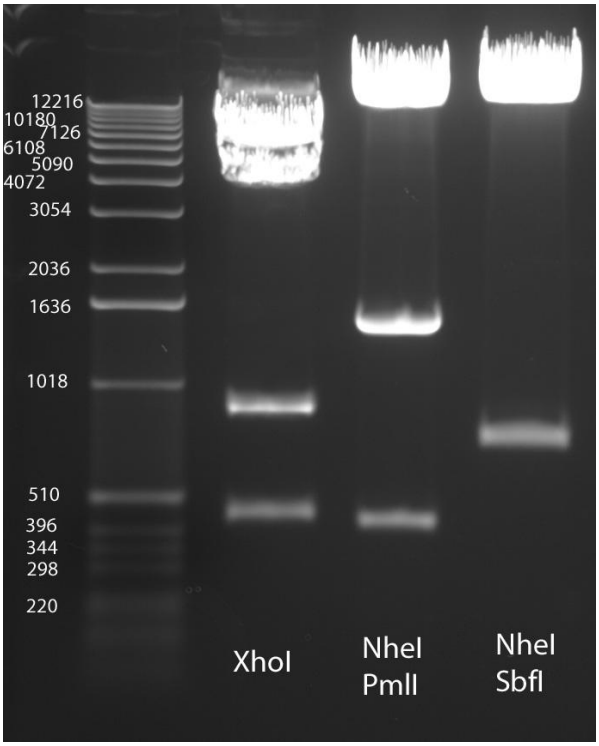

Figure 25 – Confirmatory restriction digests of pGEG-2RE2HE-Psi-CTGF

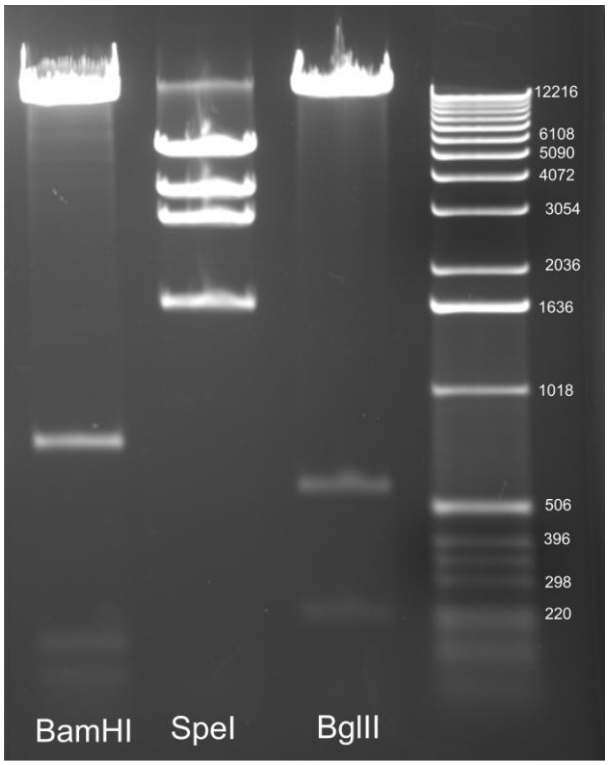

Figure 26 – Confirmatory restriction digests of pGEG-2RE2HE-Psi-FMOD

3.4.1 Polymerase chain reaction

Optimisation of the PCR reaction for the FMOD and CTGF primers was performed. The optimal conditions were as follows:

	CTGF	FMOD
Primer concentration	1μM	0.1μM
Annealing temperature	58°C	50°C

Figure 27 shows the PCR products with the CTGF primers on the original EcoRI-CTGF and new pGEG-2RE2HE-Psi-CTGF, and with the FMOD primers on the original pΔPREK1-FMOD and new pGEG-2RE2HE-Psi-FMOD. The anticipated bands of 1003bp for CTGF and 1020bp for FMOD are present confirming that both transgenes are present in the new plasmids.

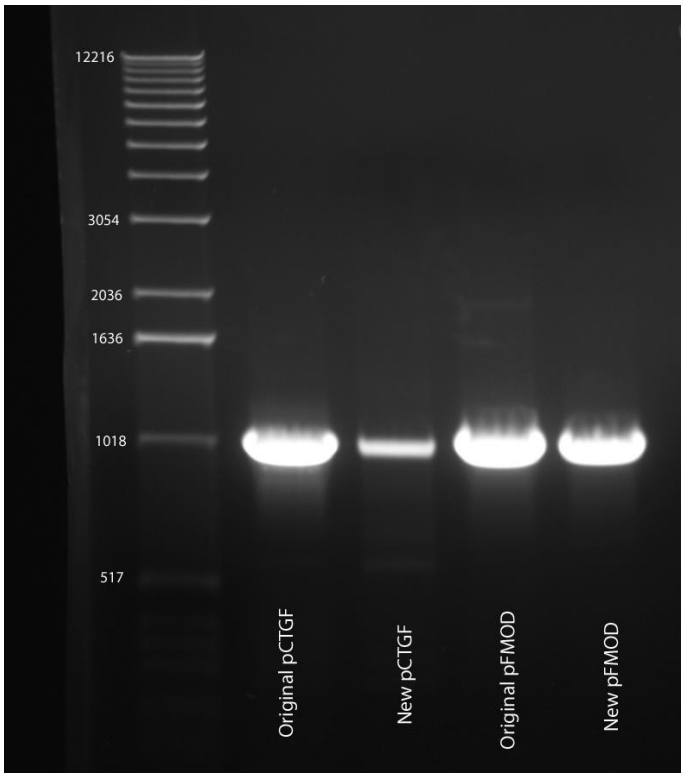

Figure 27 – PCR products from original and new plasmids containing the FMOD and CTGF cDNA

3.4.2 Functional analysis of novel plasmid constructs

Optimisation of the lipofection procedure was performed for each cell type, which involved trialling different liposome formulations and different ratios of plasmid DNA:liposome. Despite this, transfection rates of HCSMCs using the marker gene *lacZ* were consistently <5%. Therefore lipofection with the plasmids encoding for the therapeutic transgenes to be used in the *in vivo* experiments was performed for 293 cells and A10 cells only.

Successful production of the *lacZ* protein following transfection with pGEG-2RE2HE-PSi-*lacZ* was confirmed using X-gal staining and is shown in Figure 28. Successful production of CTGF and FMOD following transfection with pGEG-2RE2HE-PSi-CTGF and pGEG-2RE2HE-PSi-FMOD was confirmed with indirect immunocytochemistry and immunofluorescence which is shown in Figure 29 and Figure 30.

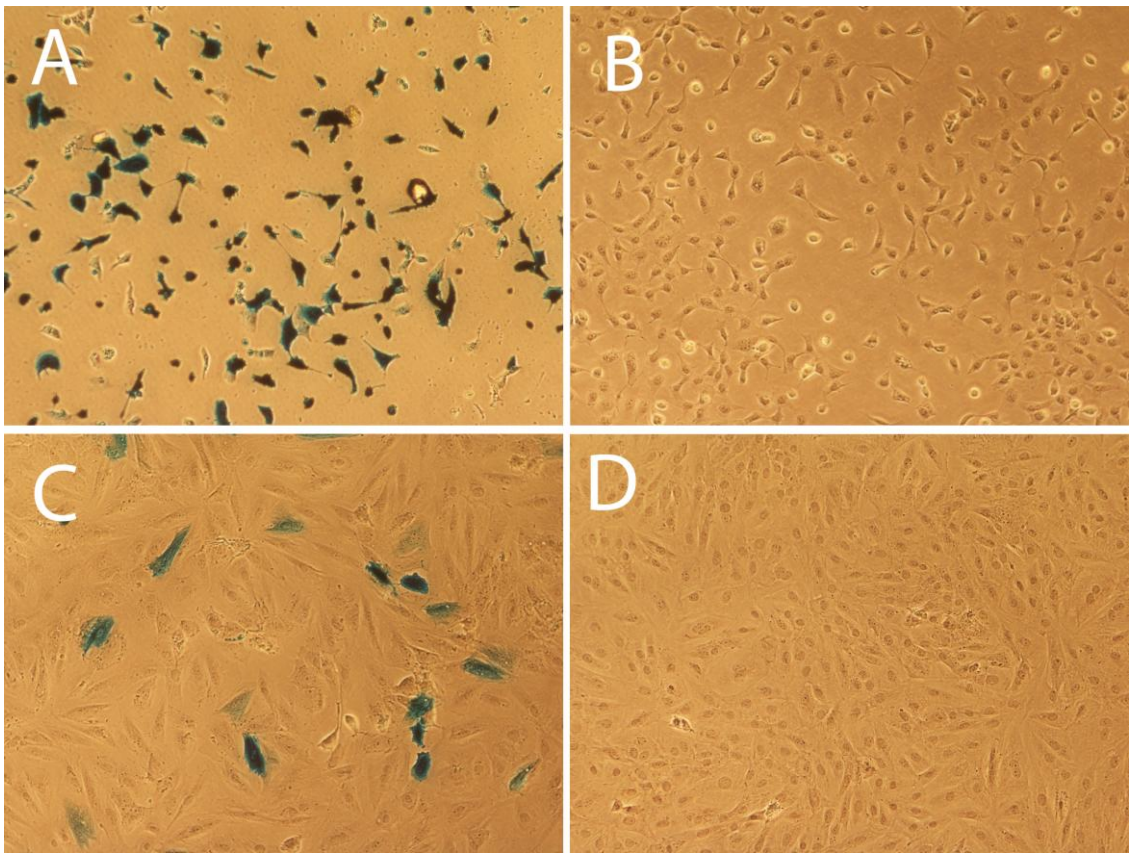

Figure 28 – Transfection with pGEG-2RE2HE-PSi-*lacZ*

Liposome-mediated transfection of 293 cells (panels A & B) and A10 cells (panels C & D). Panels A & C show successful transgene expression of lacZ following transfection with pGEG-2RE2HE-PSi-*lacZ* as indicated by blue staining with X-gal. Panels B & D show controls incubated with liposome solution but no plasmid. All images are X20 magnification.

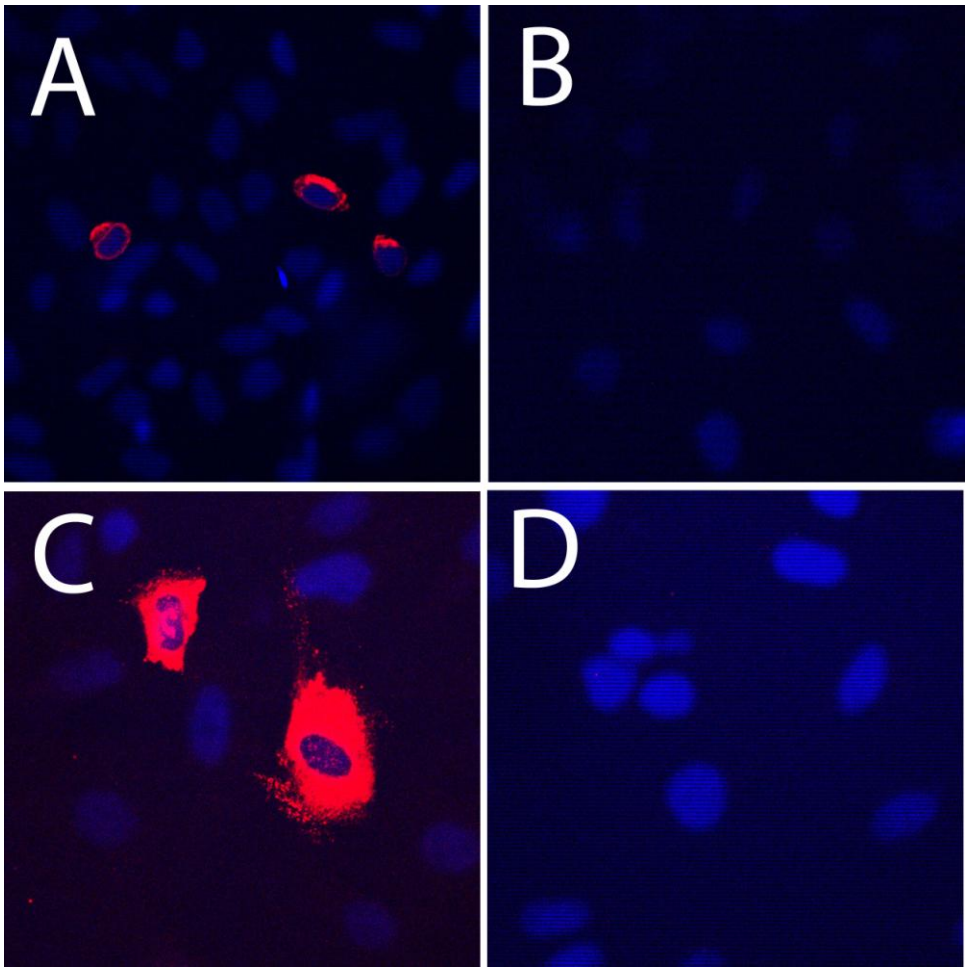

Figure 29 – Transfection with pGEG-2RE2HE-PSi-FMOD

Liposome-mediated transfection of 293 cells (panels A & B) and A10 cells (panels C & D). Panels A & C show successful transgene expression of FMOD with immunofluorescence following transfection with pGEG-2RE2HE-PSi-FMOD. The red colour represents Cy5 fluorescence, indicating antibody binding to FMOD, and the blue colour represents DAPI nuclear staining. Panels B & D show controls incubated with liposome solution but no plasmid. All images are x40 magnification.

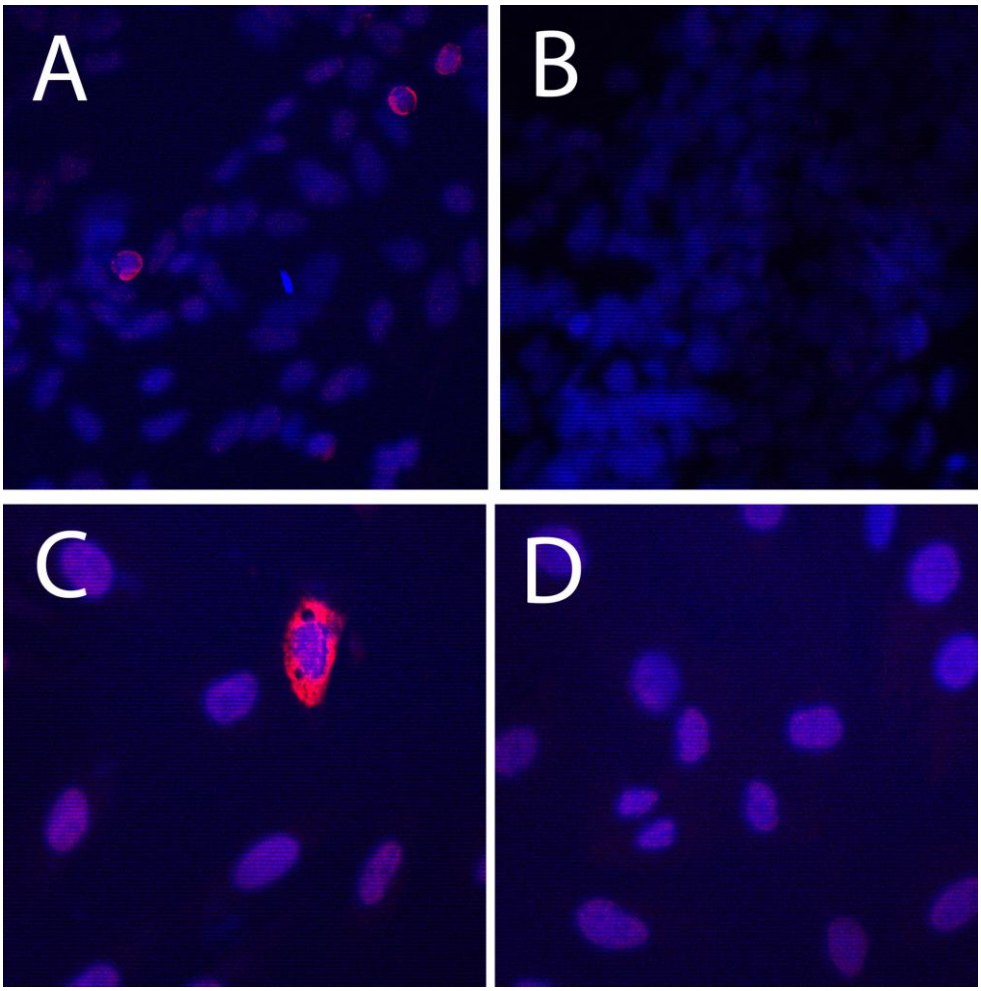

Figure 30 - Transfection with pGEG-2RE2HE-PSi-CTGF

Liposome-mediated transfection of 293 cells (panels A & B) and A10 cells (panels C & D). Panels A & C show successful transgene expression of CTGF with immunofluorescence following transfection with pGEG-2RE2HE-PSi-CTGF. The red colour represents Cy5 fluorescence, indicating antibody binding to CTGF, and the blue colour represents DAPI nuclear staining. Panels B & D show controls incubated with liposome solution but no plasmid. All images are x40 magnification.

3.5 Assessment of DNA elution from gene-eluting stents

3.5.1 Method 2: dip-coating with urethane/plasmid mix

DNA release curves for the three different weights of urethane polymer coating are shown in Figure 31**.** Following an initial burst there was a steady release of DNA over 20 days with most of the theoretical DNA load being released by this timepoint.

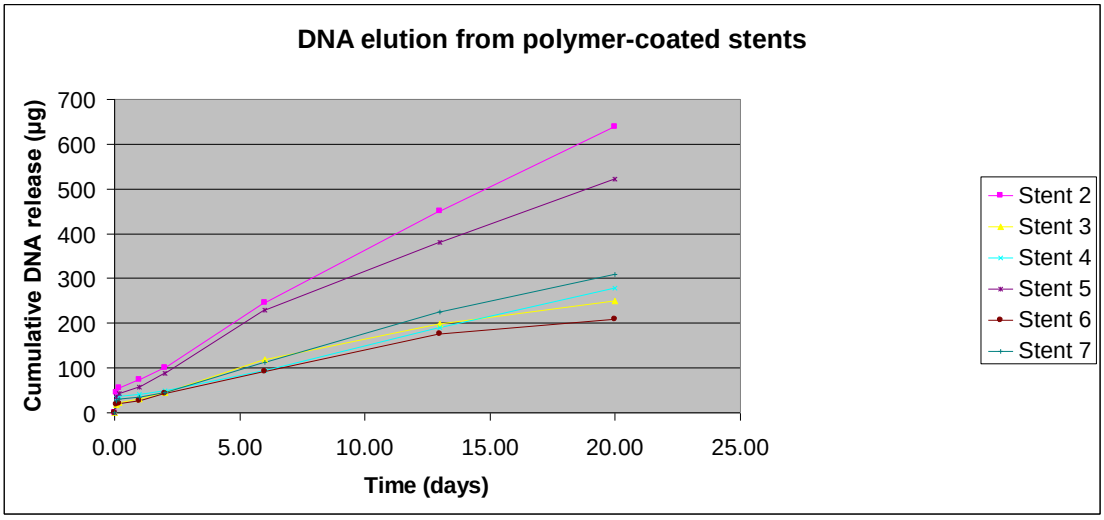

Figure 31 – Cumulative DNA elution from urethane-coated coronary stents

Stents 3 & 6 = 3 dips (theoretical DNA load: 260 µg); stents 4 & 7 = 5 dips (350 µg DNA); stents 2 & 5 = 7 dips (720 µg DNA)

Figure 32 shows gel electrophoresis of the eluted uncut plasmid (pGEG-PRIK-*lacZ*) at two timepoints. The DNA eluted in the first 6 hours is relatively pure but there is significant smearing between 6 hours and 4 days, suggesting DNA degradation.

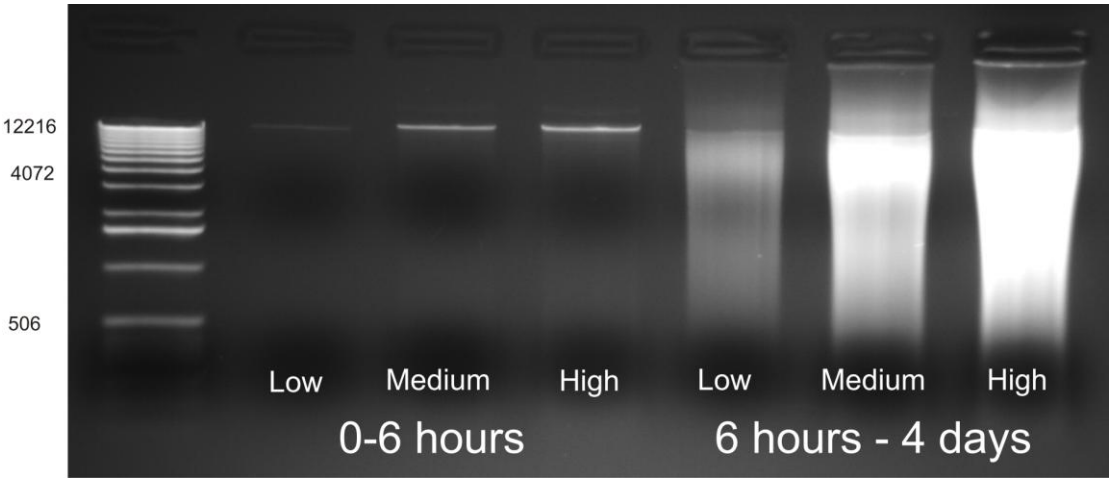

Figure 32 – Eluted uncut DNA at two different timepoints

Three different dilutions are shown for each timepoint. High = undiluted buffer solution containing eluted DNA; Medium = 1:2 dilution; Low = 1:10 dilution

Restriction digests of the eluted DNA were performed using PacI and XhoI. There is a single binding site for PacI in pGEG-PRIK-*lacZ* and digestion results in linearisation of the plasmid and a single 14kb band. There are three XhoI binding sites and digestion leads to three bands: 9106bp, 5493bp and 330bp.

Figure 33 and Figure 34 show restriction digests of eluted DNA at 0-6 hours and 6 hours-4 days incubation. The expected bands are seen showing that the plasmid remained structurally intact during stent preparation. Again there was significant smearing of the DNA at the later timepoint suggesting that DNA degradation had occurred. However the correct bands can still be seen (arrowheads) indicating that some intact plasmid remains. Note that the 330bp band following XhoI digest is partially obscured by the loading buffer tracking dye in Figure 33, although it is well seen in Figure 34.

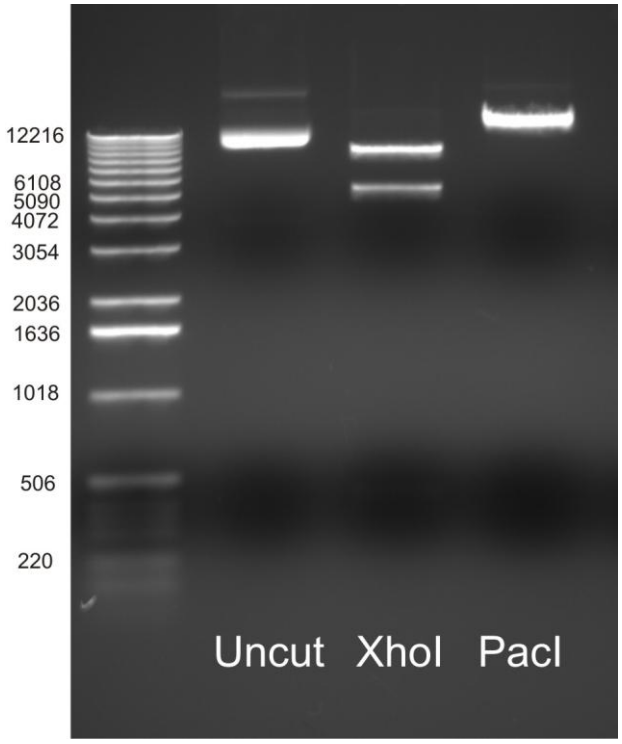

Figure 33 – Restriction digests of eluted DNA between 0-6 hours incubation

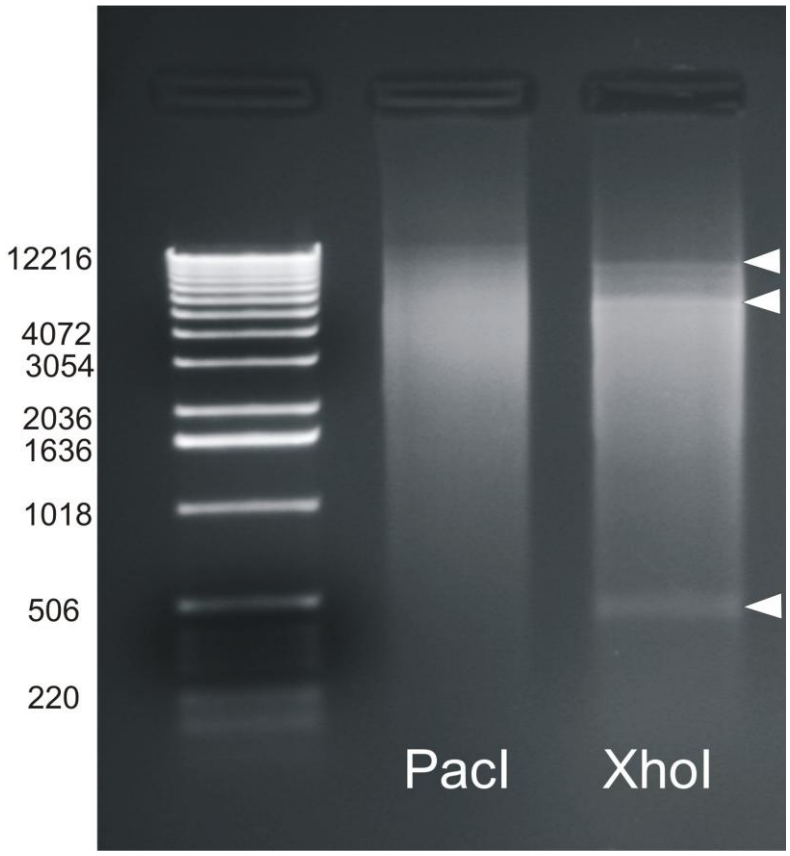

Figure 34 – Restriction digests of eluted DNA between 6 hours and 4 days incubation

Arrowheads highlight the three bands following XhoI digest

In vivo experiments were performed with eight stents (four coated with polymer-plasmid mixture, and four coated with polymer alone) deployed into the LAD and Cx coronary arteries of four pigs. At sacrifice at 7 days there was extensive neointima formation over the stent struts of all the vessels treated. Removal of the stent from the vessel resulted in peeling of the endothelium and neointima away from the media in all cases (Figure 35, Panel C).

There was diffuse non-specific blue X-gal staining in several of the segments, including the vessels treated with control (polymer only) stents (Figure 35, Panel B). However in the vessels treated with the *lacZ* plasmid there was more specific blue staining in the distribution of the stent struts (Figure 35, Panel A). This pattern of staining was not seen

in any of the control stent treated segments. All of the stents with adherent neointima were also stained with X-gal but no blue colouration was seen (Figure 35, Panel C).

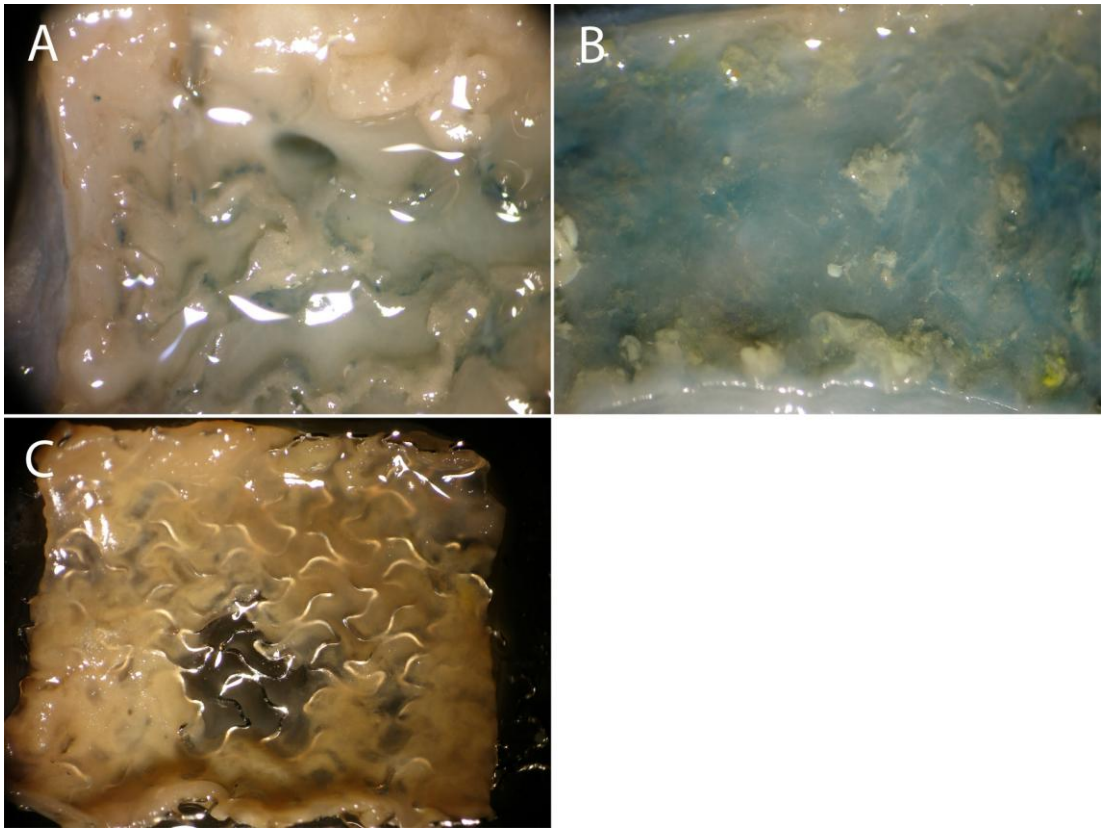

Figure 35 - X-gal staining of coronary artery segments treated with stents coated with urethane polymer mixture

Representative samples from vessels treated with stents coated with pGEG-PRIK-*lacZ* (panel A) and with polymer alone (panel B) at 7 days. Panel C shows denuded neointima which was removed whilst extracting the stent from the vessel wall.

3.5.2 Method 3: spray-coating with polymer and poragen followed by dip-coating in plasmid solution

Medtronic developed a novel coating method to apply polymer and plasmid to the stents (described in Section 2.7.3) and performed measurements of the elution rates from these plasmid-coated stents, using a stock 8kb plasmid. The estimated plasmid dose was

calculated as the difference between the weight of the stent following application of the porous polymer coating and the weight after dipping into a plasmid solution and drying.

All studies demonstrated an initial burst followed by a gradual release of DNA. Figure 36 shows results from stents which had been coated, but not crimped onto a catheter balloon and re-expanded. Plasmid appeared to be steadily eluted up to 29 days with approximately 25% of the total predicted load released at this point.

As the crimp-expansion process will stretch and potentially damage the polymer coating, which may affect plasmid elution, the experiments were repeated after a single crimp-expansion cycle. Figure 37 shows these results which demonstrate a slower initial burst of plasmid (although the first sample was taken at day 3 which will affect the results) and a higher total release, with approximately 50% eluted by day 18.

Finally DNA release curves for stents prepared with three different theoretical plasmid loads are shown in Figure 38. Following the initial burst, a gradual release of DNA was again seen such that approximately 50% of the theoretical load was eluted by day 13.

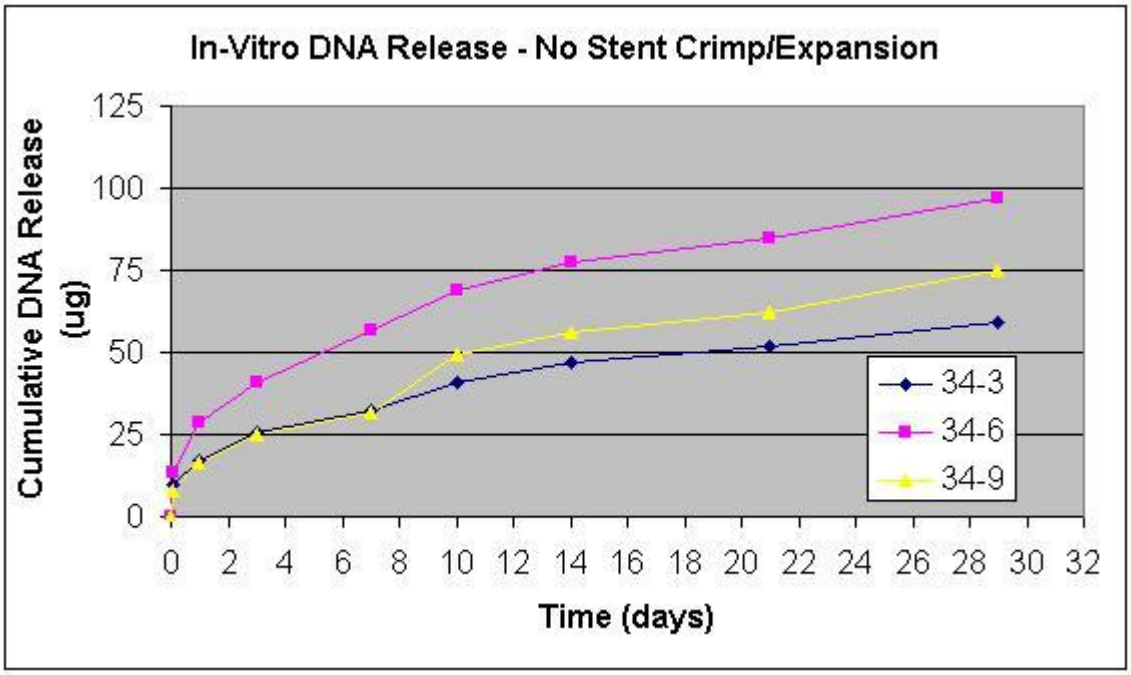

Figure 36 - Cumulative DNA elution from spray-coated stents

The cumulative DNA release up to 29 days is shown for three stents each prepared with an estimated load of 350-400µg of a stock 8kb plasmid. Graph provided by Medtronic.

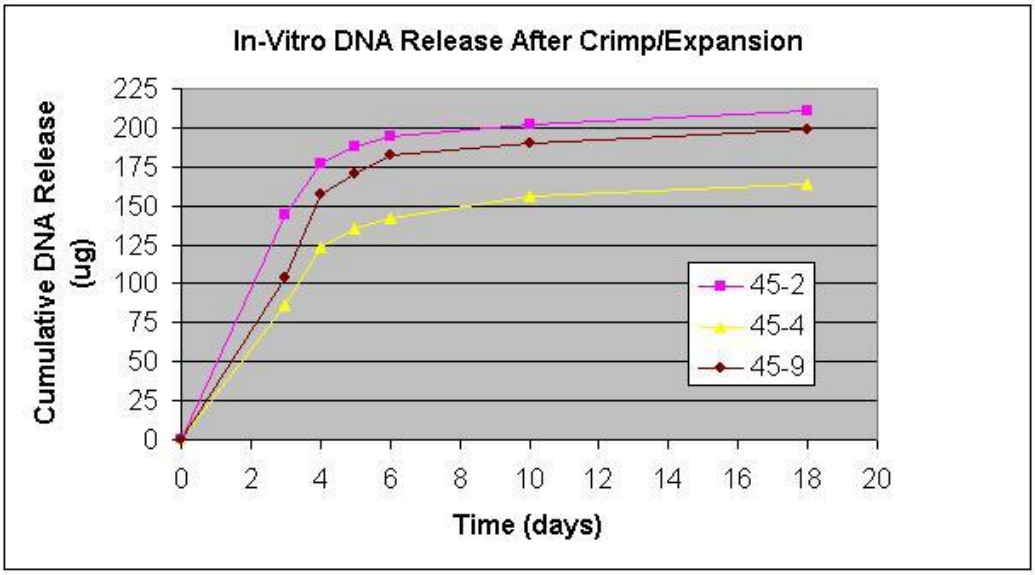

Figure 37 - Cumulative DNA elution from spray-coated stents after crimp/expansion

The cumulative DNA release is shown for three stents each prepared with an estimated load of 350-400µg of a stock 8kb plasmid, following a single crimp and expansion cycle. Graph provided by Medtronic.

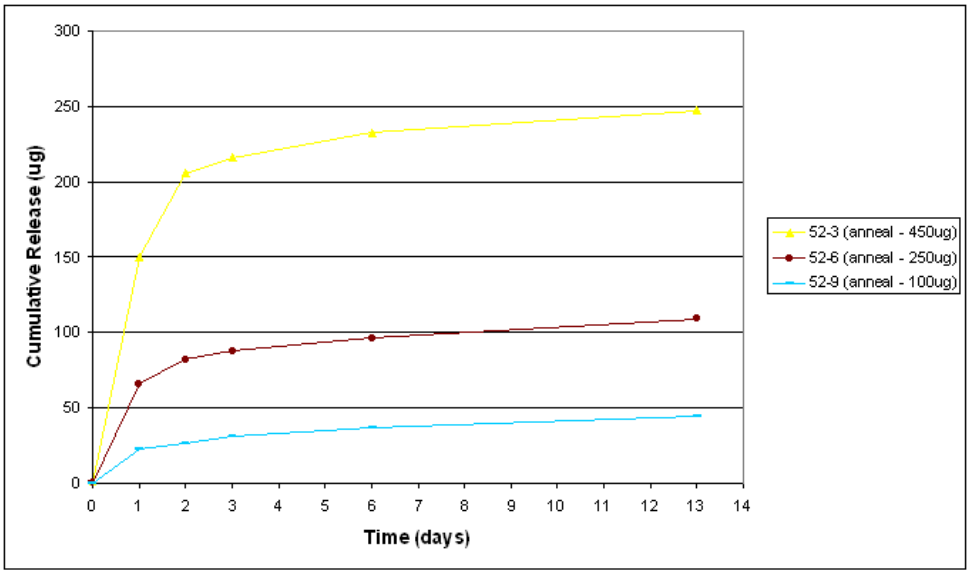

Figure 38 – Cumulative DNA elution from spray-coated stents with different plasmid loads

The cumulative DNA release is shown for three stents each prepared with a different predicted total plasmid load (stock 8kb plasmid). Graph provided by Medtronic.

The elution profiles supplied by Medtronic were considered to be sufficient to deliver a therapeutic DNA dose over an appropriate timescale. Stents were prepared by Medtronic coated with three doses of the plasmid encoding the control transgene (pGEG-2RE2HE-Psi-*lacZ*) for delivery *in vivo* to assess the optimum dose for gene delivery (see Sections 2.8.4 and 3.6). Two additional plasmid coated stents were supplied which allowed plasmid elution experiments to be performed in our laboratory to confirm the results of the elution experiments performed by Medtronic. A Nanodrop spectrophotometer was used to assess DNA concentration.

Figure 39 shows the cumulative elution profile for stents with two predicted DNA loads. DNA elution was far more rapid than had been suggested by the results provided by Medtronic with approximately 90% of the total DNA release occurring within the first 4 hours of incubation and almost all DNA eluting within 48 hours.

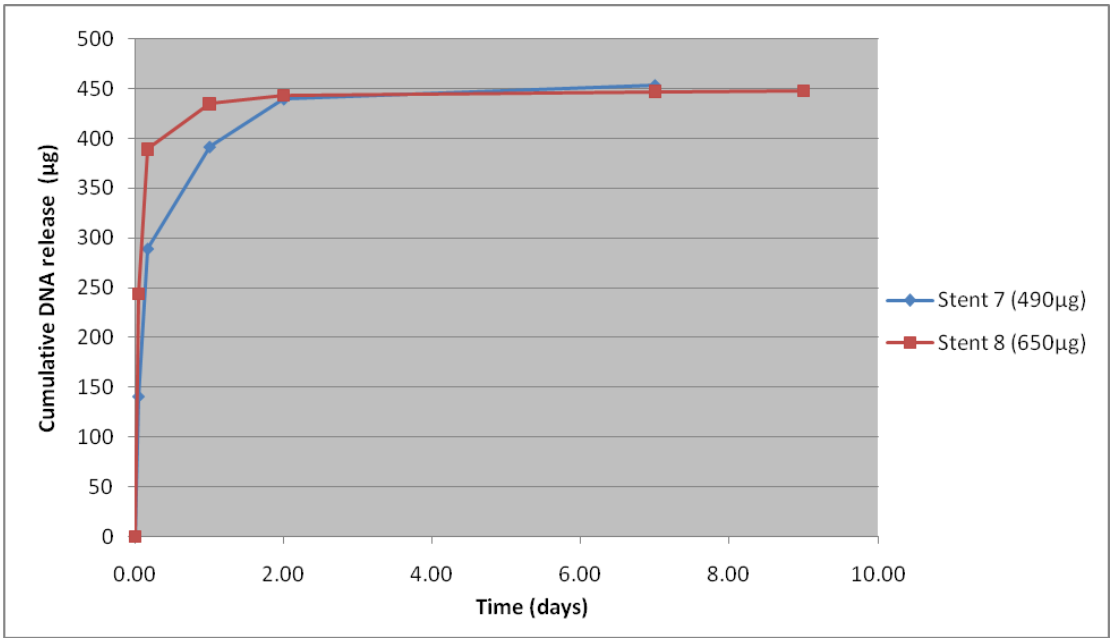

Figure 39 - Elution of DNA from stents prepared using original coating process

Predicted plasmid load is shown for each stent in brackets

Given that the rapid DNA elution demonstrated by our experiments would be unlikely to result in adequate sustained gene transfer we discussed with Medtronic possible solutions. Medtronic suggested that application of a thin cap-coat of polymer over the plasmid may slow down the elution rate of the plasmid. This so-called "capcoating" would involve application of the polymer as a dilute solution, dissolved in the solvent tetrahydrofuran (THF). As a result of the time constraints of the project there would be insufficient time for Medtronic to perform further experiments to ensure that this did not adversely affect plasmid integrity or elution. However given the suboptimal elution profile with the previous technique we felt that there was no choice but to ask Medtronic to perform the "capcoating" process on the remaining stents to be used *in vivo.*

In addition to the 30 stents to be deployed *in vivo,* two additional "capcoated" stents coated with the *lacZ* plasmid were supplied. Elution profiles for these stents were checked with spectrophotometry (Figure 40). DNA release was very similar to the previous method, with more than 90% eluted within 24 hours. This fast elution profile showed that the "capcoating" process was ineffective at slowing down release of plasmid from the polymer coating. Unfortunately there was insufficient time available at this juncture to investigate alternative coating techniques and thus these stents were accepted and used for the *in vivo* studies.

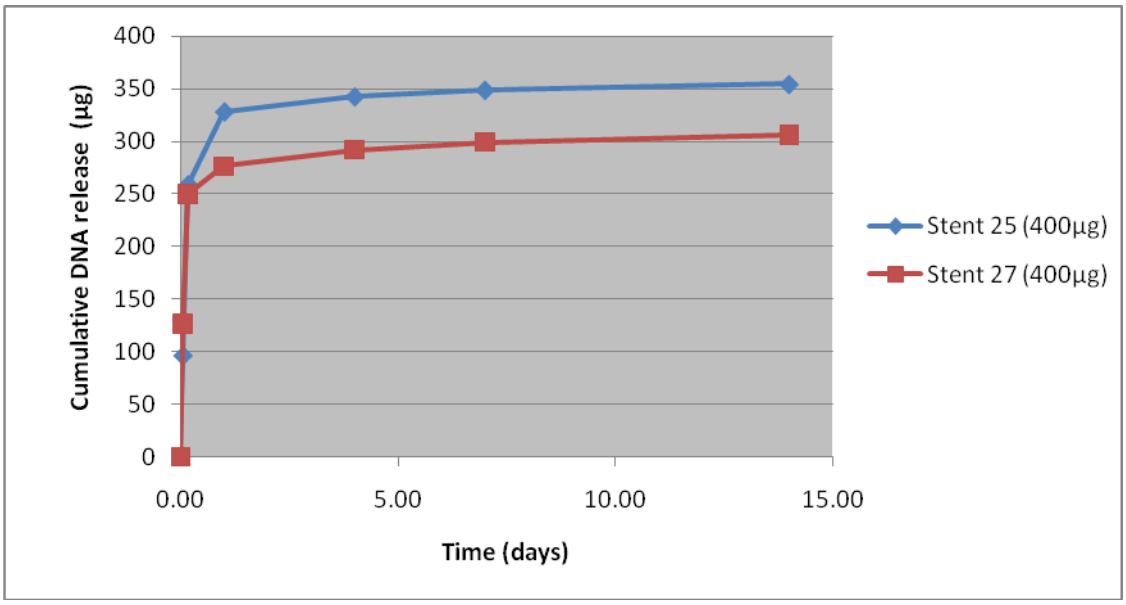

Figure 40 - Elution of DNA from stents prepared with "capcoating" process

Predicted plasmid load is shown for each stent in brackets

Restriction digests of the eluted DNA were performed using XhoI. There are four XhoI binding sites in pGEG-2RE2HE-Psi-*lacZ* and digestion leads to four bands of approximately 9100, 4400, 900 and 400bp. Figure 41 shows an XhoI digest of eluted DNA at two timepoints and confirms that the DNA was structurally intact.

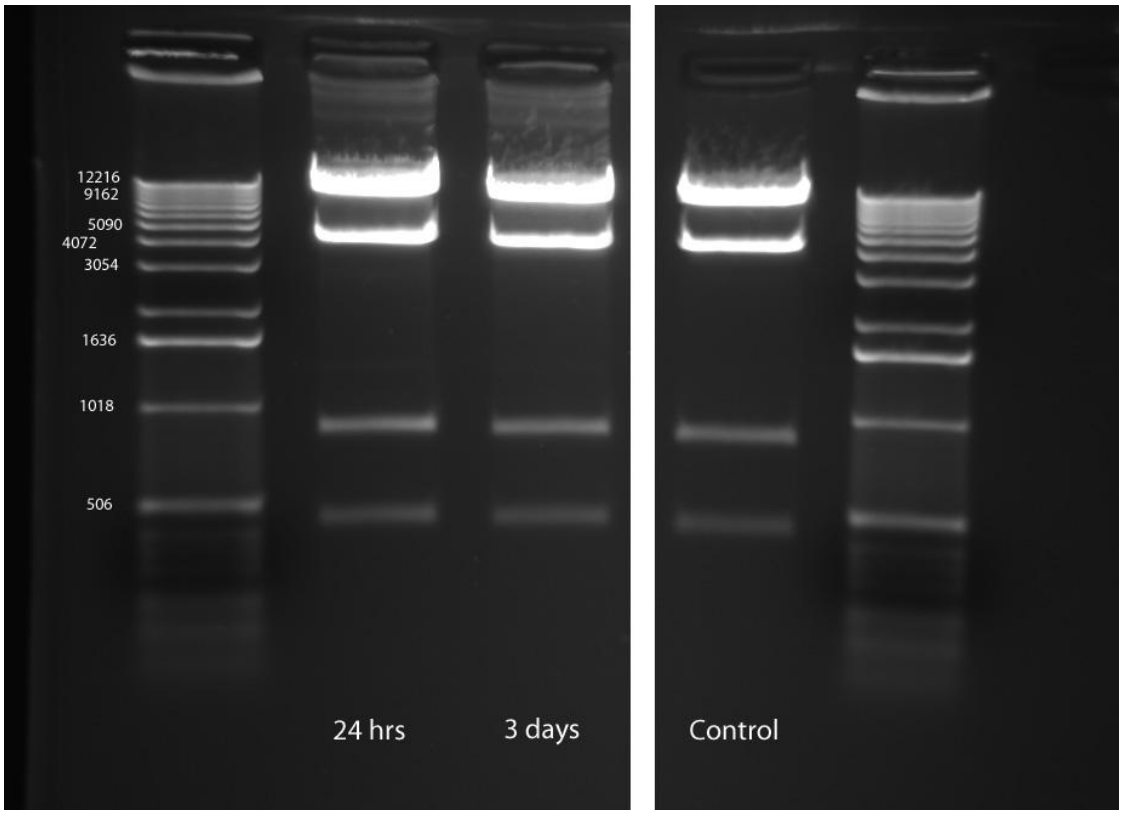

Figure 41 – XhoI restriction digest of eluted DNA from "capcoated" stents

XhoI digest of the stock pGEG-2RE2HE-Psi-*lacZ* plasmid is shown for comparison.

3.6 Assessment of optimum dose of plasmid on gene-eluting stents within porcine coronary arteries in vivo

Five stents were prepared for each of three estimated loading doses (100μg, 200μg and 400μg) of pGEG-2RE2HE-Psi-*lacZ*, the *lacZ*-expressing plasmid containing the optimal expression cassette for SMC transfection. The estimated applied dose was calculated by weighing the stents before and after dipping into plasmid solution. These stents were designated low, medium and high dose respectively and the calculated plasmid weights are shown in Table 10. Five control stents were also prepared coated with polymer only and no plasmid.

Table 10 – Estimated plasmid weights on gene-eluting stents for dose finding study

Dose	Amount of Bound Plasmid (ug)
Low Dose	84.4
	94.7
	95.2
	96.5
	85.3
Medium Dose	185.3
	180.8
	172.0
	165.5
	178.6
High Dose	400.3
	398.9
	354.5
	375.8
	363.6

The stents were deployed into pig coronary arteries as shown in Table 11. One stent embolised into the aorta following deployment and, although there were no adverse sequelae, only the circumflex artery could be used for analysis with this animal. There were no other procedural complications and all animals survived until sacrifice at day 7. In total there were segments suitable for analysis from coronary arteries treated with 5 low, 4 medium and 5 high dose gene-eluting stents, and 5 control stents.

Table 11 – *lacZ* gene expression 7 days following deployment of gene-eluting stents for dose finding study

Animal no.	Vessel	Plasmid dose	β-gal (A420)	Protein (A570)	*lacZ* gene expression (β-gal/protein)
1	Cx	Control	0.12	0.372	0.322
	LAD	Control	0.185	0.43	0.430
2	Cx	Low			Technical error
	LAD	Low	0.203	1.049	0.193
3	Cx	Medium	0.178	0.861	0.207
	LAD	Medium	0.17	1.146	0.148
4	Cx	High	0.2	0.919	0.218
	LAD	High	0.173	0.85	0.204
5	Cx	High	0.153	0.906	0.169
	LAD	Control	0.251	0.813	0.309
6	Cx	Low	0.16	0.702	0.228
	LAD	Medium	0.249	0.843	0.295
7	Cx	Control	0.167	1.174	0.142
	LAD	Medium			Embolised
8	Cx	High	0.114	0.432	0.263
	LAD	Low	0.201	0.82	0.245
9	Cx	Low	0.151	0.86	0.176
	LAD	Control	0.159	0.913	0.174
10	Cx	Medium	0.156	0.808	0.193
	LAD	High	0.161	0.819	0.197

LAD = left anterior descending coronary artery; Cx = circumflex artery; β-gal=β-galactosidase

Quantification of *lacZ* transgene expression was performed in tissue lysates using β-galactosidase and protein assays as described in Sections 2.5.2 and 2.5.3. The results are shown in Table 11. There was a pipetting error during the preparation of the tissue lysate from the Cx stent from animal 2 and this sample was not used for analysis.

The mean values for *lacZ* gene expression are shown in Table 12 (gene expression does not have a meaningful unit of measurement as it is a ratio of absorbances). There was no

statistical difference in *lacZ* gene expression between any of the 4 groups using this technique.

Table 12 – Mean *lacZ* expression following different doses of pGEG-PSi-2RE2HE-*lacZ* on gene-eluting stents

	Mean *lacZ* expression
Control	0.276
Low	0.211
Medium	0.211
High	0.210

X-gal staining of en face stented coronary artery segments was performed on two samples from each of the four groups to assess visually for *lacZ* gene expression. Representative samples are shown in Figure 42. Unexpectedly, blue staining was seen in all samples, including both of the control samples. However the pattern of staining in the control samples was of a diffuse nature between the stent struts; this pattern was also seen on some of the treated samples (see Figure 42, panel B). This pattern had the appearance of non-specific staining (ie. false positive). The plasmid-treated samples exhibited a different pattern of staining with focal areas of blue staining in the areas of artery which were exposed to the stent struts (panels B-D). This pattern was suggestive of *lacZ* gene expression (panels B-D).

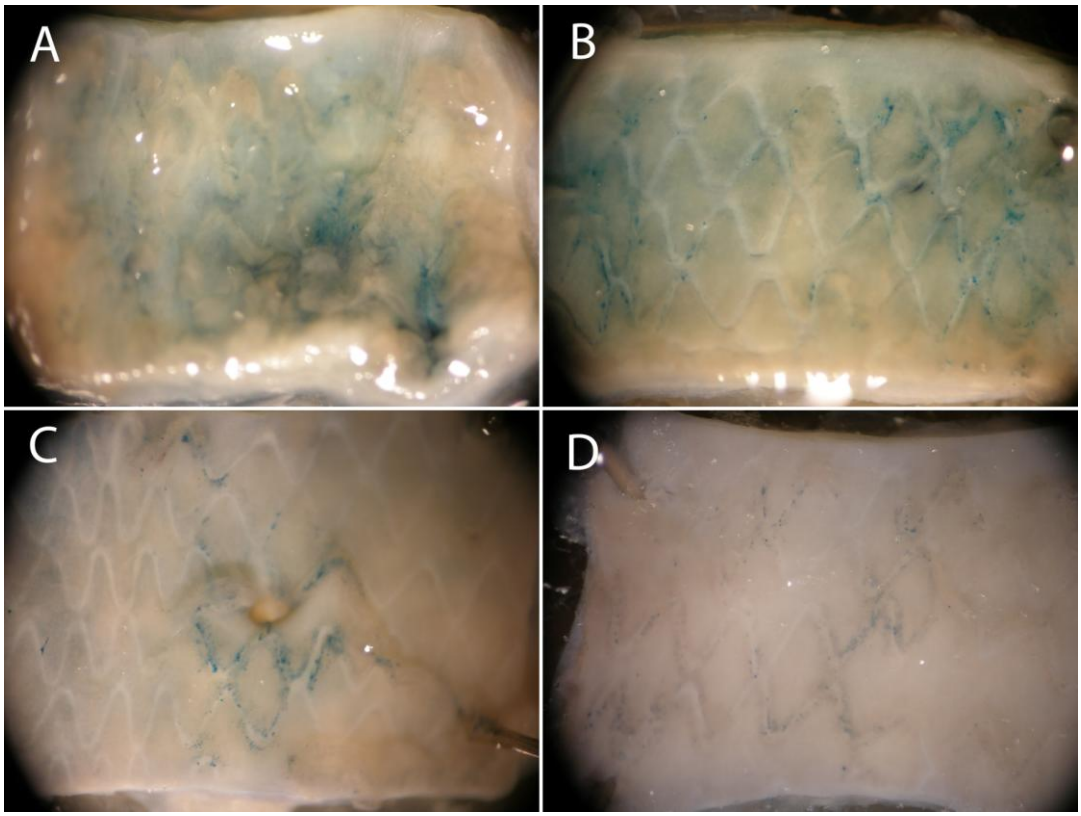

Figure 42 – X-gal staining of coronary artery segments treated with stents coated with different doses of plasmid

Samples from animals treated with a control stent (A) and low (B), medium (C) and high (D) dose plasmid-coated stents, at 7 days post-deployment. There was marked heterogeneity between samples within the same group and these samples were selected to demonstrate that there was no clear dose-effect relationship.

There was limited evidence of transgene expression, as assessed with these two techniques, but certainly no suggestion of a correlation of plasmid dose with gene expression.

Despite this lack of dose-effect correlation, it was encouraging that there was a more specific pattern of X-gal staining with the plasmid-coated stents and the highest dose of 400µg was selected for the therapeutic study. Some previous studies of gene-eluting stents have demonstrated successful transfection with even higher doses of plasmids than this (up to 1mg; see Table 1) and have not identified any safety concerns.

3.7 Effects of plasmid-mediated delivery of connective tissue growth factor and fibromodulin via gene-eluting stents in vivo

As detailed in Section 2.8.5, 30 pigs were randomised to receive a single 3mm stent deployed into the proximal LAD loaded with 400µg of plasmid encoding for either CTGF, FMOD or *lacZ* (control), resulting in a total of 10 pigs in each group. At day 28, repeat quantitative coronary angiography (QCA) was perfomed and then the pigs were sacrificed to allow vessel processing for morphometric analysis.

There were no periprocedural complications. One pig (THER9), treated with a *lacZ* stent, died suddenly at day 17. A post-mortem was performed and showed occlusive neointima within the stented area but no intracoronary thrombus. No other abnormalities were detected. The presumed mechanism of death was ischaemic ventricular fibrillation.

The QCA data for each of the groups is shown in Figure 43. There were no significant differences in target vessel diameter (TVD) or minimum lumen diameter (MLD) immediately following stent deployment. At 28 days there was numerically less late loss in the CTGF and FMOD treated arteries but this did not reach statistical significance (CTGF vs *lacZ* P=0.26; FMOD vs *lacZ* P=0.22; both 2-tailed T-tests). The full QCA data is presented in Table 14 in Appendix 6.5.

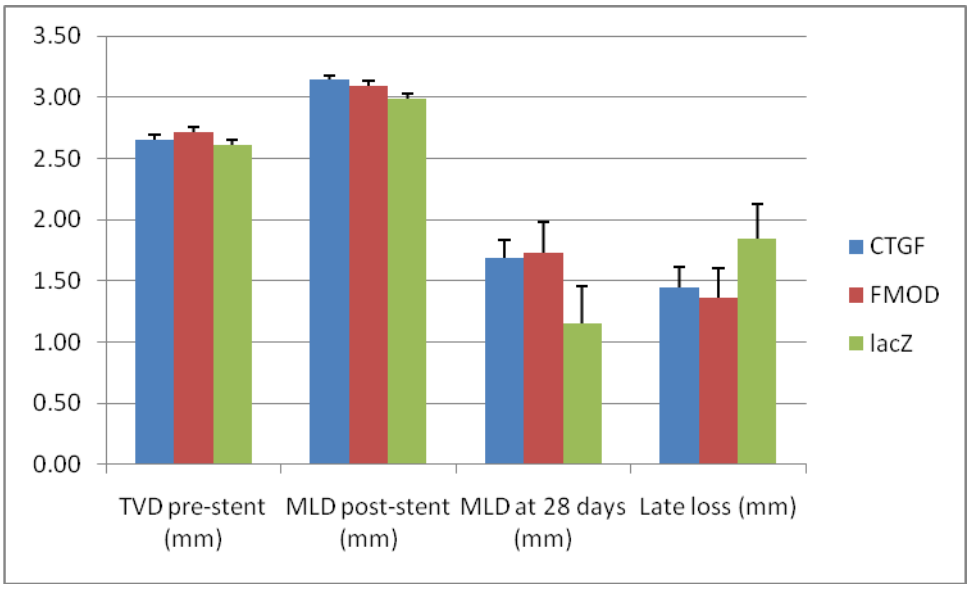

Figure 43 – Quantitative coronary angiography data from the therapeutic study

Bars represent the mean values for each group. Error bars indicate the standard error of the mean. TVD = target vessel diameter; MLD = mean lumen diameter; late loss = MLD post-stent – MLD at 28 days

Three sections were taken from each stented segment and processed for morphometric analysis as described in Section 2.8.5.1. Some sections were damaged or did not contain all of the stent struts as they were taken at the stent edge; these sections were not used for analysis. The internal elastic lamina (IEL) was severely disrupted and impossible to measure in many of the sections. The stent area was thus used as a surrogate for the IEL to allow calculation of the medial area. The section from each vessel with the smallest lumen area (and hence the greatest neointimal thickness and largest neointimal area) was used for subsequent analysis. Figure 44 shows a representative cross-section of a stented vessel.

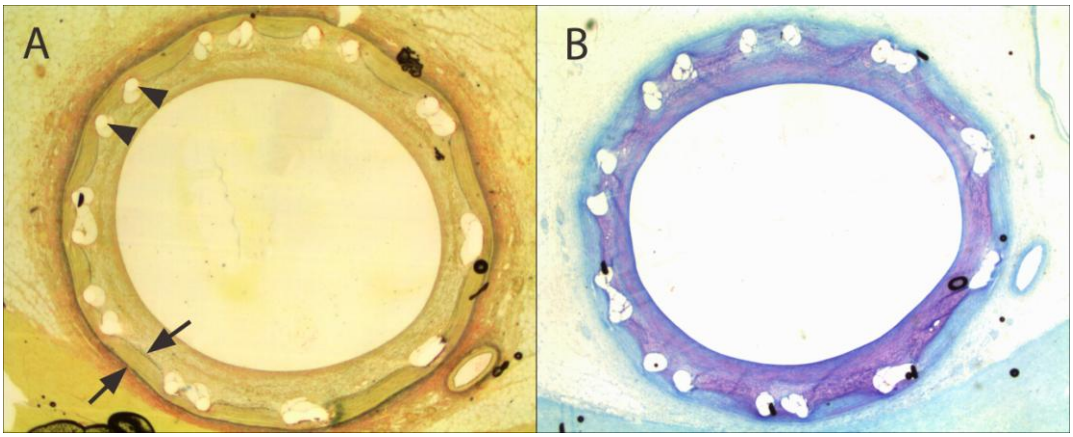

Figure 44 – Cross-section of stented vessel

The locations of the stent struts can be seen as white circles (panel A, arrowheads). The internal and external elastic laminae can be readily seen as blue lines with Miller's elastic stain (panel A, arrows). There is significant indentation but no frank disruption of the internal elastic lamina by the stent struts. Minor neointima formation has occurred. Panel A - Miller's elastic stain with picosirius red; Panel B - toluidine blue stain. The vessel shown was treated with an FMOD stent.

The mean injury score between the three groups is shown in Figure 45. Injury scores were higher than anticipated with a mean injury score of >2.8 for all groups and deep injury (ie. an injury score >2) had occurred in most of the vessels. Moderate injury without disruption of the IEL (ie. vessel injury score <=2) only occurred in 3/29 vessels analysed.

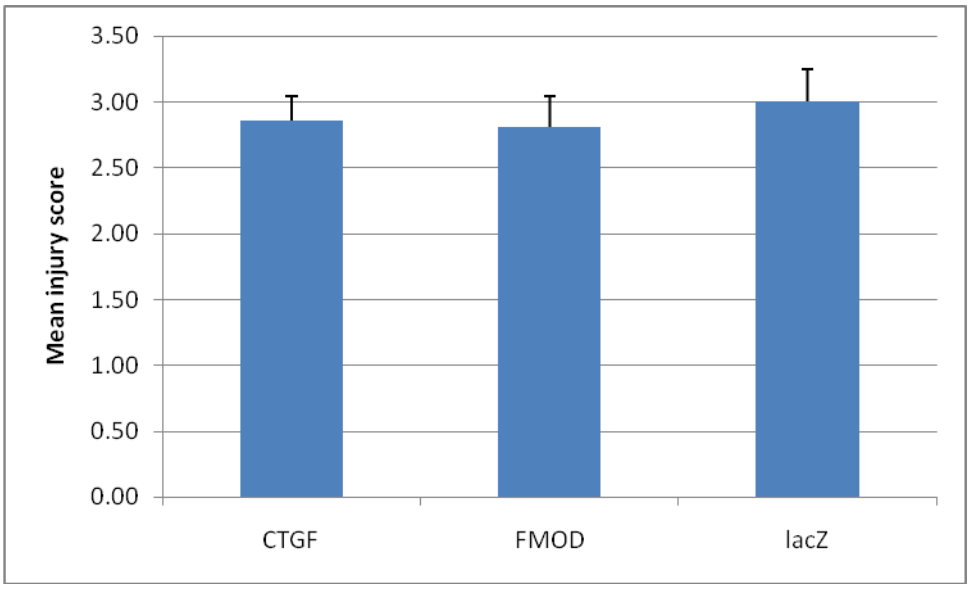

Figure 45 – Mean injury score at 28 days

Error bars indicate the standard error of the mean.

On morphometric analysis there were marked differences in neointimal formation between stented vessels, even within the same group. Figure 46 shows four different vessels treated with FMOD stents. Panel A shows only minor neointima formation, panels B-C show greater degrees of neointima formation, and panel D shows almost occlusive neointima with only a tiny residual lumen (on angiography prior to sacrifice this vessel was occluded with no anterograde flow). Similar degrees of heterogeneity were seen with the CTGF and *lacZ* treated vessels.

In many of the sections there was evidence of a small mononuclear cell infiltrate around the cell struts which was likely to be inflammatory in origin. This was often associated with significant disruption to both the IEL and external elastic lamina (EEL). This appearance is illustrated in panels C and D in Figure 46.

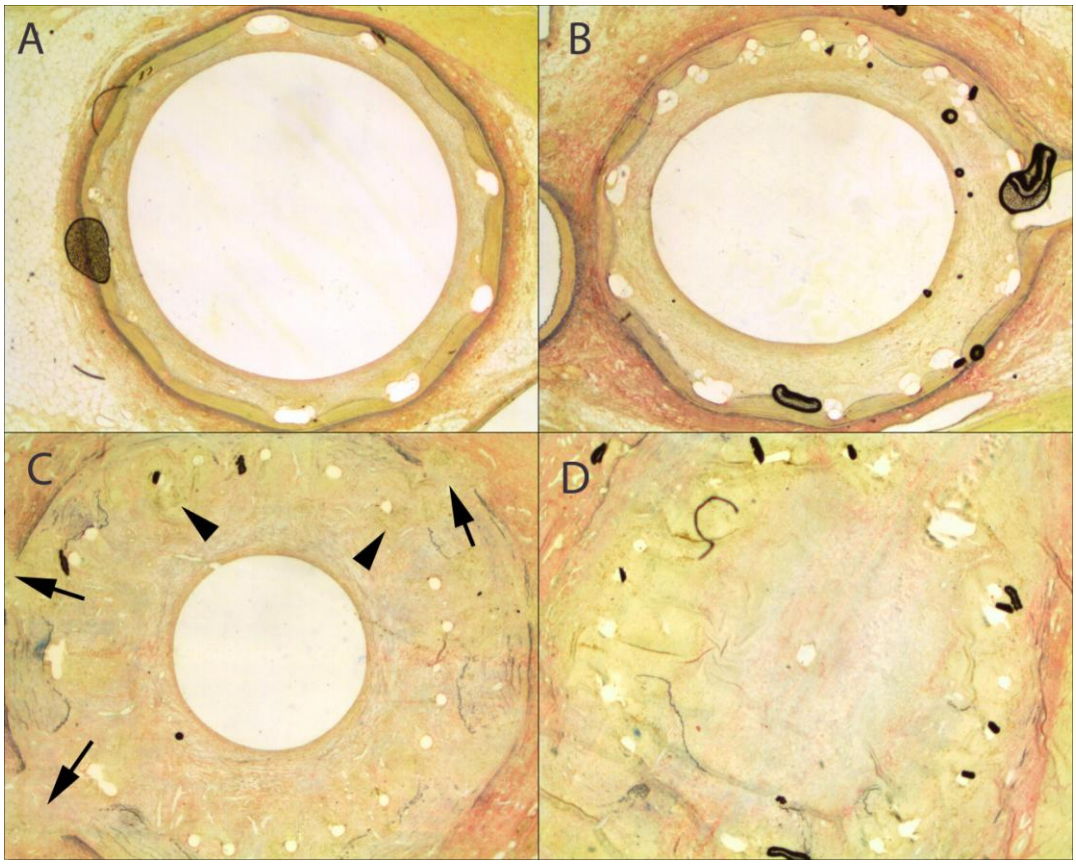

Figure 46 – Cross-sections of stented vessels showing varying degrees of neointima formation

Sections are from four different vessels treated with FMOD stents stained with Miller's elastic stain and picosirius red. Panels A & B show vessels with no significant IEL disruption and only moderate neointima formation. In panel C there is evidence of peri-stent inflammation (arrowheads) with associated disruption of both the IEL and EEL (arrowheads). There is significant neointima formation. In panel D there appears to be severe peri-stent inflammation with almost complete circumferential disruption of the IEL and EEL. Neointimal formation is severe and almost occlusive.

There was no significant difference in mean maximum neointimal thickness between the three groups (Figure 47). Lumen, EEL, stent, neointima and media areas for the three groups are shown in Figure 48. Again there was no significant difference between any of the groups.

The full morphometric data are presented in Table 15 in Appendix 6.5.

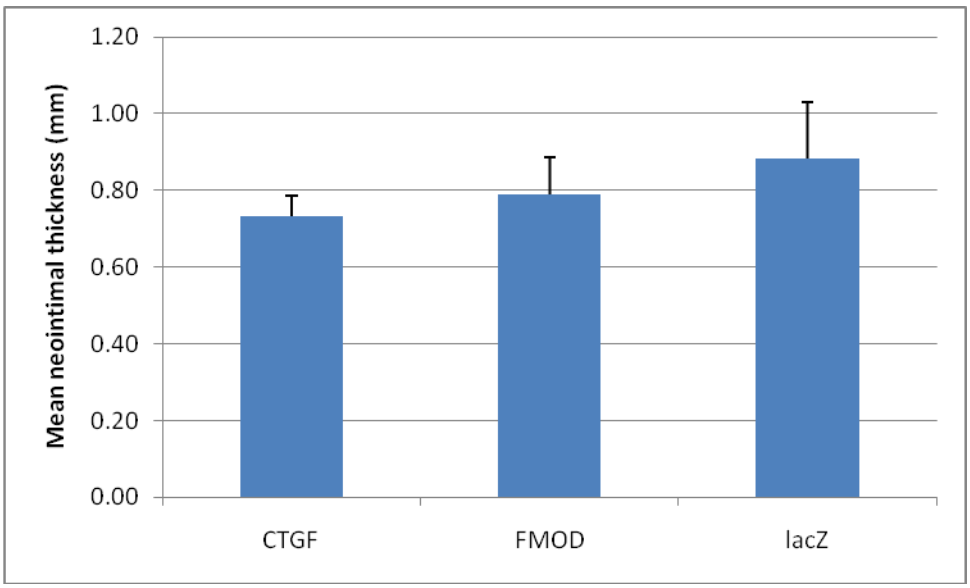

Figure 47 – Mean neointimal thickness at 28 days

Error bars indicate the standard error of the mean.

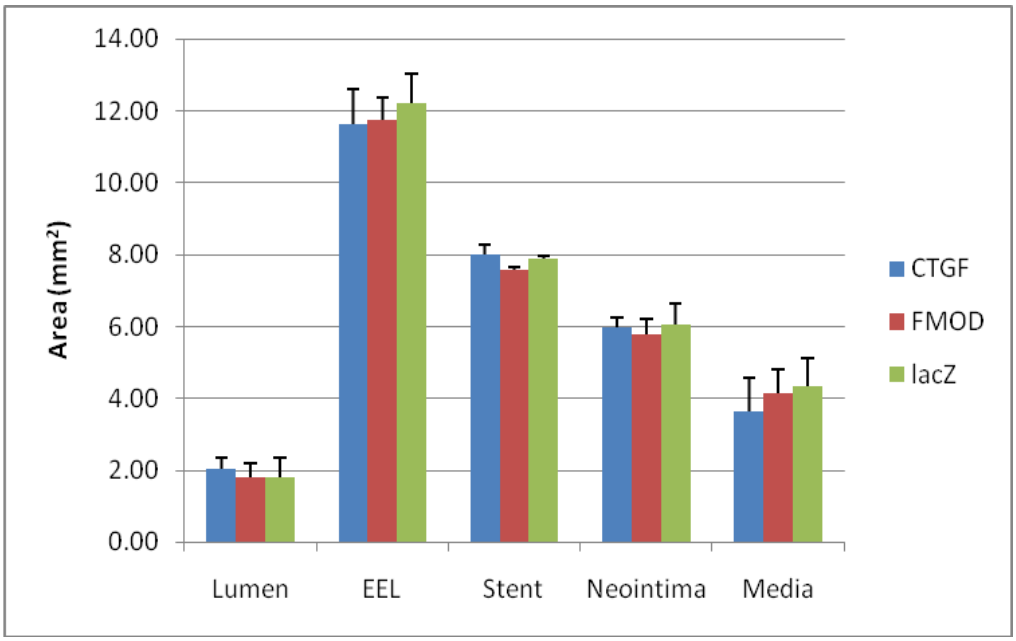

Figure 48 – Morphometric data from the therapeutic stent study

Morphometric data from the stented vessels at 28 days following deployment. Bars represent the mean for each group. Error bars indicate the standard error of the mean. EEL = external elastic lamina.

3.8 Expression of exogenous CTGF and FMOD in stented porcine coronary arteries

Given that there was no demonstrable biological effect observed with either of the putative therapeutic transgenes, no further mechanistic studies were performed.

One possible explanation for the absence of a biological effect is that there was insufficient transgene expression with the delivery system and plasmids utilised. Transgene expression in the vascular wall following plasmid-elution stent deployment was therefore quantified using the quantitative polymerase chain reaction (qPCR).

3.8.1 Quantitative PCR

As described in Section 2.8.6.1, three pCTGF-, three pFMOD- and one p*lacZ*-coated stents were deployed in the proximal LAD of 7 pigs. The stented coronary artery segments were harvested at 7 days and RNA extraction and complementary DNA synthesis was carried out. qPCR was then performed with the Taqman system using custom gene assays for human CTGF and bovine FMOD. The *lacZ* and non-targeted transgene transfected samples were used as reference controls.

Figure 49 shows the amount of transgene expression 7 days following deployment of pCTGF-coated stents. There was no detectable increase in CTGF expression at this timepoint in the pCTGF treated segments as compared to the reference controls which had been treated with either p*lacZ* or pFMOD.

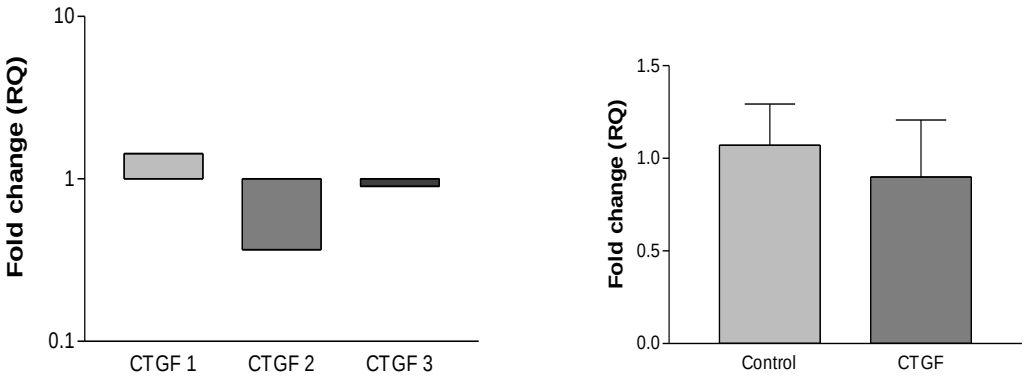

Figure 49 – CTGF transgene expression at 7 days in transfected coronary arteries *in vivo*

CTGF transgene expression as assessed by qPCR is shown for the three transfected coronary artery samples. The left graph shows values plotted for each sample as fold change in gene expression as compared to the mean of the reference samples. The mean change in gene expression for the reference samples (n=4) and for the CTGF-transfected samples (n=3) are shown in the right graph. Error bars indicate the standard error of the mean.

Figure 50 shows the amount of transgene expression at 7 days following deployment of pFMOD-coated stents. In all three treated segments there was a large increase in gene expression of FMOD, with increases in transgene expression of 118-, 5426- and 295-fold as compared to the reference segments (treated with either p*lacZ* or pCTGF).

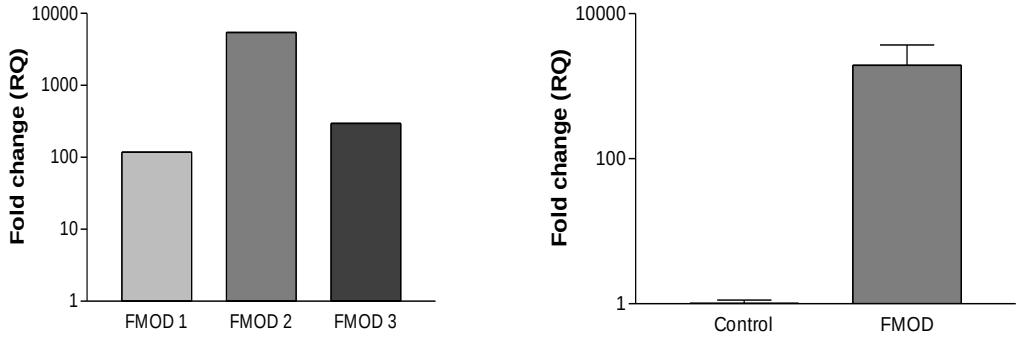

Figure 50 – FMOD transgene expression at 7 days in transfected coronary arteries *in vivo*

FMOD transgene expression as assessed by qPCR is shown for the three transfected coronary artery samples. The left graph shows values plotted for each sample as fold change in gene expression as compared to the mean of the reference samples. The mean change in gene expression for the reference samples (n=3) and for the CTGF-transfected samples (n=3) are shown in the right graph. Error bars indicate the standard error of the mean.

3.9 Effects of beta-blockers on gene expression in vivo

The effect of β-blockers on transgene expression were assessed in six pigs, three of which had been pre-treated with the β-blocker bisoprolol as discussed in Section 2.8.7. The mean heart rate following induction of general anaesthesia was 103 in the bisoprolol-treated animals and 146 in the untreated animals (P=0.009) confirming adequate β-blockade. Each pig received both a bare metal stent and a plasmid-coated stent with an estimated dose of 400µg of pGEG-2RE2HE-Psi-*lacZ* (prepared by Medtronic), as shown in Table 13. There were no procedural complications and all animals survived until sacrifice at day 7.

Table 13 – *lacZ* gene expression 7 days following deployment of gene-eluting stents for β-blocker study

Animal code	Baseline heart rate	Vessel	Stent type	β-gal (A420)	Protein (A570)	*lacZ* gene expression (β-gal/protein)
CON1	140	LAD	p*lacZ*	0.077	0.87	0.089
		Cx	BMS	0.076	0.93	0.082
CON2	136	LAD	p*lacZ*	0.16	1.18	0.135
		Cx	BMS	0.188	1.50	0.126
CON3	162	Cx	p*lacZ*	0.216	1.45	0.149
		LAD	BMS	0.172	1.35	0.127
BIS1	101	LAD	p*lacZ*	0.134	1.42	0.094
		Cx	BMS	0.146	1.24	0.118
BIS2	111	Cx	p*lacZ*	0.335	1.71	0.196
		LAD	BMS	0.137	1.32	0.104
BIS3	98	LAD	p*lacZ*	0.305	1.66	0.184
		Cx	BMS	0.222	1.51	0.147

BMS = bare metal stent; p*lacZ* = pGEG-2RE2HE-Psi-*lacZ* coated stent; β-gal = β-galactosidase

Quantification of *lacZ* transgene expression was performed in tissue lysates using β-galactosidase and protein assays as described in Sections 2.5.2 and 2.5.3. The results are shown in Table 13. The mean calculated *lacZ* gene expression for the six vessel segments treated with p*lacZ* coated stents was 0.141 and for the six treated with bare metal stents was 0.117. This difference was not statistically significant (P=0.26).

For the six segments treated with p*lacZ* coated stents, the mean *lacZ* gene expression for the three in control animals was 0.124 and for the three in β-blocker treated animals was 0.158. Again this difference was not statistically significant (P=0.41).

X-gal staining of the en face stented coronary artery segments was performed at day 7 to assess for β-galactosidase expression. There was visible blue staining in all of the segments treated with p*lacZ* coated stents and no staining visible in the segments treated

with bare metal stents. X-gal staining was patchy across the stented segment with no direct correlation with the stent struts. There subjectively appeared to be less staining in the segments from β-blocker treated animals than in the segments from animals which did not receive β-blockers. However it was not possible to quantify this accurately given the limited degree of staining. Representative sections are shown in Figure 51.

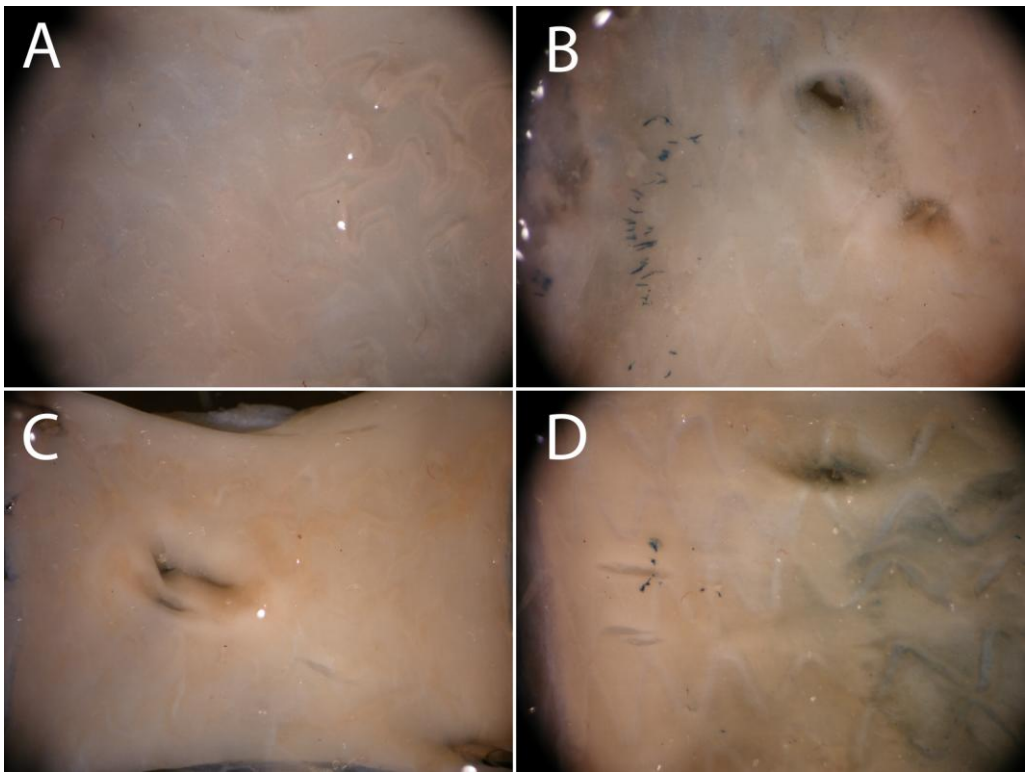

Figure 51 – X-gal staining of stented coronary artery segments in β-blocker treated animals

Control segments (panels A & B) and segments from animals treated with β-blockers (panels C & D) are shown at 7 days. Panels A & C are from animals treated with bare metal stents and panels B & D are from animals treated with stents coated with p*lacZ*.

4 Discussion

The introduction and widespread utilisation of coronary stents has revolutionised the treatment of coronary artery disease and drug-eluting stents, coated with potent anti-mitotic agents, have dramatically reduced the rate of vessel restenosis seen with the earlier generation bare metal stents. However, as well as reducing neointimal proliferation, drug-eluting stents delay re-endothelialisation of the stented vessel segment and are associated with an increased risk of late stent thrombosis. There also remains a clinically important risk of restenosis when drug-eluting stents are deployed in patients with diabetes mellitus and in complex coronary lesions including bifurcations and chronic occlusions.

Novel approaches are needed to tackle the enduring problems of restenosis and stent thrombosis following coronary stent deployment. Earlier work by our group has demonstrated a beneficial effect of gene therapy with both fibromodulin (FMOD) and connective tissue growth factor (CTGF) on neointima formation in an *ex vivo* human saphenous vein graft model. The main aim of this study was to develop gene-eluting stents, coated with vectors encoding these two transgenes, and then investigate the effect of these stents *in vivo* in a pig coronary model of instent restenosis.

Plasmids were selected as the gene delivery vector for the main study. As gene delivery via plasmid vectors is substantially less potent than with viral vectors, several novel transgene expression cassettes were developed and their effects on transgene expression in coronary artery SMCs (the likely target cell for transfection) were investigated. Planned supplementary work included investigation of the potential mechanisms for the effect of CTGF on neointimal proliferation and the effects of β-blockade on transgene expression *in vivo*.

4.1 Mechanisms of action of CTGF

Our group has previously demonstrated that *ex vivo* adenovirus mediated gene transfer of CTGF in the SVG model reduces neointimal formation as compared to a *lacZ* control (**unpublished data**). Analysis of slides prepared from this earlier work, which had been stained with picosirius red, showed a greater collagen content in the *lacZ* group as compared with the CTGF group. However this appears to be solely as a result of the

greater quantity of neointima in the *lacZ* group since, when the collagen content is controlled for total area of the segment, there is no difference between the groups. This is not entirely surprising as, although CTGF has been demonstrated to increase collagen production *in vitro*, CTGF-knockout mice do not demonstrate reduced levels of collagen[227] suggesting that the effects of CTGF on collagen may not be important *in vivo*.

A limitation is that a true control group was not available for analysis. *lacZ* gene expression would not be expected to affect collagen production, but the presence of the adenoviral vector itself may have unforeseen biological effects. Although the original experiments had included vein graft specimens which had been exposed to PBS alone (with no viral vector present), sections stained with picosirius red had not been prepared from these specimens. There was no significant difference in the degree of neointima formation between Ad5-*lacZ* and PBS control in these original experiments (**unpublished data**).

Further viral infections of SVG segments were performed using Ad5-CTGF and Ad5-*lacZ* aiming to elucidate the mechanisms responsible for the previously demonstrated reduction in neointima formation with CTGF. At all time points in both groups CTGF production was evident in the intima and endothelium, as assessed by DAB immunohistochemistry and immunofluorescence (Figure 18, Figure 19 and Figure 20). As CTGF appeared to be present in the *lacZ* control group this suggests that either CTGF is constitutively produced within saphenous veins or is produced in response to the experimental conditions of this model, which is known to induce neointimal formation analogous to that which occurs with vascular injury. CTGF is known to be endogenously produced in certain blood vessels: constitutive production of CTGF has been described in the aorta and coronary arteries of the adult mouse[226]. Although there are no previous reports of CTGF production in the venous wall of any species, it is likely that this explains the results seen in these experiments.

An alternative explanation is that the CTGF antibody used (Abcam, catalogue number: ab6992) is of limited reliability. Abcam recommends the use of human hippocampal protein extract as a positive control (http://www.abcam.com/CTGF-antibody-ab6992.html) but we were unable to source any of this tissue to study. However, this

antibody has been used successfully in several published research articles and user reviews from the Abcam website suggest that it has high specificity. Positive results were obtained with this antibody following *in vitro* transfection using a CTGF plasmid (see Figure 30) and it is therefore most likely that the results seen in the vein segments were due to genuine endogenous neointimal/endothelial CTGF production.

Surprisingly CTGF content was not higher in the Ad5-CTGF infected group than in the *lacZ* control. There are several possible reasons for this lack of difference. Firstly, it may be that, as discussed, there was endogenous production of CTGF in the vein segments and that the immunohistochemistry and immunofluoresence techniques used were of insufficient sensitivity to demonstrate an additional increase in CTGF production as a result of transgene expression.

Secondly, adequate CTGF transduction may not have occurred. This may have been due to experimental error during the luminal instillation stage of the protocol. Following virus instillation, ligation and clipping of the ends of the vein is performed and the segment is placed in culture medium for an hour. During this stage it is possible for the viral solution to escape from the vein if the ligation is inadequate. Another possible cause for poor CTGF transduction is that the virus stock had inadvertently undergone a thaw-freeze cycle due to failure of the -70°C freezer in which it was stored. However the viral titre had been calculated by serial dilution end-point assay, demonstrating that the stock could still induce cytopathic effect, and therefore the gene transfer efficacy of the virus should not have been significantly impaired.

A final limitation is that, as with the picosirius red experiments, no true control group was available for analysis. All vein graft specimens available were infected with either Ad5-*lacZ* or Ad5-CTGF and no specimens were instilled with a virus-free solution.

As a result, interpretation of results from these Ad5 SVG infection experiments is open to considerable caution. For instance, there was no difference demonstrated between the groups in proteoglycan content as assessed by Alcian Blue staining. Although this may have been due to the technique (the protocol we adopted was used on micromass cultures rather than solid tissue[270]), or the fact that there is genuinely no difference between the two groups in terms of proteoglycan production, an alternative explanation

is that there was inadequate transduction of the CTGF gene due to one of the reasons discussed above.

4.2 Promoter optimisation

The ability of RE, HE and a DNA targeting sequence (D) to increase gene transfer efficiency within human arterial coronary SMCs was investigated. The pGEG.PSi-*lacZ* plasmid has been demonstrated previously by our group to have a high level of gene transfer efficiency in SMCs **(unpublished data)**. Preliminary results from this current work suggest that the inclusion of two copies of the rabbit enhancer fragment and two copiers of the human enhancer fragment (i.e. 2RE2HE) in the expression cassette of this plasmid significantly increases transgene expression in human coronary artery SMCs further *in vitro* by a factor of 12 as compared with pGEG.PSi-*lacZ*. The other expression cassette constructs, which all included the SMC-specific DNA targeting sequence, did not improve gene transfer efficiency over the original plasmid. Importantly, the D2RE2HE insert had similar levels of transgene expression to pGEG.PSi-*lacZ* suggesting that the D element itself interferes with the enhancer effect of RE and HE.

There are several possible reasons why the inclusion of D did not improve gene expression. In previously published studies D was inserted downstream of the transgene and polyadenylation sequence[163-165] where it would not be transcribed into mRNA and potentially interfere with translation. As the D sequence contains binding sites for SRF and the NK family of transcription factors, binding of these factors to the plasmid DNA may also interfere with the function of the expression cassette regulatory elements.

A comparison of 2RE2HE with the other combinations of these enhancers (2RE, 2HE, REHE, RE) cannot be made from this data given the interference from the D element. Although, given that enhancers demonstrate copy dependency, it might be expected that this is the most potent combination further experiments will need to be completed to confirm this.

4.3 Development of gene-eluting stents

Preparation of commercial DES, coated with a mixture of polymer and drug, is a complex industrial process. Medical device manufacturers have spent considerable

resources developing their own stent coating methods, with each company having developed their own proprietary polymer which is applied to the stent in different quantities and via different methods. This allows precise control over the amount of drug present and its elution profile over a desirable timeframe. An ideal polymer should be biocompatible and resistant to fracture during stent crimping and expansion. There should be a smooth, homogenous coat over the stent struts, which enhances biocompatibility whilst ensuring consistent drug elution throughout the length of the stent. Webbing of the polymer between stent struts (which can obstruct side-branches) must be avoided.

The majority of commercial DES for use in humans have the polymer applied by spray coating. This results in a smooth layer of polymer, with a precise thickness and no intrastrut webbing, which is resistant to crimping and expansion. Given the difficulties in replicating this process in our laboratory, a research agreement had been formed with Medtronic, Inc. (Minneapolis, MN, USA), one of the largest medical technology companies in the world and one of the leading developers of coronary stents. Medtronic committed to provide polymer-plasmid coated coronary stents for use within our *in vivo* experiments, prepared using a proprietary industrial process at Medtronic's European research facility, the Bakken Institute in Maastricht.

Shortly after the research project commenced, the interventional cardiology division at the Bakken Institute was unexpectedly closed, in part as a result of the global economic downturn. This lead to considerable uncertainty as to whether Medtronic would be able to provide the plasmid-coated stents within an appropriate timescale for the *in vivo* work to be completed in. Alternative methods of coating stents with a polymer-plasmid mixture were therefore considered and preliminary experiments on two separate techniques for polymer coating stents were performed.

Egashira and colleagues have previously described the use of stents dip-coated with a mixture of polyvinyl alcohol and plasmid[178]. The authors reported that a film of polymer formed over the outside surface of the stent, but these stents were successfully deployed in iliac arteries of rabbits and monkeys with demonstration of transgene expression. Stents were prepared using this technique in our laboratory but there was an uneven, irregular distribution of polymer coating which resulted in marked webbing and

bridging between the stent struts. Although this external polymer film may not have been a concern in iliac arteries, it is extremely undesirable in coronary arteries. If there is webbing between the stent struts then the polymer could embolise distally or interfere with flow in side-branches during stent deployment causing intraprocedural myocardial infarction. Another limitation of this process is that it proved impossible to control the exact amount of polymer (and hence amount of DNA) which will bind to the stent; multiple dips were often required which exacerbated the problem. It was decided not to investigate this technique further.

Subsequently a collaboration was formed with Surface Solutions Laboratories (Carlisle, MA, USA), a specialist American polymer company with previous experience in preparing gene-eluting stents which were deployed successfully by Takahashi and colleagues in rabbit iliac arteries[137]. Surface Solutions also applied the polymer-DNA solution to stents by hand dip-coating and the stents provided had a thin film of polymer webbing between the stent struts. However this was of a far more homogenous nature than that obtained with dip-coating of polyvinyl alcohol in our laboratory and survived a crimp-expansion cycle without cracking. DNA elution experiments showed a satisfactory elution profile. However although the initial eluted DNA was intact, there appeared to be significant degradation of the DNA eluted after the first six hours.

The polymer coated stents prepared by Surface Solutions were subject to preliminary investigation *in vivo*. There was an aggressive neointimal response, with the stent struts completely covered at 7 days in every case. This was in marked contrast to the stents provided by Medtronic, and used in the later experiments, in which no stent struts were covered at 7 days following deployment. This coating technique was not investigated any further, as Medtronic were able to perform the stent coating process as originally agreed in an appropriate timeframe.

The technique Medtronic utilised involved initial spray coating of the stent to create a porous coat followed by immersion in a plasmid solution and gentle heating to close the pores. As this process also necessitated a dip-coating step, there was still some webbing between the stent struts but this was far thinner than with the other two processes and the amount of polymer on the stent struts was visibly thicker. Although still not ideal for *in vivo* use, this process was considered to be the best of the three options available.

The lengthy process in obtaining suitable polymer-coated coated stents for the *in vivo* experiments illustrates the difficulties in performing complex translational basic science research. Collaboration with industrial partners is often required which has the potential to cause significant delays and intellectual property concerns mean that detailed methodology is often unavailable.

4.4 Use of lacZ as a marker gene in pig coronary arteries

lacZ has been used as the marker gene in numerous studies of stent-mediated vascular gene transfer in rabbit carotid, rabbit iliac, rat carotid and money iliac arteries[134, 137, 172, 176, 178, 181]. Our group has extensive experience of gene therapy using the *lacZ* transgene in pig coronary arteries *in vivo* delivered via viral vectors, applied via a specialised delivery catheter[155] and via collagen-coated stents (**unpublished data**). These experiments demonstrated convincing staining in the treated arteries and absence of staining in the control arteries. As a result of this experience, *lacZ* was selected as the marker gene in the current study of plasmid-eluting stents.

The initial studies examined the effects of stents coated with different doses of the *lacZ* plasmid, in order to ascertain whether a plasmid dose-response relationship existed. X-gal staining of the stented segments at day 7 showed blue staining along the areas of vessel exposed to stent struts, which appeared suggestive of β-galactosidase transgene expression. However staining was also seen in the vessels exposed to control stents coated with polymer alone. In these vessels, the staining had a more diffuse nature, being present throughout the vessel wall and not specifically related to the stent struts. Some of the plasmid treated vessels exhibited both non-specific staining, and specific strut-related staining.

The finding of blue staining with the X-gal stain in vessels not exposed to a *lacZ* gene vector is surprising. However false positives, presumed related to endogenous β-galactosidase activity has been described in a variety of different mammals[279]. Lim and colleagues investigated delivery of *lacZ* via plasmid vectors (mixed with Lipofectin) in canine coronary arteries and assessed β-galactosidase expression with X-gal staining[280]. They reported that 13 out of 18 transfected arterial segments showed positive X-gal staining, but activity was also detected in three of 11 non-transfected segments and four out of six segments exposed to Lipofectin alone. Luciferase, an alternative marker gene,

was far more specific with absent activity in non-transfected vessels. They concluded that *lacZ* may not be an appropriate marker gene for use in the canine vasculature.

A potential mechanism for endogenous β-galactosidase staining is related to cellular senescence. Senescent cells have entered a permanent state of growth arrest and are enlarged in morphology and express negative regulators of the cell cycle[281]. Atherosclerosis and neointima formation following vascular injury have been associated with the development of senescent cells as a result of increased cellular replication[281]. β-galactosidase positivity (at pH 6) is considered to be a biomarker of replicative senescence and has been demonstrated following vascular injury to the rabbit carotid artey[282] and in atherosclerotic coronary arteries[283].

The false positive staining appears to be related to the use of the polymer coatings on the stents. Blue staining was seen in the preliminary *in vivo* experiments with stents coated with urethane polymer only (Figure 35) as well as in the dose-finding study with stents coated with Medtronic's proprietary polymer only (Figure 42). In the β-blocker studies, the control stents used were "bare metal" stainless steel without a polymer coating. There was no blue X-gal staining in any of these control vessels.

It can be hypothesised that the inflammatory response to the polymer can induce endogenous β-galactosidase expression in porcine coronary arteries. The mechanism for this may be the development of cellular senescence due to increased cellular replication as discussed above. Future experiments investigating the deployment of polymer-coated stents as gene delivery vehicles in the porcine coronary artery model should consider the use of alternative control genes such as luciferase or green fluorescent protein (GFP).

4.5 Lack of biological effect with FMOD and CTGF gene-eluting stents

The main study compared the action of stents coated with plasmids encoding for the "therapeutic" genes: CTGF and FMOD, and the control gene *lacZ*. The plasmid backbone identified from the *in vitro* experiments as resulting in the maximum gene expression in SMCs was used. Stents were deployed *in vivo* in juvenile pig coronary arteries and the effects on neointimal hyperplasia and instent restenosis, as assessed by

quantitative coronary angiography and by morphometric analysis were assessed at 28 days. At this timepoint there was no difference in the degree of neointimal hyperplasia or restenosis between either of the two therapeutic transgenes and the control group.

Why was there a lack of observed effect? It is unlikely that there was an issue with the plasmid DNA itself. All three transgenes used in this study (human CTGF, bovine FMOD and *lacZ*) have been utilised by our group previously and effective transgene expression has been demonstrated using viral vectors. Following plasmid construction in this study, great care was taken to ensure that plasmid identity was correct before proceeding with the *in vivo* experiments. Three separate techniques were used for this. Firstly, selective restriction enzyme digestion was performed which confirmed that the anticipated DNA bands were present. Secondly PCR was performed, using custom primers for CTGF and FMOD, on both the newly constructed plasmids and the original plasmids from which the transgenes were derived. Finally, the plasmids were shown to be functional, and successful *in vitro* transfection was demonstrated with all three transgenes.

The *in vivo* experiments suggested that transgene expression was occurring, but at much lower levels than anticipated. The dose-finding and β-blocker studies showed that *lacZ* expression was sparse and not seen adjacent to all stent struts. To assess for gene expression of the therapeutic transgenes, quantitative PCR using gene assays for CTGF and FMOD was performed. Evidence of transgene expression was demonstrated for FMOD, but there was no evidence of increased gene expression with the CTGF stents as compared to the control group. The reason for this probably relates to endogenous CTGF production, which has been previously demonstrated to occur within both healthy and diseased blood vessels. CTGF is produced at high levels within atheromatous lesions in human aortas[210] and constitutive production of CTGF has also been described in uninjured coronary arteries in the healthy adult mouse[226]. Earlier work from this study suggested that there was significant endogenous expression of CTGF in the neointima which forms during tissue culture of human saphenous vein grafts. These combined results imply that there is likely to be significant endogenous expression of CTGF within the injured coronary artery wall following stent deployment. Therefore any increase in gene expression as a result of transgene transfer may have been

insufficient to be measurable with the techniques used (i.e. the signal:noise ratio was too low to be detected).

Although it is possible that the proteins chosen are simply ineffective at reducing restenosis, earlier work in the SVG model using viral vectors demonstrated a positive biological effect and the most likely explanation for the neutral results of the current study is that the degree of transgene expression was inadequate to exert any potential beneficial effect. These results therefore should not be interpreted as indicating that FMOD and CTGF are ineffective at reducing restenosis, but rather that the methods used to deliver these genes to the vasculature were inadequate to produce sufficient transgene expression and protein production.

4.6 Lack of impact of β –blockers on plasmid-mediated transgene expression

β-blockers have been demonstrated to reduce transgene expression from CMV promoters following viral gene transfer into the vascular wall[264]. Unpublished data from our group has shown that the β-adrenergic agonist isoprenaline does not affect transgene expression in cultured SMC transfected with plasmid, but the effect of β-blockers on plasmid-mediated gene expression has not been studied *in vivo*.

In this study, there was no difference in *lacZ* gene expression at 7 days in β-blocker (bisoprolol) treated animals, compared to those not treated with β-blockers, following deployment of coronary stents coated with pGEG-2RE2HE-Psi-*lacZ*. There was a significant reduction in heart rate in the bisoprolol treated group indicating adequate β-blockade.

These results are difficult to interpret as, although numerically higher, there was no statistically significant difference in *lacZ* gene production between the p*lacZ* stent and control stent groups. En face staining of the stented segments suggested only very patchy *lacZ* expression in the p*lacZ* group. This suggests that the degree of transgene expression in this study was minimal and insufficient to draw any meaningful conclusions on the effect of β-blockade on plasmid-mediated gene expression.

Given that a clear increase in gene expression was only identified in pFMOD-treated vessels, as compared to control vessels, it may be that the use of pFMOD stents would have generated meaningful results. Unfortunately the p*lacZ* stents used in the β-blocker experiments were prepared at the same time as the stents used in the main experiments and no additional pFMOD coated stents were available.

4.7 Reasons for inadequate transgene expression

Poor gene transfer efficacy represents the Achilles heel of plasmid-mediated gene therapy. This shortcoming was manifest in this study and the likely reason for the failure to demonstrate meaningful results in either the therapeutic or β-blocker studies. Although numerous factors may contribute to this (discussed in detail in Section 1.5 of the Introduction), several issues are pertinent to this study and will be discussed in detail.

4.7.1 Plasmid issues

The likely target cell for stent based coronary gene therapy is the medial or neointimal SMC and these cells are notoriously difficult to transfect. In this study the *in vitro* transfection rate of human coronary SMCs using a lipofection technique was consistently <5%, despite attempts to optimise the protocol. For comparison, the transfection rate with 293 cells was >95% and the rate with A10 cells (which resemble neointimal SMCs) was approximately 10% (see Figure 28). A high transfection rate may not be necessary to result in successful protein production: Dulak and colleagues reported high levels of VEGF production following plasmid-mediated transfection of SMCs *in vitro* despite a low transfection efficiency of <5%[272]. However if the transfection rate is low *in vitro*, then the transfection rate *in vivo* is likely to be even lower, especially given the inability to use lipofection agents with stent based vector delivery. Therefore efforts to maximise SMC transfection are justified.

Our group has developed a complex expression cassette which has been shown to improve gene expression in SMCs (the likely target cells) *in vitro*. Attempts were made in this study to optimise this expression cassette further, and the addition of enhancer elements was shown to increase SMC transfection. The plasmids used for the *in vivo* studies contained the following elements (Figure 6): the woodchuck hepatitis virus post-

transcriptional regulatory element (WPRE), an intron, the Epstein-Barr nuclear antigen-1 (EBNA-1) and its binding site *oriP*, two copies of the rabbit smooth muscle myosin heavy chain promoter (RE) and two copies of the human VSMC α-actin promoter (HE). The addition of these elements to a 'simple' plasmid vector has resulted in large plasmids: pGEG-2RE2HE-Psi-*lacZ* (14.5 kb), pGEG-2RE2HE-Psi-CTGF (12.1 kb) and pGEG-2RE2HE-Psi-FMOD (13.7 kb). For comparison, other preclinical studies of gene-eluting stents which have shown successful transgene expression have used much smaller plasmids: phVEGF-2 (5.2 kb)[62], pEGFP-C1 (4.7 kb)[180, 182], pQBI25-fPA (6.2 kb)[137] and pCMVβ (7.2 kb)[137].

Plasmid size has been shown to be inversely proportional to the efficiency of gene transfer, particularly if carrier vehicles are not used[284]; smaller molecules enter the cell more rapidly by endocytosis and have a more rapid rate of nuclear transport through the cytoplasm to the nuclear pore complex[285]. Another potential benefit of simpler plasmids is that additional backbone elements may be immunogenic, particularly if they include unmethylated CpG dinucleotides which can lead to innate immune system activation[170]. Completely CpG-free plasmids reduce inflammation and increase gene expression[171]. DNA minicircles are derived from plasmid DNA and consist solely of an expression cassette, lacking any bacterial components. They increase gene transfer efficiency both *in vitro* and *in vivo* but are currently complex and expensive to produce and have not been used in human studies of cardiovascular gene therapy[284, 286].

There is clearly a balance between including additional elements which may increase gene expression or confer cell-type specificity (such as enhancers, DNA targeting sequences and cis-acting elements), and attempting to minimise plasmid size to enhance cellular uptake and nuclear trafficking and reduce immunogenicity. Factors such as immunogenicity would not be applicable *in vitro* and it is possible that the size and complexity of the plasmids used in this study impaired *in vivo* transgene expression, despite being efficacious *in vitro*. It would be worth considering substantially reducing the size of the plasmid backbone for future experiments in order to improve gene transfer efficiency.

The choice of plasmid dose is another important factor and is largely empirical. Previous published studies have used doses of between 100μg and 1700μg per stent

(Table 1) and a clear dose-effect relationship is often absent from studies of plasmid mediated gene therapy. For instance, Walter and colleagues reported a reduction in neointima following deployment of pVEGF-eluting stents in rabbit iliac arteries[62]. However there was no difference in efficacy between the two doses of VEGF studied (100µg and 200µg). In the current dose-finding study three doses were examined: 100µg , 200µg and 400µg per stent. Given the lack of a clear dose-effect correlation, the 400µg dose was selected for the therapeutic studies in an attempt to maximise transgene expression. Although it is possible that simply increasing the dose of plasmid would be sufficient to increase transgene expression, the fact that doses as low as 100µg/stent have been reported to be effective suggests that other factors may have been more important in the failure of efficacy in this study.

4.7.2 Polymer issues

The stent coating process used in the *in vivo* studies has already been discussed and several potential issues can be identified which may contribute to the poor gene transfer efficacy seen.

Commercial drug-eluting stents (DES) typically elute their therapeutic agent over a period of months as a result of specially developed polymer coatings, and this prolonged release is essential for optimal results. The XIENCE V stent (Abbott, IL, USA), which has arguably the most impressive clinical data of the currently available DES, elutes everolimus in a controlled manor for 120 days[287]. Conversely the ENDEAVOR stent developed by Medtronic (MA, USA) possessed a rapid drug elution profile and was associated with a high rate of restenosis[288]. This prompted Medtronic to redesign the polymer coating to provide extended drug release and the new RESOLUTE stent, with the same drug and stent backbone as ENDEAVOR, demonstrated significantly improved clinical results[289].

Although the optimal release profile for drug elution from DES has been established in clinical trials, the best release profile for gene therapy vectors as a treatment for instent restenosis is not well understood and will depend on the vector studied. The neointimal process induces rapid cell division and typically takes weeks to months to complete. Drug elution from DES has been shown to be needed for the duration of this process to

attain optimal clinical results. As plasmids are not well retained in dividing cells, it is likely that the optimal elution profile will be similar to that of DES.

The polymer-coated stents used in this study were prepared with a proprietary process by Medtronic in the USA for which the full details were not available. The *in vitro* DNA elution experiments performed by Medtronic appeared to show satisfactory results for use *in vivo.* This data showed an initial burst of plasmid release from the stents followed by a steady release extending out to 29 days. Although the initial experiments showed that only about 25% of plasmid had eluted at this point, once a crimp-expansion cycle had been applied to the stents, approximately 50% had eluted by day 13. Given these results, Medtronic were instructed to provide the first batch of stents for use in the *in vivo* dose-finding study.

Once these stents arrived, the elution profiles were repeated. The results from these experiments were substantially different to those provided by Medtronic: approximately 90% of the predicted DNA load eluted within the first 4 hours, with minimal further elution occurring after 48 hours. Following discussion with Medtronic they suggested that an additional step of "capcoating" the stents with an extra layer of polymer could be applied to try and reduce the rate of elution. Given the time constraints on the project, there was insufficient time for confirmatory experiments to ensure that this did not adversely affect plasmid integrity or elution. However, it was felt that the initial method of stent coating would be extremely unlikely to result in sustained plasmid elution and this additional "capcoating" step was performed on the remainder of stents to be used *in vivo*.

Unfortunately elution experiments on the new stents showed very similar results to the previous method, with more than 90% of the predicted load eluted within 24 hours, confirming that the "capcoating" process was ineffective at slowing down release of plasmid from the polymer coating. There was insufficient time available at this juncture to investigate alternative coating techniques and thus these stents were used for the *in vivo* studies. This rapid elution of plasmid from the polymer coating almost certainly represents a major factor in the poor transgene expression demonstrated in this study.

The conflicting results from the elution experiments performed by Medtronic and in our laboratory are difficult to reconcile. The DNA assays were different: Medtronic used the Quant-iT Picogreen dsDNA assay kit (Invitrogen) and our laboratory used a Nanodrop spectrophotometer (Thermo Scientific). However both methods should provide an accurate measurement of DNA concentration and the experimental protocol was otherwise identical. The most likely explanation relates to the fact that Medtronic was going through a process of staff restructuring at the time of the study. The researcher originally allocated to the project developed the stent coating protocol and completed the initial experiments demonstrating a desirable elution profile. After the main experimental work had been performed another researcher was allocated to the project, who performed the stent coating process using the original researcher's notes. It is feasible that there was an error in interpreting these notes and the coating process was not performed in an identical manner to the first researcher.

Another issue which warrants discussion is the heterogenous nature of the neointimal process. Even between stents in the same group there were marked variations in neointimal hyperplasia, with some vessels only demonstrating minimal late loss and others developing occlusive neointima. In the vessels with the greatest neointima there was extensive mononuclear infiltrate around the stent struts suggesting an inflammatory process may be responsible for this phenomenon. This heterogeneity made it very difficult to ascertain whether there were any genuine differences between the treatment groups.

There were no obvious factors in the methodology to explain this observation. Stent polymers have been shown to induce a significant inflammatory response[183] . Given that the details of the stent coating process were not divulged by Medtronic, one can speculate that inconsistencies in polymer application may explain the variability seen.

5 Future directions

Plasmid-mediated gene therapy has the potential to result in therapeutic gene expression with an acceptable safety profile, and instent restenosis offers an ideal target as prolonged site-specific therapy can be achieved with gene-eluting stents. Despite this promise, the results from this thesis clearly demonstrate that several hurdles have to be crossed before therapeutic gene therapy can be extended past the preclinical stage.

Promoter optimisation offers the potential to increase gene expression and cell specificity. The addition of 2RE2HE has been shown to substantially increase gene expression in vascular SMCs. As addition of the D element interfered with the function of the other expression cassettes assessed, plasmids with various combinations of RE and HE but with the D element removed will need to be constructed. Insertion of the D element after the polyA sequence, where it will not be transcribed, has the potential to increase SMC gene expression and is the subject of active investigation by our group.

An alternative approach to increase transgene expression is to minimise the size of the plasmid backbone. The plasmids used in this study contained the EBNA-1 gene and its binding site *oriP*, which have been shown to increase nuclear transport via a *cis* acting mechanism but substantially increase the size of the plasmid. Co-transfection with two smaller plasmids, one containing the transgene and *oriP* and a second containing the EBNA-1 gene, offers a novel method to minimise plasmid size whilst preserving the enhanced nuclear transport. Although not suitable for large scale plasmid production using current techniques, DNA minicircles offer another intriguing prospect for further studies of non-viral gene transfer.

For future studies of gene-eluting stents, more preliminary work will need to be performed on the stent platform and the polymer application. In particular DNA elution from the stent should be deemed acceptable prior to proceeding with animal experiments. This is likely to require further liaison with industrial partners who have access to state of the art polymer and stent technology.

Given the minimal gene expression seen *in vivo*, it would be worth considering using a higher dose of plasmid for future experiments as, unlike viral vectors, there is less potential for toxicity with higher doses. Certainly there seems to be little role for

performing formal dose-finding studies given the lack of correlation seen in this study. Given the issues with “false positive” blue X-gal staining seen in the segments exposed to polymer coated stents, it would be reasonable to investigate alternative marker genes for future studies.

Once the above issues have been remedied, further studies of CTGF and FMOD gene therapy to the coronary arteries are warranted given the positive results demonstrated in reducing neointimal formation in the SVG model.

6 Appendix

6.1 Composition of solutions

All chemicals and reagents were obtained from Invitrogen unless otherwise stated.

293 medium	
Minimum Essential Medium (#21090/022)	500ml
Foetal bovine serum (#10106-169)	50ml (10%)
MEM non-essential amino-acids 1x (#11140-035)	5ml
L-glutamine 200mM (#25030-024)	5ml (2mM)
Penicillin/streptomycin (5000iu/ml-5000µg/ml)	5ml
A10 medium	
Dulbecco's Modified Eagle Medium (#41965-039)	500ml
Foetal bovine serum (#10106-169)	50ml (10%)
Penicillin/streptomycin (5000iu/ml-5000µg/ml)	5ml
SMC culture medium (TCS Cellworks)	
Smooth muscle cell basal medium (#ZHC-3933)	500ml
Growth supplement (insulin, human epidermal growth factor, human fibroblast growth factor and foetal bovine serum) (#ZHS-8951)	5ml (5%)
Antibiotic supplement (25mg/ml gentamicin and 50µg/ml amphotericin B) (#ZHR-9939)	5ml
Organ transfer medium	
RPMI 1640 with 20mM HEPES	500ml
Penicillin/streptomycin (5000iu/ml-5000µg/ml)	5ml
Gentamicin (25mg/ml stock)	5ml
Amphotericin B (50µg/ml stock)	5ml
Sodium heparin	2000U
Organ culture medium	
RPMI 1640 with 2g/l sodium bircarbonate	500ml
Penicillin/streptomycin (5000iu/ml-5000µg/ml)	5ml
Gentamicin (25mg/ml stock)	5ml
Amphotericin B (50µg/ml stock)	5ml
Foetal bovine serum (to make 30% concentration)	150ml
Freezing medium	

Dulbecco's Modified Eagle Medium (#41965-039)	5ml
Dimethyl sulphoxide (DMSO) (Sigma-Aldrich)	1ml
Foetal bovine serum (#10106-169)	4ml
Cell lysis buffer	
100mM Tris-HCl (pH 7.8)	12.5ml
Glycerol	7.5ml
1M $MgCl_2$	500µl
Triton X-100	500µl
0.5M EDTA (pH 8)	100µl
ddH_2O	28.9ml
Buffer solution for X-gal assay	
Potassium ferrocyanide	42mg (5mM)
Potassium ferricyanide	32mg (5mM)
Magnesium chloride	4mg (2mM)
0.1M PBS	19.5ml
X-gal solution	
X-gal (bromo-chloro-indolyl-galactopyranoside)	20mg
DMSO	500µl

6.2 1kb ladder

The 1kb ladder was supplied by Invitrogen (15615-024) and gives the following band sizes during gel electrophoresis:

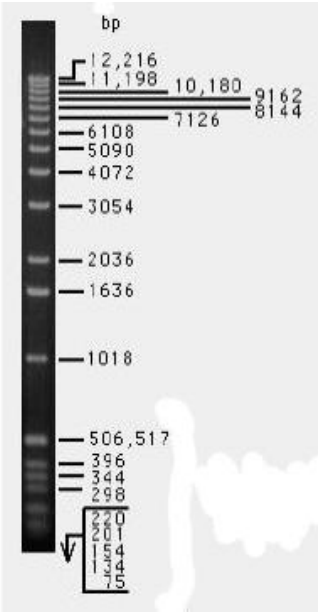

6.3 Cloning protocol for novel plasmids

6.3.1 DNA sequences of expression cassette inserts

The DNA sequences of the DNA targeting sequence and fragments of the rabbit and human enhancer elements are listed below.

Chicken Smooth Muscle Gamma Actin Promoter (GenBank accession number: AF012348)

CACTAAAGGGAAACGCGAACGAAACCACGCTTTGCAGGCACGCTTTATTTGCTTCAACAACGAGGGCTGC
ATGTTTTGCAGGGACTCCCCCCCACCCCTGCCTATCTGGTGCCCTCACACAAAGGAACGGAACCAAGCCC
GTGGCCCGAGCTCCCAGCCAGGAGCCCTCAGCAGCAGCAGAACGTGTGAGCGTTACCCATATAGGGAGGT
GCAGAGGGCTGGTGGTGCACGGGGAGCTCTGCATCCCCCCGCGGCCCTCAGCCTGCAGCCCCCTCCCGCT
CGTGGCACCGGGTTGGCCTCGCGTGCCGTGGGGTAGCCGGGCGTTCCTGCGAGCATCCCAGGCCGGCCAG
CAGGCCCTCCCTGCAGCCCGGGCACAGCCATGCTCCGACAGCTGATTGGCTGCGGTGGCCGAACCTTTCC
TTTTTAGGCTGCATCTGCTCTGGCTCTGGCTCTGCCTCCGCGGTCCCAACTTCAGCCTCCCCGTGCCGAG
GCTCAGCTCCAACAGAGGGACTGCTGCACGGTGGGACGCCCTGCATGGCTGGGTGAGACCAGGGGGCTGG
GGAGGGCTGGGATGGCTCTGGCTTGGACACGGCGGGGCTCGTGCGCTATGGGCAGAAGTGCTGTGGCTTT
TGGCACCGTTCCCTTTCCTATGGCTGGGATACAGCTGTCGCATCGGCTCCGTGTGGCCGTGGTCCCCCCC
CCCCCCTCCCCCGCAGCGTGGGCGCAATGGACCCGGTGGCCAACCTGCCTCCATCCCACTCCCTTCTGAT
TCCTTTTTCCTTACGCTCTGCTGGGTTGGGTTGTTTTTTTTTTTAATTTTTTTTTTTTTTTTGCAGCAT
GTCATATATGGCAACCTTTTGCCTCGGTGACCTCATGTTTGGCAGCAGGCCGGGTGACGCGGGCTGGGAT
GAAAGCAGCTGTGGGTGTCTCGCGTGAGGCTGCGGTGCAGAGCATGCTGAGACGCACAGCTGGGACCTGG
GGACACATCCAGCCCAGGGATGGGGGGGACCGGGCAGTGCACCGCTGTGGGACGCTCTGAGACCGTGCCC
ACATCCTCATTGCACGATGACAGCTCCGAGCTGCACCCACACCTCCGCATCCTCGCCCCGAGAATGGATC
GGGATGCAGCAAAACGAAGCAGAAGCGGCGCCTGCTCGTGCCTCAGTTTCCCAGCTGCAGCCTCACTTCC
CACAACTCTCAAGTAGCAGCTCCGTGGCTTCCTCCCATCCTCAGGCTCCAGAGAGAGGCCCCAGAACGGG
ATGGCTGCCCTTAAAAAGGCACTGGGCCGATCAGCAGGTGCTGTGCGAGGGATGGGGGCCGATGCCTTTG
CCATGGTGGGGCATTGAGGTGTCCCCAGTGCTGCTCGGGGGCAGCAGACCTCCACCTCCCCTGGGACTGG
GGCTCATCCTGCTTCCAAACCTCCTGGAGGGAAGCTGAGGGCGCACCCACCGTACAGGGCCAGGTTTGGA
AGGACCCACATGGGGCTCAACGATGAGGGGTTTGGGGTTTTGGCCAGGCTGTGTGGTGCCCAGAGGACCT
TTTTGGTGTCAGGGTAAACGCAGCACTGCCAGGACTCCCGCAGCACCTTTCAGCCTTGCACTGAATTGGG
CCCATCTGCCCTGGGGGTCCCTGCCCCCAATAACTGCAACGATGGGAGGGAAAAAATCCCACAGAGGGAA
CCCCAGGGTGGGGATGCCGGGTCGCAGGGATGGAGCAGCACCTCGAGGCTGTGACGCACCGCCCATCACC
TGGTGTGCAGCTGGGATGCTGAACCTCTTCCAAATCAGGATATGCCATGGTTCTATGACTCAGGTGCACA
GCAGCCCCGGGCCATCCCTACAGCCACCGCCTTCCTGGGCAGGGCTGTGGTCAGAGAGGACCAAAGGCCA
TCGACTGGAGTACCTCCACCTCGCTTTTGCTGAACGTCGCTTATAAGGACTTGTGTCTCGCCTGTTTATC
GAAGCATAGCATAAAAAGGAACAGACTCACCAATGGGATGTTGCCTCCTAAGCATAGCCCCACGTAGATT
TTTTTTTTTCCCCTTACAATAATTTAACT***GTTGCTGGGTCCTACCCATCAGTCCAAGGTCAATTTTAATG***

CAATAAAACACCTTATATGGCCATATGGCTAACACACCATCACTTAGCCTATTTAGGGTCTTTGTGTAGA
GAGGATCCGCCTCTGAGGTTTCGTGGGCTCGTGGTATTTATACCAAAGCAGATCGGGATTCGGTC

The bold sequence represents the 176bp fragment of the chicken SMGA promoter that acts as a SMC-specific DNA nuclear transport sequence (D; bp 2060 to 2235 of the published sequence).

SRE2 = initial underlined sequence (***CCTTATATGG)***

NKE1 = second underlined sequence (***CACTTAGCCT)***

SRE1 = overlapping sequence with NKE1 (***CCTATTTAGG)***

Enhancer fragment of the rabbit smooth muscle myosin heavy chain promoter (RE; 107bp)

CGCGCGGGGTGCAGGGTGCCCTCCCCCGCACCGGCCGAGCCGAGAGGCCGCGAGGCACCATATTTAGTCA
GCGGGAGCGGGCAGCCCCGGGCTGGTATGCGGCGCTG

Enhancer fragment of the human smooth muscle myosin heavy chain promoter (HE; 109bp)

ATCGTGAGAACTCACTCACTTTCATGAGAACAGCATGGTATAAAACGCCCCCATCGATCCAGTCACCTCC
CACCATGCCTTTCTCTGGACATGGGATTATGGAGATTAG

Full cloned DNA sequence (D2RE2HE; 708bp)

GCGGCCGCACGTGTTGCTGGGTCCTACCCATCAGTCCAAGGTCAATTTTAATGCAATAAAACACCTTATA
TGGCCATATGGCTAACACACCATCACTTAGCCTATTTAGGGTCTTTGTGTAGAGAGGAT**A**CCGCCTCTGA
GGTTTCGTGGGCTCGTGGTATTTATACCAAAGCAGATCGGGATTCGGTCATTTAAATCACGTGTTCGAAC
GCGCGGGGTGCAGGGTGCCCTCCCCCGCACCGGCCGAGCCGAGAGGCCGCGAGGCACCATATTTAGTCAG
CGGGAGCGGGCAGCCCCGGGCTGGTATGCGGCGCTGCTCGAGCCTAGGTTCGAATATTCGCGCGGGGTGC

AGGGTGCCCTCCCCCGCACCGGCCGAGCCGAGAGGCCGCGAGGCACCATATTTAGTCAGCGGGAGCGGGC
AGCCCCGGGCTGGTATGCGGCGCTGCGATCGCTTCGAATCGTGAGAACTCACTCACTTTCATGAGAACAG
CATGGTATAAAACGCCCCCATCGATCCAGTCACCTCCCACCATGCCTTTCTCTGGACATGGGATTATGGA
GATTAGATGCATCCTAGGATCGTGAGAACTCACTCACTTTCATGAGAACAGCATGGTATAAAACGCCCCC
ATCGATCCAGTCACCTCCCACCATGCCTTTCTCTGGACATGGGATTATGGAGATTAGCGATCGCATTTAA
ATACTAGT

A = additional A to remove BamHI site from D sequence

This sequence contains the following restriction sites to allow digestion and ligation of various combinations of D, RE and HE:

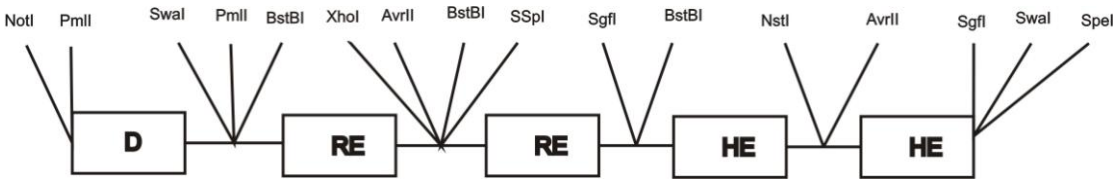

6.3.2 Cloning protocol for novel expression cassettes

pΔPSi-*lacZ* (an intermediary plasmid obtained from Dr Kingston) was double digested with NotI and SpeI and the D2RE2HE insert was ligated into the plasmid immediately before the MIEmCMV promoter to create pΔ-**D2RE2HE**-PSilacZ. The entire expression cassette (consisting of the D2RE2HE insert, the truncated murine CMV promoter, the pCI intron, the lacZ gene, WPRE and the polyA sequence) was then removed with double digestion using NotI and BamHI. pGEGPSilacZ was also double digested with NotI and BamHI to remove its expression cassette and the expression cassette from pΔ-**D2RE2HE**-PSi-*lacZ* was ligated into the pGEG backbone to create pGEG-**D2RE2HE**-PSi-*lacZ*.

Restriction enzyme digestion and religation of pGEG- **D2RE2HE** –Psi-*lacZ* was performed to create further plasmids with the following combinations of HE, RE and D as follows (all enzymes cleave sticky ends and incubation was performed at 37°C unless otherwise specified) :

PmlI digestion (blunt end)	⇒	pGEG- **2RE2HE** –Psi-*lacZ*
BstBI digestion (65°C)	⇒	pGEG- **D2HE** –Psi-*lacZ*
SgfI digestion	⇒	pGEG- **D2RE** –Psi-*lacZ*
AvrII digestion	⇒	pGEG- **DREHE** –Psi-*lacZ*
SgfI digestion then BstBI digestion	⇒	pGEG- **DRE** –Psi-*lacZ*
SwaI digestion (25°C)	⇒	pGEG- **D** –Psi-*lacZ*

Confirmatory digests were performed using various restriction enzymes as described in Section 3.2.

6.4 DNA sequences of transgenes

Base pair sequences highlighted in red are the targets for the custom primers designed for PCR in section 2.6.4.1.

6.4.1 Connective tissue growth factor

Human CTGF consensus coding DNA sequence (CCDNS)

1050bp

ATGACCGCCGCCAGTATGGGCCCCGTCCGCGTCGCCTTCGTGGTCCTCCTCGCCCTCTGCAGCCGGCCGG
CCGTCGGCCAGAACTGCAGCGGGCCGTGCCGGTGCCCGGACGAGCCGGCGCCGCGCTGCCCGGCGGGCGT
GAGCCTCGTGCTGGACGGCTGCGGCTGCTGCCGCGTCTGCGCCAAGCAGCTGGGCGAGCTGTGCACCGAG
CGCGACCCATGCGACCCGCACAAGGGCCTATTCTGTCACTTCGGCTCCCCGGCCAACCGCAAGATCGGCG
TGTGCACCGCCAAAGATGGTGCTCCCTGCATCTTCGGTGGTACGGTGTACCGCAGCGGAGAGTCCTTCCA
GAGCAGCTGCAAGTACCAGTGCACGTGCCTGGACGGGGCGGTGGGCTGCATGCCCCTGTGCAGCATGGAC
GTTCGTCTGCCCAGCCCTGACTGCCCCTTCCCGAGGAGGGTCAAGCTGCCCGGGAAATGCTGCGAGGAGT
GGGTGTGTGACGAGCCCAAGGACCAAACCGTGGTTGGGCCTGCCCTCGCGGCTTACCGACTGGAAGACAC
GTTTGGCCCAGACCCAACTATGATTAGAGCCAACTGCCTGGTCCAGACCACAGAGTGGAGCGCCTGTTCC
AAGACCTGTGGGATGGGCATCTCCACCCGGGTTACCAATGACAACGCCTCCTGCAGGCTAGAGAAGCAGA
GCCGCCTGTGCATGGTCAGGCCTTGCGAAGCTGACCTGGAAGAGAACATTAAGAAGGGCAAAAAGTGCAT
CCGTACTCCCAAAATCTCCAAGCCTATCAAGTTTGAGCTTTCTGGCTGCACCAGCATGAAGACATACCGA
GCTAAATTCTGTGGAGTATGTACCGACGGCCGATGCTGCACCCCCCACAGAACCACCACCCTGCCGGTGG

AGTTCAAGTGCCCTGACGGCGAGGTCATGAAGAAGAACATGATGTTCATCAAGACCTGTGCCTGCCATTA
CAACTGTCCCGGAGACAATGACATCTTTGAATCGCTGTACTACAGGAAGATGTACGGAGACATGGCATGA

6.4.2 Fibromodulin

Bovine fibromodulin cDNA

2656bp

AAGGAGGCCAGACAGAGGGACGTGGTCACTCTCTGAAAGATTCAACTTCAAGAAACACAAAATGCAGTGG
GCGTCCATCCTGCTGCTGGCAGGGCTCTGCTCCCTCTCCTGGGCCCAATATGAGGAAGACTCTCACTGGT
GGTTTCAGTTCCTCCGCAACCAGCAGTCCACCTACGACGATCCCTATGACCCCTACCCCTATGAGCCTTA
TGAGCCTTACCCTACGGGAGAAGAAGGTCCAGCTTATGCTTACGGCTCTCCACCCCAACCAGAGCCCCGA
GACTGCCCCCAGGAGTGCGACTGTCCCCCCAACTTCCCCACAGCCATGTACTGCGACAATCGCAATCTCA
AGTACCTGCCCTTCGTCCCCTCCCGCATGAAATACGTCTACTTCCAGAACAACCAGATCTCTTCCATCCA
GGAGGGTGTCTTCGACAATGCCACTGGGCTGCTCTGGATTGCTCTCCATGGCAACCAGATCACCAGTGAT
AAGGTGGGCAAGAAGGTTTTCTCCAAGCTGAGGCACCTGGAGAGGCTGTATCTGGACCACAACAACCTGA
CCCGGATACCCAGCCCACTGCCTCGGTCCCTGAGAGAGCTCCATCTTGACCACAACCAGATCTCAAGGGT
CCCCAACAATGCGCTGGAGGGGCTGGAGAACCTCACAGCCTTGTACCTTCATCACAACGAGATCCAGGAA
GTGGGCAGTTCTATGAAAGGCCTCCGATCATTGATCTTGCTGGACCTGAGCTACAACCACCTTAGGAAGG
TACCTGATGGACTGCCCTCAGCCCTTGAGCAGCTGTACCTGGAGCACAACAACGTCTTCTCAGTCCCCGA
CAGCTACTTCCGGGGGTCACCCAAGCTGCTGTATGTGCGGCTATCCCACAACAGCCTCACCAACAATGGC
CTGGCCTCAAATACCTTCAATTCCAGCAGCCTCCTTGAGCTCGACCTCTCCTACAACCAGCTGCAGAAGA
TCCCCCCAGTCAGCACCAACCTGGAGAACCTCTACCTCCAAGGCAATAGGATCAATGAGTTCTCCATCAG
CAGCTTCTGCACCGTGGTGGATGTCATGAACTTCTCCAAGCTGCAGGTGCAGCGCCTGGATGGCAACGAG
ATCAAGCGCAGCGCCATGCCCGCTGACGCGCCCCTCTGCCTGCGCCTGGCTAGCCTCATCGAGATCTGAG
CGCCACTGGGCGAGGGCCATGCCCCCACGCCTCTTTGCATTTGGCTTGATGGTTTGGTTTGGCTTATGGA
AGGTCTGGGACAGACCGTGTGACAGAGGTCCATGGGCTCTCTCTCTAGTCTTCTTCTTCCCTGTAGGCAG
TTTTAGGTGGAGTCAGGGGACAGGCAGCTTTCTGCTGAGGGACATGACACGTCCGTTTCCAAGACAGAAA
GTGGTTGGCAGAAGGTGTAAACCCTGAAGTCCCAGTCCCCGAAATCTCATTACCCTCAAGGTCTTCACAG
TGATCCAGTGTCCTGAACCATTGCCTGAGCAATAGAATAACTGTGCTTTTGAAGTAATGTCTGACTCTGA
AGGCAGCACCTGACCGCTCCCCCGCGTGCTGGGCTGGTCGTGCCGATACTCTGGGCTCCCAGTTGCTGCT
TCTCAGATATACCTCTTGCCCGACTGCCGCCTCCTCAGTCCACCTCATCCACTCAACCATGCCCCACAGA
CATCTTAGGTAGAGGCAGGAGAAGCCAAGGCGTATGCACAGCTGCCCAGTGACTGCGCAGAGAACTCACA
CTGGTGGCTGAGGCTGGAAGGACACCAAGAGTCACCTTTTCACCACAGGTCACCAGTGTGATGACAATAT
TCCAGGCTTGACGTGGGAGGAGACAGCCAACCTCAGACTTAGCTAAATGCGTGGGGCTGTATTTTAACAA
CTGGGCAGTTCTCTGAAGGTGGGTCAGACTTCAGAAAAGGAAAGCGACCTGATGTTGCGTATTACCAGCA
TCCATAGTGGAGGCAAATACACCTTGAATTGGCTGAACTGAGGAGGCAGCCCAGGAGTGTCATTCTTGCC
CAGCACTCTCTGCATTCCCAGCAGCTCCCTACTTGAGTTTTTATCTTCAAAGGCAGAGGCCATGTGGCTC

TCAAAGTATGAGAGAGGTAATTTGTCCTCTTATGCAAGCAGAAAGGTCAATAACCTGATTGGAGAGACAG
ACTCCAACCAGCCCTGGAGTTGCCACCCTCGTTACTGAAGCTGGCTGTTGCTTTATAGCTTGGCTGGAGA
GCAATTAATCTTTCCCGTTTCTGAAAGTAGTGCTGCCTGGGGACCTAACCCCTGCTTTGTGGGGTACCAC
TGGGATGGGGCCATCTGGGCAGCCATGGGCAGAGACTGCTTGAGGAGAGCTCCCTGCACAGATGCTGTTG
CTTCCCTGATACCGTGTATGCTTTGAAGCAGTTCCCTGAAGAAAGAAGAGGGGATCCTTGAACTATGTTC
TTGGCTCCAGAACCTCAAATCCACAAAAGCCAAACCAGCTCATTTCAACAAAGAAGCTCTGATGTGAGGG
GCAAGGCTGCCCCTTGCCCCAGGGCTCTTCAGAAAGCATCTGCATGTGGACACCATCATGCCTCTATAAA
GGATCCTTATTACAGGAAAAGCATGAGTGGTGGCTAACCCAACCAATAAAGTTATTTTACAATTGC

6.4.3 lacZ

lacZ cDNA

3386bp

CTCGAGCGGGGCTGGGACACTTCACATGAGCGAAAAATACATCGTCACCTGGGACATGTTGCAGATCCAT
GCACGTAAACTCGCAAGCCGACTGATGCCTTCTGAACAATGGAAAGGCATTATTGCCGTAAGCCGTGGCG
GTCTGGTACCGGTGGGTGAAGACCAGAAACAGCACCTCGAACTGAGCCGCGATATTGCCCAGCGTTTCAA
CGCGCTGTATGGCGAGATCGATCCCGTCGTTTTACAACGTCGTGACTGGGAAAACCCTGGCGTTACCCAA
CTTAATCGCCTTGCAGCACATCCCCCTTTCGCCAGCTGGCGTAATAGCGAAGAGGCCCGCACCGATCGCC
CTTCCCAACAGTTGCGCAGCCTGAATGGCGAATGGCGCTTTGCCTGGTTTCCGGCACCAGAAGCGGTGCC
GGAAAGCTGGCTGGAGTGCGATCTTCCTGAGGCCGATACTGTCGTCGTCCCCTCAAACTGGCAGATGCAC
GGTTACGATGCGCCCATCTACACCAACGTAACCTATCCCATTACGGTCAATCCGCCGTTTGTTCCCACGG
AGAATCCGACGGGTTGTTACTCGCTCACATTTAATGTTGATGAAAGCTGGCTACAGGAAGGCCAGACGCG
AATTATTTTTGATGGCGTTAACTCGGCGTTTCATCTGTGGTGCAACGGGCGCTGGGTCGGTTACGGCCAG
GACAGTCGTTTGCCGTCTGAATTTGACCTGAGCGCATTTTTACGCGCCGGAGAAAACCGCCTCGCGGTGA
TGGTGCTGCGTTGGAGTGACGGCAGTTATCTGGAAGATCAGGATATGTGGCGGATGAGCGGCATTTTCCG
TGACGTCTCGTTGCTGCATAAACCGACTACACAAATCAGCGATTTCCATGTTGCCACTCGCTTTAATGAT
GATTTCAGCCGCGCTGTACTGGAGGCTGAAGTTCAGATGTGCGGCGAGTTGCGTGACTACCTACGGGTAA
CAGTTTCTTTATGGCAGGGTGAAACGCAGGTCGCCAGCGGCACCGCGCCTTTCGGCGGTGAAATTATCGA
TGAGCGTGGTGGTTATGCCGATCGCGTCACACTACGTCTGAACGTCGAAAACCCGAAACTGTGGAGCGCC
GAAATCCCGAATCTCTATCGTGCGGTGGTTGAACTGCACACCGCCGACGGCACGCTGATTGAAGCAGAAG
CCTGCGATGTCGGTTTCCGCGAGGTGCGGATTGAAAATGGTCTGCTGCTGCTGAACGGCAAGCCGTTGCT
GATTCGAGGCGTTAACCGTCACGAGCATCATCCTCTGCATGGTCAGGTCATGGATGAGCAGACGATGGTG
CAGGATATCCTGCTGATGAAGCAGAACAACTTTAACGCCGTGCGCTGTTCGCATTATCCGAACCATCCGC
TGTGGTACACGCTGTGCGACCGCTACGGCCTGTATGTGGTGGATGAAGCCAATATTGAAACCCACGGCAT
GGTGCCAATGAATCGTCTGACCGATGATCCGCGCTGGCTACCGGCGATGAGCGAACGCGTAACGCGAATG
GTGCAGCGCGATCGTAATCACCCGAGTGTGATCATCTGGTCGCTGGGGAATGAATCAGGCCACGGCGCTA
ATCACGACGCGCTGTATCGCTGGATCAAATCTGTCGATCCTTCCCGCCCGGTGCAGTATGAAGGCGGCGG

AGCCGACACCACGGCCACCGATATTATTTGCCCGATGTACGCGCGCGTGGATGAAGACCAGCCCTTCCCG
GCTGTGCCGAAATGGTCCATCAAAAAATGGCTTTCGCTACCTGGAGAGACGCGCCCGCTGATCCTTTGCG
AATACGCCCACGCGATGGGTAACAGTCTTGGCGGTTTCGCTAAATACTGGCAGGCGTTTCGTCAGTATCC
CCGTTTACAGGGCGGCTTCGTCTGGGACTGTTTATCCGGGCAAACCATCGAAGTGACCAGCGAATACCTG
TTCCGTCATAGCGATAACGAGCTCCTGCACTGGATGGTGGCGCTGGATGGTAAGCCGCTGGCAAGCGGTG
AAGTGCCTCTGGATGTCGCTCCACAAGGTAAACAGTTGATTGAACTGCCTGAACTACCGCAGCCGGAGAG
CGCCGGGCAACTCTGGCTCACAGTACGCGTAGTGCAACCGAACGCGACCGCATGGTCAGAAGCCGGGCAC
ATCAGCGCCTGGCAGCAGTGGCGTCTGGCGGAAAACCTCAGTGTGACGCTCCCCGCCGCGTCCCACGCCA
TCCCGCATCTGACCACCAGCGAAATGGATTTTTGCATCGAGCTGGGTAATAAGCGTTGGCAATTTAACCG
CCAGTCAGGCTTTCTTTCACAGATGTGGATTGGCGATAAAAAACAACTGCTGACGCCGCTGCGCGATCAG
TTCACCCGTGCACCGCTGGATAACGACATTGGCGTAAGTGAAGCGACCCGCATTGACCCTAACGCCTGGG
TCGAACGCTGGAAGGCGGCGGGCCATTACCAGGCCGAAGCAGCGTTGTTGCAGTGCACGGCAGATACACT
TGCTGATGCGGTGCTGATTACGACCGCTCACGCGTGGCAGCATCAGGGGAAAACCTTATTTATCAGCCGG
AAAACCTACCGGATTGATGGTAGTGGTCAAATGGCGATTACCGTTGATGTTGAAGTGGCGAGCGATACAC
CGCATCCGGCGCGGATTGGCCTGAACTGCCAGCTGGCGCAGGTAGCAGAGCGGGTAAACTGGCTCGGATT
AGGGCCGCAAGAAAACTATCCCGACCGCCTTACTGCCGCCTGTTTTGACCGCTGGGATCTGCCATTGTCA
GACATGTATACCCCGTACGTCTTCCCGAGCGAAAACGGTCTGCGCTGCGGGACGCGCGAATTGAATTATG
GCCCACACCAGTGGCGCGGCGACTTCCAGTTCAACATCAGCCGCTACAGTCAACAGCAACTGATGGAAAC
CAGCCATCGCCATCTGCTGCACGCGGAAGAAGGCACATGGCTGAATATCGACGGTTTCCATATGGGGATT
GGTGGCGACGACTCCTGGAGCCCGTCAGTATCGGCGGAATTCCAGCTGAGCGCCGGTCGCTACCATTACC
AGTTGGTCTGGTGTCAAAAATAATAATAACCGGGCAGGCCATGTCTGCCCGTATTTCGCGTAAGGAAATC
CATTATGTACTATTTAAAAAACACAAACTTTTGGATGTTCGGTTTATTCTTTTTCTTTTACTTTTTTATC
ATGGGAGCCTACTTCCCGTTTTTCCCGATTTGGCTACATGACATCAACCATATCAGCAAAAGTGATACGG
GTATTATTTTTGCCGCTATTTCTCTGTTCTCGCTATTATTCCAACCGCTGTTTGGTCTGCTTTCTGACAA
ACTCGGAACTTGTTTATTGGTCTAGA

6.5 Therapeutic stent study

Table 14 shows the QCA data for the therapeutic stent study. THER9 died at 17 days and was found to have occlusive neointima at post-mortem. Table 15 shows the morphometric data from the stented sections suitable for analysis. No morphometric data was available for THER9.

Table 14 – Quantitative coronary angiography data for therapeutic stent study

Pig code	Weight (kg)	Transgene	TVD pre-stent (mm)	MLD post-stent (mm)	Stent:vessel oversize ratio	MLD at 28 days (mm)	Late loss (mm)
THER1	27	FMOD	2.8	3	1.19	1.1	1.9
THER2	28.5	CTGF	2.8	3.1	1.19	1.1	2
THER3	31	*lacZ*	2.5	3	1.33	1.9	1.1
THER4	27	FMOD	2.7	3.1	1.23	2	1.1
THER5	26	CTGF	2.5	3.1	1.33	2	1.1
THER6	26	*lacZ*	2.8	3	1.19	2.8	0.2
THER7	21	FMOD	2.6	3	1.28	2.5	0.5
THER8	21	CTGF	2.6	3	1.28	2.4	0.6
THER9	20	*lacZ*	2.6	3	1.28	N/A	N/A
THER10	23	*lacZ*	2.5	2.9	1.33	1.5	1.4
THER11	22	CTGF	2.6	3.1	1.28	1.1	2
THER12	21	FMOD	2.4	2.9	1.39	0	2.9
THER13	22	*lacZ*	2.6	3	1.28	1.1	1.9
THER14	16	CTGF	2.6	3.1	1.28	2	1.1
THER15	27	FMOD	2.8	3.1	1.19	1.9	1.2
THER16	26	CTGF	2.5	3.1	1.33	1.7	1.4
THER17	23	*lacZ*	2.5	3.2	1.33	1.3	1.9
THER18	19	*lacZ*	2.7	3.1	1.23	0.9	2.2
THER19	24	CTGF	2.5	3.2	1.33	1.5	1.7
THER20	23.5	FMOD	2.6	3.3	1.28	1.4	1.9
THER21	26	*lacZ*	2.5	2.9	1.33	0	2.9
THER22	23	CTGF	2.7	3.1	1.23	1.4	1.7
THER23	22	FMOD	2.6	3	1.28	2.8	0.2
THER24	24	*lacZ*	2.6	2.8	1.28	0	2.8
THER25	25	FMOD	2.8	3.1	1.19	1.7	1.4
THER26	27	CTGF	2.9	3.4	1.15	1.4	2
THER27	29	FMOD	2.9	3.3	1.15	2.3	1
THER28	26	FMOD	2.9	3.1	1.15	1.6	1.5
THER29	24	CTGF	2.8	3.2	1.19	2.3	0.9
THER30	27	*lacZ*	2.8	3	1.19	2	1

TVD = target vessel diameter; MLD = minimum lumen diameter; late loss = MLD post-stent – MLD at 28 days

Table 15 – Morphometric data for therapeutic stent study

Animal code	Transgene	Segment	Mean neointima (mm)	Mean injury score	Lumen (mm^2)	IEL (mm^2)	EEL (mm^2)	Stent (mm^2)	Neointima area (mm^2)	Media area (mm^2)
THER1	FMOD	2	0.94	3.18	0.91	5.97	10.72	7.49	6.58	3.22
		3	0.82	2.94	1.73	6.28	10.05	7.85	6.13	2.20
THER2	CTGF	1	0.61	3.05	1.76	8.82	14.07	7.25	5.49	6.82
		2	0.95	3.17	1.19	N/A	16.22	7.52	6.33	8.70
		3	0.97	3.21	0.92	N/A	17.84	7.71	6.79	10.13
THER3	*lacZ*	1	0.34	2.35	4.19	7.44	9.12	7.47	3.29	1.65
		2	0.45	1.79	3.43	7.00	8.74	7.16	3.73	1.58
		3	0.31	1.95	3.73	6.87	8.00	6.87	3.14	1.12
THER4	FMOD	1	0.88	3.25	1.20	N/A	13.60	7.44	6.24	6.16
		2	0.85	3.15	1.44	N/A	17.02	7.71	6.27	9.31
		3	0.64	3.50	2.28	N/A	18.88	7.47	5.19	11.40
THER5	CTGF	1	0.27	1.40	4.84	7.54	8.84	7.58	2.74	1.26
		2	0.48	1.70	2.94	6.94	8.40	7.47	4.53	0.93
		3	0.58	1.95	2.70	7.51	8.84	7.56	4.85	1.29
THER6	*lacZ*	1	0.32	2.50	4.60	8.29	10.19	7.97	3.37	2.23
		2	0.11	2.00	6.91	8.78	10.37	8.17	1.26	2.21
THER7	FMOD	1	0.21	2.31	5.57	7.84	8.75	7.63	2.05	1.12
		2	0.42	1.15	3.58	7.34	8.96	7.55	3.97	1.41
		3	0.32	1.45	3.47	6.40	7.85	6.18	2.70	1.67
THER8	CTGF	1	0.48	2.20	3.33	7.54	8.98	7.53	4.20	1.45
		2	0.39	2.10	3.71	7.59	9.00	7.39	3.68	1.61
		3	0.31	1.90	4.88	8.10	9.62	8.30	3.41	1.33

THER10	*lacZ*	1	0.87	2.90	1.77	7.75	13.06	7.75	5.98	5.32
		2	0.92	3.40	1.03	N/A	13.99	7.81	6.78	6.18
THER11	CTGF	2	0.69	3.32	1.84	N/A	9.45	7.37	5.53	2.08
		3	0.82	3.35	1.31	N/A	10.39	7.99	6.68	2.40
THER12	FMOD	1	1.31	4.00	0.14	N/A	10.35	7.31	7.17	3.04
		2	1.41	4.00	0.02	N/A	15.65	7.60	7.58	8.05
		3	1.40	3.85	0.06	N/A	12.82	7.75	7.69	5.08
THER13	*lacZ*	1	0.98	3.90	1.02	N/A	17.66	7.76	6.74	9.90
		2	1.00	3.65	0.97	N/A	13.10	8.20	7.23	4.90
THER14	CTGF	1	0.51	2.40	3.84	8.17	9.47	8.28	4.44	1.18
		2	0.65	3.80	2.61	N/A	9.43	7.87	5.26	1.55
		3	0.70	3.10	1.95	N/A	8.65	7.77	5.83	0.87
THER15	FMOD	2	0.81	2.75	1.41	N/A	14.93	7.48	6.07	7.46
		3	0.80	3.30	1.67	N/A	15.23	7.51	5.84	7.72
THER16	CTGF	1	0.75	3.80	2.44	N/A	11.24	8.85	6.41	2.38
		2	0.71	3.75	2.89	N/A	14.25	9.75	6.86	4.50
		3	0.77	3.00	2.68	N/A	13.95	9.49	6.81	4.46
THER17	*lacZ*	1	0.69	3.80	2.16	N/A	18.34	7.66	5.50	10.68
		2	0.82	3.10	1.55	N/A	16.86	7.71	6.17	9.14
		3	0.90	3.90	1.30	N/A	14.65	8.26	6.96	6.39
THER18	*lacZ*	1	0.79	3.25	1.51	N/A	15.72	7.29	5.79	8.42
		2	0.82	2.95	1.48	N/A	17.67	7.56	6.08	10.11
		3	0.79	3.00	1.64	N/A	15.73	7.82	6.18	7.91
THER19	CTGF	2	0.64	2.35	2.21	7.47	9.95	7.93	5.72	2.03
		3	0.22	2.45	5.36	8.07	9.42	7.96	2.60	1.46
THER20	FMOD	2	0.80	2.92	1.47	N/A	13.26	7.43	5.96	5.82

		3	0.71	3.40	1.82	N/A	15.75	7.67	5.85	8.07
THER21	*lacZ*	1	1.52	3.35	0.00	N/A	12.84	7.60	7.60	5.24
		2	1.55	2.90	0.00	N/A	12.05	7.81	7.81	4.24
		3	1.36	3.10	0.06	N/A	12.63	7.39	7.33	5.25
THER22	CTGF	2	0.83	3.10	1.02	N/A	13.34	6.90	5.88	6.44
THER23	FMOD	1	0.25	1.60	4.55	6.96	8.11	6.94	2.39	1.18
		2	0.27	2.10	4.49	7.18	8.52	7.28	2.79	1.23
		3	0.21	2.09	5.10	7.36	8.56	7.34	2.24	1.21
THER24	*lacZ*	1	1.48	4.00	0.00	N/A	12.24	7.62	7.62	4.62
		2	1.53	3.80	0.00	N/A	12.17	7.85	7.85	4.31
		3	1.55	3.75	0.00	N/A	12.43	8.02	8.02	4.41
THER25	FMOD	2	0.99	3.17	1.26	N/A	10.82	7.60	6.34	3.22
		3	0.84	3.10	1.35	N/A	11.08	7.80	6.44	3.28
THER26	CTGF	1	0.99	3.20	0.90	N/A	13.87	7.89	6.98	5.99
		2	0.75	2.75	1.69	N/A	10.43	7.54	5.85	2.89
		3	0.68	2.67	1.77	N/A	11.04	7.67	5.90	3.37
THER27	FMOD	2	0.80	2.95	1.79	N/A	11.21	7.89	6.10	3.32
		3	0.74	3.25	1.81	N/A	12.68	7.68	5.87	5.00
THER28	FMOD	1	0.75	2.90	1.71	N/A	12.23	7.62	5.91	4.61
		2	0.72	3.15	1.78	N/A	13.01	7.42	5.64	5.59
		3	0.80	2.88	2.23	7.99	13.24	7.80	5.58	5.44
THER29	CTGF	2	0.61	2.40	3.21	8.55	10.09	9.00	5.79	1.09
		3	0.52	1.95	3.72	8.55	9.94	8.77	5.04	1.18
THER30	*lacZ*	2	0.45	2.17	3.25	7.67	8.91	7.82	4.57	1.09
		3	0.28	2.50	5.02	8.09	9.30	8.17	3.15	1.14

IEL = internal elastic lamina; EEL = external elastic lamina

7 References

1. World Health Organisation. The world health report 2004 - changing history. Statistical Annex. 2004.
2. Cook S, Walker A, Hügli O, Togni M, Meier B. Percutaneous coronary interventions in Europe. *Clinical Research in Cardiology* 2007;**96**:375-382.
3. Thom T, Haase N, Rosamond W, Howard VJ, Rumsfeld J, Manolio T, *et al.* Heart disease and stroke statistics--2006 update: a report from the American Heart Association Statistics Committee and Stroke Statistics Subcommittee. *Circulation* 2006;**113**:e85-151.
4. Williams DO, Holubkov R, Yeh W, Bourassa MG, Al-Bassam M, Block PC, *et al.* Percutaneous coronary intervention in the current era compared with 1985-1986: the National Heart, Lung, and Blood Institute Registries. *Circulation* 2000;**102**:2945-2951.
5. Ryan J, Cohen DJ. Are drug-eluting stents cost-effective? It depends on whom you ask. *Circulation* 2006;**114**:1736-1743; discussion 1744.
6. Serruys PW, Foley DP, Pieper M, Kleijne JA, de Feyter PJ. The TRAPIST Study. A multicentre randomized placebo controlled clinical trial of trapidil for prevention of restenosis after coronary stenting, measured by 3-D intravascular ultrasound. *Eur Heart J* 2001;**22**:1938-1947.
7. Holmes DR, Jr., Savage M, LaBlanche JM, Grip L, Serruys PW, Fitzgerald P, *et al.* Results of Prevention of REStenosis with Tranilast and its Outcomes (PRESTO) trial. *Circulation* 2002;**106**:1243-1250.
8. Grube E, Silber S, Hauptmann KE, Mueller R, Buellesfeld L, Gerckens U, *et al.* TAXUS I: six- and twelve-month results from a randomized, double-blind trial on a slow-release paclitaxel-eluting stent for de novo coronary lesions. *Circulation* 2003;**107**:38-42.
9. Morice MC, Serruys PW, Sousa JE, Fajadet J, Ban Hayashi E, Perin M, *et al.* A randomized comparison of a sirolimus-eluting stent with a standard stent for coronary revascularization. *N Engl J Med* 2002;**346**:1773-1780.
10. Jenkins NP, Prendergast BD, Thomas M. Drug eluting coronary stents. *BMJ* 2002;**325**:1315-1316.
11. Holmes DR, Jr., Leon MB, Moses JW, Popma JJ, Cutlip D, Fitzgerald PJ, *et al.* Analysis of 1-year clinical outcomes in the SIRIUS trial: a randomized trial of a sirolimus-eluting stent versus a standard stent in patients at high risk for coronary restenosis. *Circulation* 2004;**109**:634-640.
12. McFadden EP, Stabile E, Regar E, Cheneau E, Ong AT, Kinnaird T, *et al.* Late thrombosis in drug-eluting coronary stents after discontinuation of antiplatelet therapy. *Lancet* 2004;**364**:1519-1521.
13. Nordmann AJ, Briel M, Bucher HC. Mortality in randomized controlled trials comparing drug-eluting vs. bare metal stents in coronary artery disease: a meta-analysis. *Eur Heart J* 2006;**27**:2784-2814.
14. Pfisterer M, Brunner-La Rocca HP, Buser PT, Rickenbacher P, Hunziker P, Mueller C, *et al.* Late clinical events after clopidogrel discontinuation may limit the benefit of drug-eluting stents: an observational study of drug-eluting versus bare-metal stents. *Journal of the American College of Cardiology* 2006;**48**:2584-2591.

15. Kastrati A, Mehilli J, Pache J, Kaiser C, Valgimigli M, Kelbaek H, *et al.* Analysis of 14 trials comparing sirolimus-eluting stents with bare-metal stents. *N Engl J Med* 2007;**356**:1030-1039.
16. Lagerqvist B, James SK, Stenestrand U, Lindback J, Nilsson T, Wallentin L. Long-term outcomes with drug-eluting stents versus bare-metal stents in Sweden. *N Engl J Med* 2007;**356**:1009-1019.
17. Mauri L, Hsieh WH, Massaro JM, Ho KK, D'Agostino R, Cutlip DE. Stent thrombosis in randomized clinical trials of drug-eluting stents. *N Engl J Med* 2007;**356**:1020-1029.
18. Spaulding C, Daemen J, Boersma E, Cutlip DE, Serruys PW. A pooled analysis of data comparing sirolimus-eluting stents with bare-metal stents. *N Engl J Med* 2007;**356**:989-997.
19. Stone GW, Moses JW, Ellis SG, Schofer J, Dawkins KD, Morice MC, *et al.* Safety and efficacy of sirolimus- and paclitaxel-eluting coronary stents. *N Engl J Med* 2007;**356**:998-1008.
20. Vermeersch P, Agostoni P, Verheye S, Van den Heuvel P, Convens C, Van den Branden F, *et al.* Increased late mortality after sirolimus-eluting stents versus bare-metal stents in diseased saphenous vein grafts: results from the randomized DELAYED RRISC Trial. *Journal of the American College of Cardiology* 2007;**50**:261-267.
21. Di Mario C, Gil R, Camenzind E, Ozaki Y, von Birgelen C, Umans V, *et al.* Quantitative assessment with intracoronary ultrasound of the mechanisms of restenosis after percutaneous transluminal coronary angioplasty and directional coronary atherectomy. *Am J Cardiol* 1995;**75**:772-777.
22. Mintz GS, Popma JJ, Pichard AD, Kent KM, Satler LF, Wong C, *et al.* Arterial remodeling after coronary angioplasty: a serial intravascular ultrasound study. *Circulation* 1996;**94**:35-43.
23. Shi Y, Pieniek M, Fard A, O'Brien J, Mannion JD, Zalewski A. Adventitial remodeling after coronary arterial injury. *Circulation* 1996;**93**:340-348.
24. Dussaillant GR, Mintz GS, Pichard AD, Kent KM, Satler LF, Popma JJ, *et al.* Small stent size and intimal hyperplasia contribute to restenosis: a volumetric intravascular ultrasound analysis. *Journal of the American College of Cardiology* 1995;**26**:720-724.
25. Costa MA, Simon DI. Molecular basis of restenosis and drug-eluting stents. *Circulation* 2005;**111**:2257-2273.
26. Forrester JS, Fishbein M, Helfant R, Fagin J. A paradigm for restenosis based on cell biology: clues for the development of new preventive therapies. *Journal of the American College of Cardiology* 1991;**17**:758-769.
27. Geary RL, Nikkari ST, Wagner WD, Williams JK, Adams MR, Dean RH. Wound healing: a paradigm for lumen narrowing after arterial reconstruction. *J Vasc Surg* 1998;**27**:96-106; discussion 106-108.
28. Furie B, Furie BC. Mechanisms of thrombus formation. *N Engl J Med* 2008;**359**:938-949.
29. Diacovo TG, Roth SJ, Buccola JM, Bainton DF, Springer TA. Neutrophil rolling, arrest, and transmigration across activated, surface-adherent platelets via sequential action of P-selectin and the beta 2-integrin CD11b/CD18. *Blood* 1996;**88**:146-157.

30. Rogers C, Welt FG, Karnovsky MJ, Edelman ER. Monocyte recruitment and neointimal hyperplasia in rabbits. Coupled inhibitory effects of heparin. *Arteriosclerosis, thrombosis, and vascular biology* 1996;**16**:1312-1318.
31. Stewart HJ, Guildford AL, Lawrence-Watt DJ, Santin M. Substrate-induced phenotypical change of monocytes/macrophages into myofibroblast-like cells: A new insight into the mechanism of in-stent restenosis. *J Biomed Mater Res A* 2008.
32. Libby P, Simon DI. Inflammation and thrombosis: the clot thickens. *Circulation* 2001;**103**:1718-1720.
33. Owens GK, Kumar MS, Wamhoff BR. Molecular regulation of vascular smooth muscle cell differentiation in development and disease. *Physiol Rev* 2004;**84**:767-801.
34. Tanner FC, Yang ZY, Duckers E, Gordon D, Nabel GJ, Nabel EG. Expression of cyclin-dependent kinase inhibitors in vascular disease. *Circ Res* 1998;**82**:396-403.
35. Violaris AG, de Jong M, MacLeod DC, Umans VA, Verdouw PD, Serruys PW. Increased extracellular matrix synthesis by smooth-muscle cells obtained from in vivo restenotic lesions by directional coronary atherectomy. *Am Heart J* 1996;**131**:613-615.
36. Shi Y, O'Brien JE, Jr., Fard A, Zalewski A. Transforming growth factor-beta 1 expression and myofibroblast formation during arterial repair. *Arteriosclerosis, thrombosis, and vascular biology* 1996;**16**:1298-1305.
37. Shi Y, O'Brien JE, Fard A, Mannion JD, Wang D, Zalewski A. Adventitial myofibroblasts contribute to neointimal formation in injured porcine coronary arteries. *Circulation* 1996;**94**:1655-1664.
38. Li G, Chen SJ, Oparil S, Chen YF, Thompson JA. Direct in vivo evidence demonstrating neointimal migration of adventitial fibroblasts after balloon injury of rat carotid arteries. *Circulation* 2000;**101**:1362-1365.
39. Siow RC, Mallawaarachchi CM, Weissberg PL. Migration of adventitial myofibroblasts following vascular balloon injury: insights from in vivo gene transfer to rat carotid arteries. *Cardiovascular research* 2003;**59**:212-221.
40. Christen T, Verin V, Bochaton-Piallat M, Popowski Y, Ramaekers F, Debruyne P, *et al.* Mechanisms of neointima formation and remodeling in the porcine coronary artery. *Circulation* 2001;**103**:882-888.
41. Schwartz RS, Holmes DR, Jr., Topol EJ. The restenosis paradigm revisited: an alternative proposal for cellular mechanisms. *Journal of the American College of Cardiology* 1992;**20**:1284-1293.
42. Chung IM, Gold HK, Schwartz SM, Ikari Y, Reidy MA, Wight TN. Enhanced extracellular matrix accumulation in restenosis of coronary arteries after stent deployment. *Journal of the American College of Cardiology* 2002;**40**:2072-2081.
43. Farb A, Kolodgie FD, Hwang JY, Burke AP, Tefera K, Weber DK, *et al.* Extracellular matrix changes in stented human coronary arteries. *Circulation* 2004;**110**:940-947.
44. O'Brien ER, Urieli-Shoval S, Garvin MR, Stewart DK, Hinohara T, Simpson JB, *et al.* Replication in restenotic atherectomy tissue. *Atherosclerosis* 2000;**152**:117-126.
45. Evanko SP, Angello JC, Wight TN. Formation of hyaluronan- and versican-rich pericellular matrix is required for proliferation and migration of vascular smooth

muscle cells. *Arteriosclerosis, thrombosis, and vascular biology* 1999;**19**:1004-1013.
46. Bauters C, Marotte F, Hamon M, Oliviero P, Farhadian F, Robert V, *et al.* Accumulation of fetal fibronectin mRNAs after balloon denudation of rabbit arteries. *Circulation* 1995;**92**:904-911.
47. Southgate KM, Fisher M, Banning AP, Thurston VJ, Baker AH, Fabunmi RP, *et al.* Upregulation of basement membrane-degrading metalloproteinase secretion after balloon injury of pig carotid arteries. *Circ Res* 1996;**79**:1177-1187.
48. Strauss BH, Robinson R, Batchelor WB, Chisholm RJ, Ravi G, Natarajan MK, *et al.* In vivo collagen turnover following experimental balloon angioplasty injury and the role of matrix metalloproteinases. *Circ Res* 1996;**79**:541-550.
49. Fischer JW, Kinsella MG, Clowes MM, Lara S, Clowes AW, Wight TN. Local expression of bovine decorin by cell-mediated gene transfer reduces neointimal formation after balloon injury in rats. *Circ Res* 2000;**86**:676-683.
50. Kim WH, Hong MK, Virmani R, Kornowski R, Jones R, Leon MB. Histopathologic analysis of in-stent neointimal regression in a porcine coronary model. *Coron Artery Dis* 2000;**11**:273-277.
51. Kuroda N, Kobayashi Y, Nameki M, Kuriyama N, Kinoshita T, Okuno T, *et al.* Intimal hyperplasia regression from 6 to 12 months after stenting. *Am J Cardiol* 2002;**89**:869-872.
52. Kimura T, Yokoi H, Nakagawa Y, Tamura T, Kaburagi S, Sawada Y, *et al.* Three-year follow-up after implantation of metallic coronary-artery stents. *N Engl J Med* 1996;**334**:561-566.
53. Asakura M, Ueda Y, Nanto S, Hirayama A, Adachi T, Kitakaze M, *et al.* Remodeling of in-stent neointima, which became thinner and transparent over 3 years: serial angiographic and angioscopic follow-up. *Circulation* 1998;**97**:2003-2006.
54. Kimura T, Abe K, Shizuta S, Odashiro K, Yoshida Y, Sakai K, *et al.* Long-term clinical and angiographic follow-up after coronary stent placement in native coronary arteries. *Circulation* 2002;**105**:2986-2991.
55. Nachman RL, Rafii S. Platelets, petechiae, and preservation of the vascular wall. *N Engl J Med* 2008;**359**:1261-1270.
56. Palmer RM, Ferrige AG, Moncada S. Nitric oxide release accounts for the biological activity of endothelium-derived relaxing factor. *Nature* 1987;**327**:524-526.
57. Fishman JA, Ryan GB, Karnovsky MJ. Endothelial regeneration in the rat carotid artery and the significance of endothelial denudation in the pathogenesis of myointimal thickening. *Lab Invest* 1975;**32**:339-351.
58. van Beusekom HM, Whelan DM, Hofma SH, Krabbendam SC, van Hinsbergh VW, Verdouw PD, *et al.* Long-term endothelial dysfunction is more pronounced after stenting than after balloon angioplasty in porcine coronary arteries. *Journal of the American College of Cardiology* 1998;**32**:1109-1117.
59. Evans DJ, Jackman LE, Chamberlain J, Crosdale DJ, Judge HM, Jetha K, *et al.* Platelet P2Y(12) receptor influences the vessel wall response to arterial injury and thrombosis. *Circulation* 2009;**119**:116-122.
60. Aoki J, Serruys PW, van Beusekom H, Ong AT, McFadden EP, Sianos G, *et al.* Endothelial progenitor cell capture by stents coated with antibody against CD34: the HEALING-FIM (Healthy Endothelial Accelerated Lining Inhibits

Neointimal Growth-First In Man) Registry. *Journal of the American College of Cardiology* 2005;**45**:1574-1579.
61. Inoue T, Sata M, Hikichi Y, Sohma R, Fukuda D, Uchida T, *et al.* Mobilization of CD34-positive bone marrow-derived cells after coronary stent implantation: impact on restenosis. *Circulation* 2007;**115**:553-561.
62. Walter DH, Cejna M, Diaz-Sandoval L, Willis S, Kirkwood L, Stratford PW, *et al.* Local gene transfer of phVEGF-2 plasmid by gene-eluting stents: an alternative strategy for inhibition of restenosis. *Circulation* 2004;**110**:36-45.
63. Van Belle E, Maillard L, Tio FO, Isner JM. Accelerated endothelialization by local delivery of recombinant human vascular endothelial growth factor reduces in-stent intimal formation. *Biochem Biophys Res Commun* 1997;**235**:311-316.
64. Asahara T, Chen D, Tsurumi Y, Kearney M, Rossow S, Passeri J, *et al.* Accelerated restitution of endothelial integrity and endothelium-dependent function after phVEGF165 gene transfer. *Circulation* 1996;**94**:3291-3302.
65. Van Belle E, Tio FO, Chen D, Maillard L, Kearney M, Isner JM. Passivation of metallic stents after arterial gene transfer of phVEGF165 inhibits thrombus formation and intimal thickening. *Journal of the American College of Cardiology* 1997;**29**:1371-1379.
66. Kong D, Melo LG, Gnecchi M, Zhang L, Mostoslavsky G, Liew CC, *et al.* Cytokine-induced mobilization of circulating endothelial progenitor cells enhances repair of injured arteries. *Circulation* 2004;**110**:2039-2046.
67. Kong D, Melo LG, Mangi AA, Zhang L, Lopez-Ilasaca M, Perrella MA, *et al.* Enhanced inhibition of neointimal hyperplasia by genetically engineered endothelial progenitor cells. *Circulation* 2004;**109**:1769-1775.
68. Cooney R, Hynes SO, Sharif F, Howard L, O'Brien T. Effect of gene delivery of NOS isoforms on intimal hyperplasia and endothelial regeneration after balloon injury. *Gene therapy* 2007;**14**:396-404.
69. Garas SM, Huber P, Scott NA. Overview of therapies for prevention of restenosis after coronary interventions. *Pharmacol Ther* 2001;**92**:165-178.
70. Kay IP, Wardeh AJ, Kozuma K, Foley DP, Knook AH, Thury A, *et al.* Radioactive stents delay but do not prevent in-stent neointimal hyperplasia. *Circulation* 2001;**103**:14-17.
71. Teirstein PS, Massullo V, Jani S, Popma JJ, Russo RJ, Schatz RA, *et al.* Three-year clinical and angiographic follow-up after intracoronary radiation : results of a randomized clinical trial. *Circulation* 2000;**101**:360-365.
72. Farb A, Burke AP, Kolodgie FD, Virmani R. Pathological mechanisms of fatal late coronary stent thrombosis in humans. *Circulation* 2003;**108**:1701-1706.
73. Thomas MR. Brachytherapy: here today, gone tomorrow? *Heart* 2005;**91 Suppl 3**:iii32-34.
74. Moses JW, Leon MB, Popma JJ, Fitzgerald PJ, Holmes DR, O'Shaughnessy C, *et al.* Sirolimus-eluting stents versus standard stents in patients with stenosis in a native coronary artery. *N Engl J Med* 2003;**349**:1315-1323.
75. Stone GW, Ellis SG, Cox DA, Hermiller J, O'Shaughnessy C, Mann JT, *et al.* One-year clinical results with the slow-release, polymer-based, paclitaxel-eluting TAXUS stent: the TAXUS-IV trial. *Circulation* 2004;**109**:1942-1947.
76. Cosgrave J, Corbett SJ, Melzi G, Babic R, Biondi-Zoccai GG, Airoldi F, *et al.* Late restenosis following sirolimus-eluting stent implantation. *Am J Cardiol* 2007;**100**:41-44.

77. Cosgrave J, Qasim A, Latib A, Aranzulla TC, Colombo A. Very late restenosis after paclitaxel-eluting stent implantation. *Ann Intern Med* 2007;**147**:885-887.
78. Byrne RA, Iijima R, Mehilli J, Pinieck S, Bruskina O, Schomig A, *et al.* Durability of Antirestenotic Efficacy in Drug-Eluting Stents With and Without Permanent Polymer. *J Am Coll Cardiol Intv* 2009;**2**:291-299.
79. Nilsen DW, Melberg T, Larsen AI, Barvik S, Bonarjee V. Late complications following the deployment of drug eluting stents. *Int J Cardiol* 2006;**109**:398-401.
80. Ako J, Morino Y, Honda Y, Hassan A, Sonoda S, Yock PG, *et al.* Late incomplete stent apposition after sirolimus-eluting stent implantation: a serial intravascular ultrasound analysis. *Journal of the American College of Cardiology* 2005;**46**:1002-1005.
81. Iakovou I, Schmidt T, Bonizzoni E, Ge L, Sangiorgi GM, Stankovic G, *et al.* Incidence, predictors, and outcome of thrombosis after successful implantation of drug-eluting stents. *JAMA* 2005;**293**:2126-2130.
82. Burzotta F, Parma A, Pristipino C, Manzoli A, Belloni F, Sardella G, *et al.* Angiographic and clinical outcome of invasively managed patients with thrombosed coronary bare metal or drug-eluting stents: the OPTIMIST study. *Eur Heart J* 2008;**29**:3011-3021.
83. de la Torre-Hernandez JM, Alfonso F, Hernandez F, Elizaga J, Sanmartin M, Pinar E, *et al.* Drug-Eluting Stent Thrombosis: Results From the Multicenter Spanish Registry ESTROFA (Estudio ESpanol sobre TROmbosis de stents FArmacoactivos). *Journal of the American College of Cardiology* 2008;**51**:986-990.
84. Drachman DE, Edelman ER, Seifert P, Groothuis AR, Bornstein DA, Kamath KR, *et al.* Neointimal thickening after stent delivery of paclitaxel: change in composition and arrest of growth over six months. *Journal of the American College of Cardiology* 2000;**36**:2325-2332.
85. Farb A, Heller PF, Shroff S, Cheng L, Kolodgie FD, Carter AJ, *et al.* Pathological analysis of local delivery of paclitaxel via a polymer-coated stent. *Circulation* 2001;**104**:473-479.
86. Finn AV, Kolodgie FD, Harnek J, Guerrero LJ, Acampado E, Tefera K, *et al.* Differential response of delayed healing and persistent inflammation at sites of overlapping sirolimus- or paclitaxel-eluting stents. *Circulation* 2005;**112**:270-278.
87. Joner M, Finn AV, Farb A, Mont EK, Kolodgie FD, Ladich E, *et al.* Pathology of drug-eluting stents in humans: delayed healing and late thrombotic risk. *Journal of the American College of Cardiology* 2006;**48**:193-202.
88. Finn AV, Nakazawa G, Joner M, Kolodgie FD, Mont EK, Gold HK, *et al.* Vascular responses to drug eluting stents: importance of delayed healing. *Arteriosclerosis, thrombosis, and vascular biology* 2007;**27**:1500-1510.
89. Kotani J, Awata M, Nanto S, Uematsu M, Oshima F, Minamiguchi H, *et al.* Incomplete neointimal coverage of sirolimus-eluting stents: angioscopic findings. *Journal of the American College of Cardiology* 2006;**47**:2108-2111.
90. Oyabu J, Ueda Y, Ogasawara N, Okada K, Hirayama A, Kodama K. Angioscopic evaluation of neointima coverage: sirolimus drug-eluting stent versus bare metal stent. *Am Heart J* 2006;**152**:1168-1174.

91. Cook S, Wenaweser P, Togni M, Billinger M, Morger C, Seiler C, *et al.* Incomplete stent apposition and very late stent thrombosis after drug-eluting stent implantation. *Circulation* 2007;**115**:2426-2434.
92. Cook S, Ladich E, Nakazawa G, Eshtehardi P, Neidhart M, Vogel R, *et al.* Correlation of Intravascular Ultrasound Findings With Histopathological Analysis of Thrombus Aspirates in Patients With Very Late Drug-Eluting Stent Thrombosis. *Circulation* 2009.
93. Kochiadakis GE, Marketou ME, Panutsopulos D, Arfanakis DA, Skalidis EI, Igoumenidis NE, *et al.* Vascular endothelial growth factor protein levels and gene expression in peripheral monocytes after stenting: a randomized comparative study of sirolimus: eluting and bare metal stents. *Eur Heart J* 2008;**29**:733-740.
94. Nebeker JR, Virmani R, Bennett CL, Hoffman JM, Samore MH, Alvarez J, *et al.* Hypersensitivity cases associated with drug-eluting coronary stents: a review of available cases from the Research on Adverse Drug Events and Reports (RADAR) project. *Journal of the American College of Cardiology* 2006;**47**:175-181.
95. Grines CL, Bonow RO, Casey DE, Jr., Gardner TJ, Lockhart PB, Moliterno DJ, *et al.* Prevention of premature discontinuation of dual antiplatelet therapy in patients with coronary artery stents: a science advisory from the American Heart Association, American College of Cardiology, Society for Cardiovascular Angiography and Interventions, American College of Surgeons, and American Dental Association, with representation from the American College of Physicians. *Circulation* 2007;**115**:813-818.
96. Daemen J, Wenaweser P, Tsuchida K, Abrecht L, Vaina S, Morger C, *et al.* Early and late coronary stent thrombosis of sirolimus-eluting and paclitaxel-eluting stents in routine clinical practice: data from a large two-institutional cohort study. *Lancet* 2007;**369**:667-678.
97. Stone GW, Midei M, Newman W, Sanz M, Hermiller JB, Williams J, *et al.* Comparison of an everolimus-eluting stent and a paclitaxel-eluting stent in patients with coronary artery disease: a randomized trial. *JAMA* 2008;**299**:1903-1913.
98. Fajadet J, Wijns W, Laarman GJ, Kuck KH, Ormiston J, Munzel T, *et al.* Randomized, double-blind, multicenter study of the Endeavor zotarolimus-eluting phosphorylcholine-encapsulated stent for treatment of native coronary artery lesions: clinical and angiographic results of the ENDEAVOR II trial. *Circulation* 2006;**114**:798-806.
99. Erbel R, Di Mario C, Bartunek J, Bonnier J, de Bruyne B, Eberli FR, *et al.* Temporary scaffolding of coronary arteries with bioabsorbable magnesium stents: a prospective, non-randomised multicentre trial. *Lancet* 2007;**369**:1869-1875.
100. Ormiston JA, Serruys PW, Regar E, Dudek D, Thuesen L, Webster MW, *et al.* A bioabsorbable everolimus-eluting coronary stent system for patients with single de-novo coronary artery lesions (ABSORB): a prospective open-label trial. *Lancet* 2008;**371**:899-907.
101. Serruys PW, Ormiston JA, Onuma Y, Regar E, Gonzalo N, Garcia-Garcia HM, *et al.* A bioabsorbable everolimus-eluting coronary stent system (ABSORB): 2-year outcomes and results from multiple imaging methods. *Lancet* 2009;**373**:897-910.

102. Miglionico M, Patti G, D'Ambrosio A, Di Sciascio G. Percutaneous coronary intervention utilizing a new endothelial progenitor cells antibody-coated stent: a prospective single-center registry in high-risk patients. *Catheter Cardiovasc Interv* 2008;**71**:600-604.
103. Bystron M, Cervinka P, Spacek R, Kvasnak M, Jakabcin J, Cervinkova M, *et al.* Randomized comparison of endothelial progenitor cells capture stent versus cobalt-chromium stent for treatment of ST-elevation myocardial infarction. Six-month clinical, angiographic, and IVUS follow-up. *Catheter Cardiovasc Interv* 2010;**76**:627-631.
104. Nabel EG, Plautz G, Boyce FM, Stanley JC, Nabel GJ. Recombinant gene expression in vivo within endothelial cells of the arterial wall. *Science* 1989;**244**:1342-1344.
105. Rissanen TT, Yla-Herttuala S. Current status of cardiovascular gene therapy. *Mol Ther* 2007;**15**:1233-1247.
106. Gaffney MM, Hynes SO, Barry F, O'Brien T. Cardiovascular gene therapy: current status and therapeutic potential. *British journal of pharmacology* 2007;**152**:175-188.
107. Sharif F, Daly K, Crowley J, O'Brien T. Current status of catheter- and stent-based gene therapy. *Cardiovascular research* 2004;**64**:208-216.
108. Appleby CE, Kingston PA. Gene therapy for restenosis--what now, what next? *Current gene therapy* 2004;**4**:153-182.
109. Hu YC. Baculovirus vectors for gene therapy. *Adv Virus Res* 2006;**68**:287-320.
110. Williams P, Ranjzad P, Kakar S, Kingston P. Development of Viral Vectors for Use in Cardiovascular Gene Therapy. *Viruses* 2010;**2**:334-371.
111. Kingston PA, Sinha S, Appleby CE, David A, Verakis T, Castro MG, *et al.* Adenovirus-mediated gene transfer of transforming growth factor-beta3, but not transforming growth factor-beta1, inhibits constrictive remodeling and reduces luminal loss after coronary angioplasty. *Circulation* 2003;**108**:2819-2825.
112. Hedman M, Hartikainen J, Syvanne M, Stjernvall J, Hedman A, Kivela A, *et al.* Safety and feasibility of catheter-based local intracoronary vascular endothelial growth factor gene transfer in the prevention of postangioplasty and in-stent restenosis and in the treatment of chronic myocardial ischemia: phase II results of the Kuopio Angiogenesis Trial (KAT). *Circulation* 2003;**107**:2677-2683.
113. Kingston PA, Sinha S, David A, Castro MG, Lowenstein PR, Heagerty AM. Adenovirus-mediated gene transfer of a secreted transforming growth factor-beta type II receptor inhibits luminal loss and constrictive remodeling after coronary angioplasty and enhances adventitial collagen deposition. *Circulation* 2001;**104**:2595-2601.
114. Laitinen M, Hartikainen J, Hiltunen MO, Eranen J, Kiviniemi M, Narvanen O, *et al.* Catheter-mediated vascular endothelial growth factor gene transfer to human coronary arteries after angioplasty. *Human gene therapy* 2000;**11**:263-270.
115. Tahlil O, Brami M, Feldman LJ, Branellec D, Steg PG. The Dispatch catheter as a delivery tool for arterial gene transfer. *Cardiovascular research* 1997;**33**:181-187.
116. Laitinen M, Pakkanen T, Donetti E, Baetta R, Luoma J, Lehtolainen P, *et al.* Gene transfer into the carotid artery using an adventitial collar: comparison of the effectiveness of the plasmid-liposome complexes, retroviruses, pseudotyped retroviruses, and adenoviruses. *Human gene therapy* 1997;**8**:1645-1650.

117. Rome JJ, Shayani V, Newman KD, Farrell S, Lee SW, Virmani R, *et al.* Adenoviral vector-mediated gene transfer into sheep arteries using a double-balloon catheter. *Human gene therapy* 1994;**5**:1249-1258.
118. Gene Therapy Clinical Trials Worldwide.
119. Newman KD, Dunn PF, Owens JW, Schulick AH, Virmani R, Sukhova G, *et al.* Adenovirus-mediated gene transfer into normal rabbit arteries results in prolonged vascular cell activation, inflammation, and neointimal hyperplasia. *J Clin Invest* 1995;**96**:2955-2965.
120. Schulick AH, Vassalli G, Dunn PF, Dong G, Rade JJ, Zamarron C, *et al.* Established immunity precludes adenovirus-mediated gene transfer in rat carotid arteries. Potential for immunosuppression and vector engineering to overcome barriers of immunity. *J Clin Invest* 1997;**99**:209-219.
121. Palmer DJ, Ng P. Helper-dependent adenoviral vectors for gene therapy. *Human gene therapy* 2005;**16**:1-16.
122. Marshall E. Gene therapy death prompts review of adenovirus vector. *Science* 1999;**286**:2244-2245.
123. Volpers C, Kochanek S. Adenoviral vectors for gene transfer and therapy. *The journal of gene medicine* 2004;**6 Suppl 1**:S164-171.
124. Campos SK, Barry MA. Current advances and future challenges in Adenoviral vector biology and targeting. *Current gene therapy* 2007;**7**:189-204.
125. Wang Z, Zhu T, Qiao C, Zhou L, Wang B, Zhang J, *et al.* Adeno-associated virus serotype 8 efficiently delivers genes to muscle and heart. *Nat Biotechnol* 2005;**23**:321-328.
126. Bish LT, Morine K, Sleeper MM, Sanmiguel J, Wu D, Gao G, *et al.* AAV9 Provides Global Cardiac Gene Transfer Superior to AAV1, AAV6, AAV7, and AAV8 in the Mouse and Rat. *Human gene therapy* 2008.
127. McCarty DM. Self-complementary AAV vectors; advances and applications. *Mol Ther* 2008;**16**:1648-1656.
128. Kerstin E, Patricia S, Jörg RS. Update on the prevalence of serum antibodies (IgG and IgM) to adeno-associated virus (AAV). *Journal of Medical Virology* 1999;**59**:406-411.
129. Zaiss AK, Muruve DA. Immunity to adeno-associated virus vectors in animals and humans: a continued challenge. *Gene therapy* 2008;**15**:808-816.
130. Mingozzi F, High KA. Immune responses to AAV in clinical trials. *Current gene therapy* 2007;**7**:316-324.
131. Manno CS, Arruda VR, Pierce GF, Glader B, Ragni M, Rasko J, *et al.* Successful transduction of liver in hemophilia by AAV-factor IX and limitations imposed by the host immune response. *Nat Med* 2006;**12**:342-347.
132. Mingozzi F, Maus MV, Hui DJ, Sabatino DE, Murphy SL, Rasko JEJ, *et al.* CD8+ T-cell responses to adeno-associated virus capsid in humans. *Nat Med* 2007;**13**:419-422.
133. Hajjar RJ, Zsebo K, Deckelbaum L, Thompson C, Rudy J, Yaroshinsky A, *et al.* Design of a phase 1/2 trial of intracoronary administration of AAV1/SERCA2a in patients with heart failure. *J Card Fail* 2008;**14**:355-367.
134. Sharif F, Hynes SO, McMahon J, Cooney R, Conroy S, Dockery P, *et al.* Gene-eluting stents: comparison of adenoviral and adeno- associated viral gene delivery to the blood vessel wall in vivo. *Human gene therapy* 2006;**17**:741-750.

135. Yanez-Munoz RJ, Balaggan KS, MacNeil A, Howe SJ, Schmidt M, Smith AJ, *et al.* Effective gene therapy with nonintegrating lentiviral vectors. *Nat Med* 2006;**12**:348-353.
136. Bonci D, Cittadini A, Latronico MV, Borello U, Aycock JK, Drusco A, *et al.* 'Advanced' generation lentiviruses as efficient vectors for cardiomyocyte gene transduction in vitro and in vivo. *Gene therapy* 2003;**10**:630-636.
137. Takahashi A, Palmer-Opolski M, Smith RC, Walsh K. Transgene delivery of plasmid DNA to smooth muscle cells and macrophages from a biostable polymer-coated stent. *Gene therapy* 2003;**10**:1471-1478.
138. Indolfi C, Avvedimento EV, Rapacciuolo A, Esposito G, Di Lorenzo E, Leccia A, *et al.* In vivo gene transfer: prevention of neointima formation by inhibition of mitogen-activated protein kinase kinase. *Basic Res Cardiol* 1997;**92**:378-384.
139. Kawabata K, Takakura Y, Hashida M. The fate of plasmid DNA after intravenous injection in mice: involvement of scavenger receptors in its hepatic uptake. *Pharm Res* 1995;**12**:825-830.
140. Dean DA, Strong DD, Zimmer WE. Nuclear entry of nonviral vectors. *Gene therapy* 2005;**12**:881-890.
141. Isaka Y, Imai E. Electroporation-mediated gene therapy. *Expert Opin Drug Deliv* 2007;**4**:561-571.
142. Young JL, Benoit JN, Dean DA. Effect of a DNA nuclear targeting sequence on gene transfer and expression of plasmids in the intact vasculature. *Gene therapy* 2003;**10**:1465-1470.
143. Seidler RW, Allgauer S, Ailinger S, Sterner A, Dev N, Rabussay D, *et al.* In vivo human MCP-1 transfection in porcine arteries by intravascular electroporation. *Pharm Res* 2005;**22**:1685-1691.
144. Leong-Poi H, Kuliszewski MA, Lekas M, Sibbald M, Teichert-Kuliszewska K, Klibanov AL, *et al.* Therapeutic arteriogenesis by ultrasound-mediated VEGF165 plasmid gene delivery to chronically ischemic skeletal muscle. *Circ Res* 2007;**101**:295-303.
145. Kawakami S, Higuchi Y, Hashida M. Nonviral approaches for targeted delivery of plasmid DNA and oligonucleotide. *J Pharm Sci* 2008;**97**:726-745.
146. DeYoung MB, Zamarron C, Lin AP, Qiu C, Driscoll RM, Dichek DA. Optimizing vascular gene transfer of plasminogen activator inhibitor 1. *Human gene therapy* 1999;**10**:1469-1478.
147. Ribault S, Neuville P, Mechine-Neuville A, Auge F, Parlakian A, Gabbiani G, *et al.* Chimeric smooth muscle-specific enhancer/promoters: valuable tools for adenovirus-mediated cardiovascular gene therapy. *Circ Res* 2001;**88**:468-475.
148. Addison CL, Hitt M, Kunsken D, Graham FL. Comparison of the human versus murine cytomegalovirus immediate early gene promoters for transgene expression by adenoviral vectors. *J Gen Virol* 1997;**78 (Pt 7)**:1653-1661.
149. Kim YS, Risser R. TAR-independent transactivation of the murine cytomegalovirus major immediate-early promoter by the Tat protein. *J Virol* 1993;**67**:239-248.
150. Kim SY, Lee JH, Shin HS, Kang HJ, Kim YS. The human elongation factor 1 alpha (EF-1 alpha) first intron highly enhances expression of foreign genes from the murine cytomegalovirus promoter. *J Biotechnol* 2002;**93**:183-187.
151. Zufferey R, Donello JE, Trono D, Hope TJ. Woodchuck hepatitis virus posttranscriptional regulatory element enhances expression of transgenes delivered by retroviral vectors. *J Virol* 1999;**73**:2886-2892.

152. Loeb JE, Cordier WS, Harris ME, Weitzman MD, Hope TJ. Enhanced expression of transgenes from adeno-associated virus vectors with the woodchuck hepatitis virus posttranscriptional regulatory element: implications for gene therapy. *Human gene therapy* 1999;**10**:2295-2305.
153. Kallmeier RC, Somasundaram C, Babij P. A novel smooth muscle-specific enhancer regulates transcription of the smooth muscle myosin heavy chain gene in vascular smooth muscle cells. *J Biol Chem* 1995;**270**:30949-30957.
154. Keogh MC, Chen D, Schmitt JF, Dennehy U, Kakkar VV, Lemoine NR. Design of a muscle cell-specific expression vector utilising human vascular smooth muscle alpha-actin regulatory elements. *Gene therapy* 1999;**6**:616-628.
155. Appleby CE, Kingston PA, David A, Gerdes CA, Umana P, Castro MG, *et al.* A novel combination of promoter and enhancers increases transgene expression in vascular smooth muscle cells in vitro and coronary arteries in vivo after adenovirus-mediated gene transfer. *Gene therapy* 2003;**10**:1616-1622.
156. Palmiter RD, Sandgren EP, Avarbock MR, Allen DD, Brinster RL. Heterologous introns can enhance expression of transgenes in mice. *Proc Natl Acad Sci U S A* 1991;**88**:478-482.
157. Brondyk B. pCI and pSI Mammalian Expression Vectors. *Promega Notes Magazine* 1994:7-12.
158. Carswell S, Alwine JC. Efficiency of utilization of the simian virus 40 late polyadenylation site: effects of upstream sequences. *Mol Cell Biol* 1989;**9**:4248-4258.
159. Dowty ME, Williams P, Zhang G, Hagstrom JE, Wolff JA. Plasmid DNA entry into postmitotic nuclei of primary rat myotubes. *Proc Natl Acad Sci U S A* 1995;**92**:4572-4576.
160. Capecchi MR. High efficiency transformation by direct microinjection of DNA into cultured mammalian cells. *Cell* 1980;**22**:479-488.
161. Dean DA. Import of plasmid DNA into the nucleus is sequence specific. *Exp Cell Res* 1997;**230**:293-302.
162. Dean DA, Dean BS, Muller S, Smith LC. Sequence requirements for plasmid nuclear import. *Exp Cell Res* 1999;**253**:713-722.
163. Miller AM, Dean DA. Cell-specific nuclear import of plasmid DNA in smooth muscle requires tissue-specific transcription factors and DNA sequences. *Gene therapy* 2008;**15**:1107-1115.
164. Vacik J, Dean BS, Zimmer WE, Dean DA. Cell-specific nuclear import of plasmid DNA. *Gene therapy* 1999;**6**:1006-1014.
165. Young JL, Zimmer WE, Dean DA. Smooth muscle-specific gene delivery in the vasculature based on restriction of DNA nuclear import. *Exp Biol Med (Maywood)* 2008;**233**:840-848.
166. Yates JL, Warren N, Sugden B. Stable replication of plasmids derived from Epstein-Barr virus in various mammalian cells. *Nature* 1985;**313**:812-815.
167. Mazda O, Satoh E, Yasutomi K, Imanishi J. Extremely efficient gene transfection into lympho-hematopoietic cell lines by Epstein-Barr virus-based vectors. *J Immunol Methods* 1997;**204**:143-151.
168. Langle-Rouault F, Patzel V, Benavente A, Taillez M, Silvestre N, Bompard A, *et al.* Up to 100-fold increase of apparent gene expression in the presence of Epstein-Barr virus oriP sequences and EBNA1: implications of the nuclear import of plasmids. *J Virol* 1998;**72**:6181-6185.

169. Kingston PA. Epstein-Barr Nuclear Antigen-1 markedly enhances non-virally-mediated transgene expression in cultured smooth muscle cells while inclusion of a matrix-attachment region does not. . 4th Annual meeting of the British Society for Gene Therapy. Warwick, 2007.
170. Gill DR, Pringle IA, Hyde SC. Progress and Prospects: The design and production of plasmid vectors. *Gene therapy* 2009.
171. Hyde SC, Pringle IA, Abdullah S, Lawton AE, Davies LA, Varathalingam A, *et al.* CpG-free plasmids confer reduced inflammation and sustained pulmonary gene expression. *Nat Biotechnol* 2008;**26**:549-551.
172. Ye YW, Landau C, Willard JE, Rajasubramanian G, Moskowitz A, Aziz S, *et al.* Bioresorbable microporous stents deliver recombinant adenovirus gene transfer vectors to the arterial wall. *Ann Biomed Eng* 1998;**26**:398-408.
173. Klugherz BD, Jones PL, Cui X, Chen W, Meneveau NF, DeFelice S, *et al.* Gene delivery from a DNA controlled-release stent in porcine coronary arteries. *Nat Biotech* 2000;**18**:1181-1184.
174. Klugherz BD, Song C, DeFelice S, Cui X, Lu Z, Connolly J, *et al.* Gene delivery to pig coronary arteries from stents carrying antibody-tethered adenovirus. *Human gene therapy* 2002;**13**:443-454.
175. Perlstein I, Connolly JM, Cui X, Song C, Li Q, Jones PL, *et al.* DNA delivery from an intravascular stent with a denatured collagen-polylactic-polyglycolic acid-controlled release coating: mechanisms of enhanced transfection. *Gene therapy* 2003;**10**:1420-1428.
176. Johnson TW, Wu YX, Herdeg C, Baumbach A, Newby AC, Karsch KR, *et al.* Stent-based delivery of tissue inhibitor of metalloproteinase-3 adenovirus inhibits neointimal formation in porcine coronary arteries. *Arteriosclerosis, thrombosis, and vascular biology* 2005;**25**:754-759.
177. Fishbein I, Alferiev IS, Nyanguile O, Gaster R, Vohs JM, Wong GS, *et al.* Bisphosphonate-mediated gene vector delivery from the metal surfaces of stents. *Proc Natl Acad Sci U S A* 2006;**103**:159-164.
178. Egashira K, Nakano K, Ohtani K, Funakoshi K, Zhao G, Ihara Y, *et al.* Local delivery of anti-monocyte chemoattractant protein-1 by gene-eluting stents attenuates in-stent stenosis in rabbits and monkeys. *Arteriosclerosis, thrombosis, and vascular biology* 2007;**27**:2563-2568.
179. Fishbein I, Alferiev I, Bakay M, Stachelek SJ, Sobolewski P, Lai M, *et al.* Local delivery of gene vectors from bare-metal stents by use of a biodegradable synthetic complex inhibits in-stent restenosis in rat carotid arteries. *Circulation* 2008;**117**:2096-2103.
180. Jin X, Mei L, Song C, Liu L, Leng X, Sun H, *et al.* Immobilization of plasmid DNA on an anti-DNA antibody modified coronary stent for intravascular site-specific gene therapy. *The journal of gene medicine* 2008;**10**:421-429.
181. Sharif F, Hynes SO, Cooney R, Howard L, McMahon J, Daly K, *et al.* Gene-eluting Stents: Adenovirus-mediated Delivery of eNOS to the Blood Vessel Wall Accelerates Re-endothelialization and Inhibits Restenosis. *Mol Ther* 2008.
182. Zhang LH, Luo T, Zhang C, Luo P, Jin X, Song CX, *et al.* Anti-DNA antibody modified coronary stent for plasmid gene delivery: results obtained from a porcine coronary stent model. *The journal of gene medicine* 2011;**13**:37-45.
183. van der Giessen WJ, Lincoff AM, Schwartz RS, van Beusekom HMM, Serruys PW, Holmes DR, *et al.* Marked Inflammatory Sequelae to Implantation of

Biodegradable and Nonbiodegradable Polymers in Porcine Coronary Arteries. *Circulation* 1996;**94**:1690-1697.
184. Windecker S, Serruys PW, Wandel S, Buszman P, Trznadel S, Linke A, *et al.* Biolimus-eluting stent with biodegradable polymer versus sirolimus-eluting stent with durable polymer for coronary revascularisation (LEADERS): a randomised non-inferiority trial. *Lancet* 2008;**372**:1163-1173.
185. Brito LA, Chandrasekhar S, Little SR, Amiji MM. In vitro and In vivo studies of local arterial gene delivery and transfection using lipopolyplexes-embedded stents. *J Biomed Mater Res A* 2009.
186. Yla-Herttuala S, Rissanen TT, Vajanto I, Hartikainen J. Vascular endothelial growth factors: biology and current status of clinical applications in cardiovascular medicine. *Journal of the American College of Cardiology* 2007;**49**:1015-1026.
187. Brigstock DR, Goldschmeding R, Katsube KI, Lam SC, Lau LF, Lyons K, *et al.* Proposal for a unified CCN nomenclature. *Mol Pathol* 2003;**56**:127-128.
188. Yeger H, Perbal B. The CCN family of genes: a perspective on CCN biology and therapeutic potential. *J Cell Commun Signal* 2007;**1**:159-164.
189. Shi-Wen X, Leask A, Abraham D. Regulation and function of connective tissue growth factor/CCN2 in tissue repair, scarring and fibrosis. *Cytokine & growth factor reviews* 2008;**19**:133-144.
190. Perbal B. CCN proteins: multifunctional signalling regulators. *Lancet* 2004;**363**:62-64.
191. Kubota S, Takigawa M. CCN family proteins and angiogenesis: from embryo to adulthood. *Angiogenesis* 2007;**10**:1-11.
192. Bradham DM, Igarashi A, Potter RL, Grotendorst GR. Connective tissue growth factor: a cysteine-rich mitogen secreted by human vascular endothelial cells is related to the SRC-induced immediate early gene product CEF-10. *J Cell Biol* 1991;**114**:1285-1294.
193. Brigstock DR, Steffen CL, Kim GY, Vegunta RK, Diehl JR, Harding PA. Purification and characterization of novel heparin-binding growth factors in uterine secretory fluids. Identification as heparin-regulated Mr 10,000 forms of connective tissue growth factor. *J Biol Chem* 1997;**272**:20275-20282.
194. Leask A, Abraham DJ. All in the CCN family: essential matricellular signaling modulators emerge from the bunker. *Journal of cell science* 2006;**119**:4803-4810.
195. Gao R, Brigstock DR. A novel integrin alpha5beta1 binding domain in module 4 of connective tissue growth factor (CCN2/CTGF) promotes adhesion and migration of activated pancreatic stellate cells. *Gut* 2006;**55**:856-862.
196. Segarini PR, Nesbitt JE, Li D, Hays LG, Yates JR, 3rd, Carmichael DF. The low density lipoprotein receptor-related protein/alpha2-macroglobulin receptor is a receptor for connective tissue growth factor. *J Biol Chem* 2001;**276**:40659-40667.
197. Gao R, Brigstock DR. Low density lipoprotein receptor-related protein (LRP) is a heparin-dependent adhesion receptor for connective tissue growth factor (CTGF) in rat activated hepatic stellate cells. *Hepatol Res* 2003;**27**:214-220.
198. Grotendorst GR, Duncan MR. Individual domains of connective tissue growth factor regulate fibroblast proliferation and myofibroblast differentiation. *FASEB J* 2005;**19**:729-738.

199. Grotendorst GR, Rahmanie H, Duncan MR. Combinatorial signaling pathways determine fibroblast proliferation and myofibroblast differentiation. *Faseb J* 2004;**18**:469-479.
200. Frazier K, Williams S, Kothapalli D, Klapper H, Grotendorst GR. Stimulation of fibroblast cell growth, matrix production, and granulation tissue formation by connective tissue growth factor. *J Invest Dermatol* 1996;**107**:404-411.
201. Fan WH, Pech M, Karnovsky MJ. Connective tissue growth factor (CTGF) stimulates vascular smooth muscle cell growth and migration in vitro. *Eur J Cell Biol* 2000;**79**:915-923.
202. Shimo T, Nakanishi T, Kimura Y, Nishida T, Ishizeki K, Matsumura T, *et al.* Inhibition of endogenous expression of connective tissue growth factor by its antisense oligonucleotide and antisense RNA suppresses proliferation and migration of vascular endothelial cells. *J Biochem* 1998;**124**:130-140.
203. Babic AM, Chen CC, Lau LF. Fisp12/mouse connective tissue growth factor mediates endothelial cell adhesion and migration through integrin alphavbeta3, promotes endothelial cell survival, and induces angiogenesis in vivo. *Mol Cell Biol* 1999;**19**:2958-2966.
204. Boes M, Dake BL, Booth BA, Erondu NE, Oh Y, Hwa V, *et al.* Connective tissue growth factor (IGFBP-rP2) expression and regulation in cultured bovine endothelial cells. *Endocrinology* 1999;**140**:1575-1580.
205. Inoki I, Shiomi T, Hashimoto G, Enomoto H, Nakamura H, Makino K, *et al.* Connective tissue growth factor binds vascular endothelial growth factor (VEGF) and inhibits VEGF-induced angiogenesis. *Faseb J* 2002;**16**:219-221.
206. Brigstock DR. Regulation of angiogenesis and endothelial cell function by connective tissue growth factor (CTGF) and cysteine-rich 61 (CYR61). *Angiogenesis* 2002;**5**:153-165.
207. Hishikawa K, Nakaki T, Fujii T. Connective tissue growth factor induces apoptosis via caspase 3 in cultured human aortic smooth muscle cells. *European journal of pharmacology* 2000;**392**:19-22.
208. Hishikawa K, Nakaki T, Fujii T. Transforming growth factor-beta(1) induces apoptosis via connective tissue growth factor in human aortic smooth muscle cells. *European journal of pharmacology* 1999;**385**:287-290.
209. Hishikawa K, Oemar BS, Tanner FC, Nakaki T, Fujii T, Luscher TF. Overexpression of connective tissue growth factor gene induces apoptosis in human aortic smooth muscle cells. *Circulation* 1999;**100**:2108-2112.
210. Oemar BS, Werner A, Garnier JM, Do DD, Godoy N, Nauck M, *et al.* Human connective tissue growth factor is expressed in advanced atherosclerotic lesions. *Circulation* 1997;**95**:831-839.
211. Liu LD, Shi HJ, Jiang L, Wang LC, Ma SH, Dong CH, *et al.* The repairing effect of a recombinant human connective-tissue growth factor in a burn-wounded rhesus-monkey (Macaca mulatta) model. *Biotechnol Appl Biochem* 2007;**47**:105-112.
212. Igarashi A, Okochi H, Bradham DM, Grotendorst GR. Regulation of connective tissue growth factor gene expression in human skin fibroblasts and during wound repair. *Mol Biol Cell* 1993;**4**:637-645.
213. Grotendorst GR. Connective tissue growth factor: a mediator of TGF-beta action on fibroblasts. *Cytokine & growth factor reviews* 1997;**8**:171-179.

214. Abreu JG, Ketpura NI, Reversade B, De Robertis EM. Connective-tissue growth factor (CTGF) modulates cell signalling by BMP and TGF-beta. *Nat Cell Biol* 2002;**4**:599-604.
215. Holmes A, Abraham DJ, Sa S, Shiwen X, Black CM, Leask A. CTGF and SMADs, maintenance of scleroderma phenotype is independent of SMAD signaling. *J Biol Chem* 2001;**276**:10594-10601.
216. Xu SW, Howat SL, Renzoni EA, Holmes A, Pearson JD, Dashwood MR, *et al.* Endothelin-1 induces expression of matrix-associated genes in lung fibroblasts through MEK/ERK. *J Biol Chem* 2004;**279**:23098-23103.
217. Rodriguez-Vita J, Ruiz-Ortega M, Ruperez M, Esteban V, Sanchez-Lopez E, Plaza JJ, *et al.* Endothelin-1, via ETA receptor and independently of transforming growth factor-beta, increases the connective tissue growth factor in vascular smooth muscle cells. *Circ Res* 2005;**97**:125-134.
218. Stratton R, Rajkumar V, Ponticos M, Nichols B, Shiwen X, Black CM, *et al.* Prostacyclin derivatives prevent the fibrotic response to TGF-beta by inhibiting the Ras/MEK/ERK pathway. *FASEB J* 2002;**16**:1949-1951.
219. Abraham DJ, Shiwen X, Black CM, Sa S, Xu Y, Leask A. Tumor necrosis factor alpha suppresses the induction of connective tissue growth factor by transforming growth factor-beta in normal and scleroderma fibroblasts. *J Biol Chem* 2000;**275**:15220-15225.
220. Finckenberg P, Inkinen K, Ahonen J, Merasto S, Louhelainen M, Vapaatalo H, *et al.* Angiotensin II induces connective tissue growth factor gene expression via calcineurin-dependent pathways. *Am J Pathol* 2003;**163**:355-366.
221. Chambers RC, Leoni P, Blanc-Brude OP, Wembridge DE, Laurent GJ. Thrombin is a potent inducer of connective tissue growth factor production via proteolytic activation of protease-activated receptor-1. *J Biol Chem* 2000;**275**:35584-35591.
222. Murphy M, Godson C, Cannon S, Kato S, Mackenzie HS, Martin F, *et al.* Suppression subtractive hybridization identifies high glucose levels as a stimulus for expression of connective tissue growth factor and other genes in human mesangial cells. *J Biol Chem* 1999;**274**:5830-5834.
223. Ruperez M, Lorenzo O, Blanco-Colio LM, Esteban V, Egido J, Ruiz-Ortega M. Connective tissue growth factor is a mediator of angiotensin II-induced fibrosis. *Circulation* 2003;**108**:1499-1505.
224. Higgins DF, Biju MP, Akai Y, Wutz A, Johnson RS, Haase VH. Hypoxic induction of Ctgf is directly mediated by Hif-1. *Am J Physiol Renal Physiol* 2004;**287**:F1223-1232.
225. Chen Y, Abraham DJ, Shi-Wen X, Pearson JD, Black CM, Lyons KM, *et al.* CCN2 (connective tissue growth factor) promotes fibroblast adhesion to fibronectin. *Mol Biol Cell* 2004;**15**:5635-5646.
226. Friedrichsen S, Heuer H, Christ S, Cuthill D, Bauer K, Raivich G. Gene expression of connective tissue growth factor in adult mouse. *Growth Factors* 2005;**23**:43-53.
227. Ivkovic S, Yoon BS, Popoff SN, Safadi FF, Libuda DE, Stephenson RC, *et al.* Connective tissue growth factor coordinates chondrogenesis and angiogenesis during skeletal development. *Development* 2003;**130**:2779-2791.
228. Kawaki H, Kubota S, Suzuki A, Yamada T, Matsumura T, Mandai T, *et al.* Functional requirement of CCN2 for intramembranous bone formation in embryonic mice. *Biochem Biophys Res Commun* 2008;**366**:450-456.

229. Kikuchi T, Kubota S, Asaumi K, Kawaki H, Nishida T, Kawata K, *et al.* Promotion of bone regeneration by CCN2 incorporated into gelatin hydrogel. *Tissue Eng Part A* 2008;**14**:1089-1098.
230. Shimo T, Nakanishi T, Nishida T, Asano M, Kanyama M, Kuboki T, *et al.* Connective tissue growth factor induces the proliferation, migration, and tube formation of vascular endothelial cells in vitro, and angiogenesis in vivo. *J Biochem* 1999;**126**:137-145.
231. Kuiper EJ, Roestenberg P, Ehlken C, Lambert V, van Treslong-de Groot HB, Lyons KM, *et al.* Angiogenesis is not impaired in connective tissue growth factor (CTGF) knock-out mice. *J Histochem Cytochem* 2007;**55**:1139-1147.
232. Mori T, Kawara S, Shinozaki M, Hayashi N, Kakinuma T, Igarashi A, *et al.* Role and interaction of connective tissue growth factor with transforming growth factor-beta in persistent fibrosis: A mouse fibrosis model. *J Cell Physiol* 1999;**181**:153-159.
233. Fataccioli V, Abergel V, Wingertsmann L, Neuville P, Spitz E, Adnot S, *et al.* Stimulation of angiogenesis by Cyr61 gene: a new therapeutic candidate. *Human gene therapy* 2002;**13**:1461-1470.
234. Dean RG, Balding LC, Candido R, Burns WC, Cao Z, Twigg SM, *et al.* Connective tissue growth factor and cardiac fibrosis after myocardial infarction. *J Histochem Cytochem* 2005;**53**:1245-1256.
235. Hayashi N, Kakimuma T, Soma Y, Grotendorst GR, Tamaki K, Harada M, *et al.* Connective tissue growth factor is directly related to liver fibrosis. *Hepatogastroenterology* 2002;**49**:133-135.
236. Ito Y, Aten J, Bende RJ, Oemar BS, Rabelink TJ, Weening JJ, *et al.* Expression of connective tissue growth factor in human renal fibrosis. *Kidney Int* 1998;**53**:853-861.
237. Igarashi A, Nashiro K, Kikuchi K, Sato S, Ihn H, Grotendorst GR, *et al.* Significant correlation between connective tissue growth factor gene expression and skin sclerosis in tissue sections from patients with systemic sclerosis. *J Invest Dermatol* 1995;**105**:280-284.
238. Cicha I, Yilmaz A, Klein M, Raithel D, Brigstock DR, Daniel WG, *et al.* Connective tissue growth factor is overexpressed in complicated atherosclerotic plaques and induces mononuclear cell chemotaxis in vitro. *Arteriosclerosis, thrombosis, and vascular biology* 2005;**25**:1008-1013.
239. Adam O, Lavall D, Theobald K, Hohl M, Grube M, Ameling S, *et al.* Rac1-induced connective tissue growth factor regulates connexin 43 and N-cadherin expression in atrial fibrillation. *Journal of the American College of Cardiology* 2010;**55**:469-480.
240. Ellis PD, Chen Q, Barker PJ, Metcalfe JC, Kemp PR. Nov gene encodes adhesion factor for vascular smooth muscle cells and is dynamically regulated in response to vascular injury. *Arteriosclerosis, thrombosis, and vascular biology* 2000;**20**:1912-1919.
241. Shimoyama T, Hiraoka S, Takemoto M, Koshizaka M, Tokuyama H, Tokuyama T, *et al.* CCN3 Inhibits Neointimal Hyperplasia Through Modulation of Smooth Muscle Cell Growth and Migration. *Arteriosclerosis, thrombosis, and vascular biology*;**2010**:5.
242. Matsumae H, Yoshida Y, Ono K, Togi K, Inoue K, Furukawa Y, *et al.* CCN1 knockdown suppresses neointimal hyperplasia in a rat artery balloon injury model. *Arteriosclerosis, thrombosis, and vascular biology* 2008;**28**:1077-1083.

243. Iozzo RV. The biology of the small leucine-rich proteoglycans. Functional network of interactive proteins. *J Biol Chem* 1999;**274**:18843-18846.
244. Heinegard D, Larsson T, Sommarin Y, Franzen A, Paulsson M, Hedbom E. Two novel matrix proteins isolated from articular cartilage show wide distributions among connective tissues. *J Biol Chem* 1986;**261**:13866-13872.
245. Hedbom E, Heinegard D. Interaction of a 59-kDa connective tissue matrix protein with collagen I and collagen II. *J Biol Chem* 1989;**264**:6898-6905.
246. Oldberg A, Antonsson P, Lindblom K, Heinegard D. A collagen-binding 59-kd protein (fibromodulin) is structurally related to the small interstitial proteoglycans PG-S1 and PG-S2 (decorin). *Embo J* 1989;**8**:2601-2604.
247. Talusan P, Bedri S, Yang S, Kattapuram T, Silva N, Roughley PJ, *et al.* Analysis of intimal proteoglycans in atherosclerosis-prone and atherosclerosis-resistant human arteries by mass spectrometry. *Mol Cell Proteomics* 2005;**4**:1350-1357.
248. Strom A, Ahlqvist E, Franzen A, Heinegard D, Hultgardh-Nilsson A. Extracellular matrix components in atherosclerotic arteries of Apo E/LDL receptor deficient mice: an immunohistochemical study. *Histol Histopathol* 2004;**19**:337-347.
249. Sztrolovics R, Chen XN, Grover J, Roughley PJ, Korenberg JR. Localization of the human fibromodulin gene (FMOD) to chromosome 1q32 and completion of the cDNA sequence. *Genomics* 1994;**23**:715-717.
250. Antonsson P, Heinegard D, Oldberg A. Structure and deduced amino acid sequence of the human fibromodulin gene. *Biochim Biophys Acta* 1993;**1174**:204-206.
251. Roughley PJ. The structure and function of cartilage proteoglycans. *Eur Cell Mater* 2006;**12**:92-101.
252. Plaas AH, Neame PJ, Nivens CM, Reiss L. Identification of the keratan sulfate attachment sites on bovine fibromodulin. *J Biol Chem* 1990;**265**:20634-20640.
253. Svensson L, Narlid I, Oldberg A. Fibromodulin and lumican bind to the same region on collagen type I fibrils. *FEBS Lett* 2000;**470**:178-182.
254. Svensson L, Aszodi A, Reinholt FP, Fassler R, Heinegard D, Oldberg A. Fibromodulin-null mice have abnormal collagen fibrils, tissue organization, and altered lumican deposition in tendon. *J Biol Chem* 1999;**274**:9636-9647.
255. Aigner T, Zien A, Gehrsitz A, Gebhard PM, McKenna L. Anabolic and catabolic gene expression pattern analysis in normal versus osteoarthritic cartilage using complementary DNA-array technology. *Arthritis Rheum* 2001;**44**:2777-2789.
256. Sofat N. Analysing the role of endogenous matrix molecules in the development of osteoarthritis. *Int J Exp Pathol* 2009;**90**:463-479.
257. Soo C, Hu FY, Zhang X, Wang Y, Beanes SR, Lorenz HP, *et al.* Differential expression of fibromodulin, a transforming growth factor-beta modulator, in fetal skin development and scarless repair. *Am J Pathol* 2000;**157**:423-433.
258. Stoff A, Rivera AA, Mathis JM, Moore ST, Banerjee NS, Everts M, *et al.* Effect of adenoviral mediated overexpression of fibromodulin on human dermal fibroblasts and scar formation in full-thickness incisional wounds. *J Mol Med* 2007;**85**:481-496.
259. Hildebrand A, Romaris M, Rasmussen LM, Heinegard D, Twardzik DR, Border WA, *et al.* Interaction of the small interstitial proteoglycans biglycan, decorin and fibromodulin with transforming growth factor beta. *Biochem J* 1994;**302 (Pt 2)**:527-534.

260. Nili N, Cheema AN, Giordano FJ, Barolet AW, Babaei S, Hickey R, *et al.* Decorin inhibition of PDGF-stimulated vascular smooth muscle cell function: potential mechanism for inhibition of intimal hyperplasia after balloon angioplasty. *Am J Pathol* 2003;**163**:869-878.
261. Shah M, Foreman DM, Ferguson MW. Neutralisation of TGF-beta 1 and TGF-beta 2 or exogenous addition of TGF-beta 3 to cutaneous rat wounds reduces scarring. *Journal of cell science* 1995;**108 (Pt 3)**:985-1002.
262. Ranjzad P, Salem HK, Kingston PA. Adenovirus-mediated gene transfer of fibromodulin inhibits neointimal hyperplasia in an organ culture model of human saphenous vein graft disease. *Gene therapy* 2009.
263. Ichii T, Koyama H, Tanaka S, Kim S, Shioi A, Okuno Y, *et al.* Fibrillar collagen specifically regulates human vascular smooth muscle cell genes involved in cellular responses and the pericellular matrix environment. *Circ Res* 2001;**88**:460-467.
264. Salem HK, Ranjzad P, Driessen A, Appleby CE, Heagerty AM, Kingston PA. Beta-adrenoceptor blockade markedly attenuates transgene expression from cytomegalovirus promoters within the cardiovascular system. *Arteriosclerosis, thrombosis, and vascular biology* 2006;**26**:2267-2274.
265. Anderson JL, Adams CD, Antman EM, Bridges CR, Califf RM, Casey DE, Jr., *et al.* ACC/AHA 2007 guidelines for the management of patients with unstable angina/non-ST-Elevation myocardial infarction: a report of the American College of Cardiology/American Heart Association Task Force on Practice Guidelines (Writing Committee to Revise the 2002 Guidelines for the Management of Patients With Unstable Angina/Non-ST-Elevation Myocardial Infarction) developed in collaboration with the American College of Emergency Physicians, the Society for Cardiovascular Angiography and Interventions, and the Society of Thoracic Surgeons endorsed by the American Association of Cardiovascular and Pulmonary Rehabilitation and the Society for Academic Emergency Medicine. *Journal of the American College of Cardiology* 2007;**50**:e1-e157.
266. Bassand JP, Hamm CW, Ardissino D, Boersma E, Budaj A, Fernandez-Aviles F, *et al.* Guidelines for the diagnosis and treatment of non-ST-segment elevation acute coronary syndromes. *Eur Heart J* 2007;**28**:1598-1660.
267. Losordo DW, Vale PR, Symes JF, Dunnington CH, Esakof DD, Maysky M, *et al.* Gene therapy for myocardial angiogenesis: initial clinical results with direct myocardial injection of phVEGF165 as sole therapy for myocardial ischemia. *Circulation* 1998;**98**:2800-2804.
268. Montminy M. Transcriptional regulation by cyclic AMP. *Annu Rev Biochem* 1997;**66**:807-822.
269. Rao RS, Miano JM, Olson EN, Seidel CL. The A10 cell line: a model for neonatal, neointimal, or differentiated vascular smooth muscle cells? *Cardiovascular research* 1997;**36**:118-126.
270. Hatakeyama Y, Nguyen J, Wang X, Nuckolls GH, Shum L. Smad signaling in mesenchymal and chondroprogenitor cells. *J Bone Joint Surg Am* 2003;**85-A Suppl 3**:13-18.
271. Pickering JG, Jekanowski J, Weir L, Takeshita S, Losordo DW, Isner JM. Liposome-mediated gene transfer into human vascular smooth muscle cells. *Circulation* 1994;**89**:13-21.

272. Dulak J, Jozkowicz A, Ratajska A, Szuba A, Cooke JP, Dembinska-Kiec A. Vascular endothelial growth factor is efficiently synthesized in spite of low transfection efficiency of pSG5VEGF plasmids in vascular smooth muscle cells. *Vascular Medicine* 2000;**5**:33-40.
273. Keogh MC, Chen D, Lupu F, Shaper N, Schmitt JF, Kakkar VV, *et al.* High efficiency reporter gene transfection of vascular tissue in vitro and in vivo using a cationic lipid-DNA complex. *Gene therapy* 1997;**4**:162-171.
274. Pelisek J, Engelmann MG, Golda A, Fuchs A, Armeanu S, Shimizu M, *et al.* Optimization of nonviral transfection: variables influencing liposome-mediated gene transfer in proliferating vs. quiescent cells in culture and in vivo using a porcine restenosis model. *J Mol Med* 2002;**80**:724-736.
275. Schwartz RS, Edelman ER, Carter A, Chronos N, Rogers C, Robinson KA, *et al.* Drug-eluting stents in preclinical studies: recommended evaluation from a consensus group. *Circulation* 2002;**106**:1867-1873.
276. Appleby CE, Kingston PA, Verhoeven M, Heagerty AM. Stent-based intra-coronary gene transfer of a secreted Transforming Growth Factor-ß type II receptor inhibits in-stent neointimal hyperplasia. *Circulation* 2004;**110**:III-161(Abstract).
277. Schwartz RS, Huber KC, Murphy JG, Edwards WD, Camrud AR, Vlietstra RE, *et al.* Restenosis and the proportional neointimal response to coronary artery injury: results in a porcine model. *Journal of the American College of Cardiology* 1992;**19**:267-274.
278. Gunn J, Arnold N, Chan KH, Shepherd L, Cumberland DC, Crossman DC. Coronary artery stretch versus deep injury in the development of in-stent neointima. *Heart* 2002;**88**:401-405.
279. Felton J, Meisler M, Paigen K. A locus determining beta-galactosidase activity in the mouse. *J Biol Chem* 1974;**249**:3267-3272.
280. Lim CS, Chapman GD, Gammon RS, Muhlestein JB, Bauman RP, Stack RS, *et al.* Direct in vivo gene transfer into the coronary and peripheral vasculatures of the intact dog. *Circulation* 1991;**83**:2007-2011.
281. Minamino T, Komuro I. Vascular cell senescence: contribution to atherosclerosis. *Circ Res* 2007;**100**:15-26.
282. Fenton M, Barker S, Kurz DJ, Erusalimsky JD. Cellular senescence after single and repeated balloon catheter denudations of rabbit carotid arteries. *Arteriosclerosis, thrombosis, and vascular biology* 2001;**21**:220-226.
283. Minamino T, Miyauchi H, Yoshida T, Ishida Y, Yoshida H, Komuro I. Endothelial cell senescence in human atherosclerosis: role of telomere in endothelial dysfunction. *Circulation* 2002;**105**:1541-1544.
284. Darquet AM, Cameron B, Wils P, Scherman D, Crouzet J. A new DNA vehicle for nonviral gene delivery: supercoiled minicircle. *Gene therapy* 1997;**4**:1341-1349.
285. Lanford RE, Kanda P, Kennedy RC. Induction of nuclear transport with a synthetic peptide homologous to the SV40 T antigen transport signal. *Cell* 1986;**46**:575-582.
286. Mayrhofer P, Schleef M, Jechlinger W. Use of minicircle plasmids for gene therapy. *Methods Mol Biol* 2009;**542**:87-104.
287. Perkins LEL, Boeke-Purkis KH, Wang Q, Stringer SK, Coleman LA. XIENCE V™ Everolimus-Eluting Coronary Stent System: A Preclinical Assessment. *Journal of Interventional Cardiology* 2009;**22**:S28-S40.

288. Park DW, Kim YH, Yun SC, Kang SJ, Lee SW, Lee CW, *et al.* Comparison of zotarolimus-eluting stents with sirolimus- and paclitaxel-eluting stents for coronary revascularization: the ZEST (comparison of the efficacy and safety of zotarolimus-eluting stent with sirolimus-eluting and paclitaxel-eluting stent for coronary lesions) randomized trial. *Journal of the American College of Cardiology* 2010;**56**:1187-1195.
289. Serruys PW, Silber S, Garg S, van Geuns RJ, Richardt G, Buszman PE, *et al.* Comparison of zotarolimus-eluting and everolimus-eluting coronary stents.